THE UNIVERSITY OF CALGARY

# The Dynamics of Left Ventricular Torsion Throughout the Cardiac Cycle

by

**Carol A. Gibbons Kroeker**

A Dissertation

Submitted To The Faculty Of Graduate Studies

In Partial Fulfillment Of The Requirement For The

Degree Of Doctor Of Philosophy

Department of Cardiovascular and Respiratory Sciences,

Medicine

Calgary, Alberta

September, 1994

# THE UNIVERSITY OF CALGARY
# FACULTY OF GRADUATE STUDIES

The undersigned certify that they have read, and recommend to the Faculty of Graduate Studies for acceptance, a thesis entitled, **"The Dynamics of Left Ventricular Torsion Throughout the Cardiac Cycle"** submitted by Carol A. Gibbons Kroeker in partial fulfillment of the requirements for the degree of Doctor of Philosophy.

Dr. John. V. Tyberg, Supervisor
Medicine and Medical Physiology

Dr. Rafael Beyar
Biomedical Engineering
Technion-Israel Institute

Dr. Henk E.D.J. ter Keurs
Medicine and Medical Physiology

Dr. Merril L. Knudtson
Medicine

Dr. Brian McMahon
Biology

Dr. Edward P. Shapiro, External Examiner
Division of Cardiology
John Hopkins University
Baltimore, Maryland

September 30, 1994.

# ABSTRACT

Previous studies on LV twist involved labourious techniques and analysis and many were unable to record twist continuously throughout the cardiac cycle. To study torsion in a simpler, more direct fashion, it was hypothesized that the dynamics of LV twist would be well-characterized by measurement of apex-rotation alone, since base-rotation was small. A device was designed to measure apex-rotation on-line throughout the cardiac cycle. It consisted of a light source, a position-sensitive diode, and a small mirror that was coupled to the apex by a wire. As the wire rotated with LV contraction or relaxation, apex-rotation (°) was calculated from the deflected light beam on the diode. Timing of apex-rotation was compared to simultaneous recordings of LV pressure, LV area-index (as calculated from short-axis diameters), and segment length. Under control conditions, recordings of apex-rotation were similar to previous results from more labourious methods, confirming that the device is a reliable index of LV twist. Because the method records on-line, rapid changes in apex-rotation could be measured. The dynamics of apex-rotation with changing preload (VC occlusion and volume loading), afterload (aortic constriction), contractility (paired-pacing and epinephrine injection), heart rate (atrial pacing; 90-180 bpm), and ischemia (coronary artery occlusion).

By changing preload, a single, direct, linear relationship was shown between apex-rotation and LV volume at end diastole which was significantly different from the direct, linear relationship at end systole. These relationships were not altered by

changes in afterload, contractility, or heart rate, but did seem to be altered under ischemic conditions. With VC occlusion, apex-rotation amplitude increased and maximal apex-rotation occurred earlier in the cycle. With increased preload or increased afterload, the amplitude of apex-rotation decreased slightly and maximal apex-rotation was delayed into IVR. Increased contractility by paired pacing increased apex-rotation amplitude by 42%, and the LV remained in its twisted state for a longer period. More rapid untwisting in IVR was seen with epinephrine injection. Increasing heart rate over 150 bpm decreased apex-rotation amplitude, with maximal apex-rotation delayed into IVR. With ischemia, there is an initial increase in apex-rotation amplitude. At 10, 30, and 50 seconds of ischemia, maximal apex-rotation was delayed into the IVR period. At 30 and 50 sec, there is a period of paradoxical twisting in the IVR period. These changes may be a result of a changing balance of moments between epicardial and endocardial fibres, which may affect restoring forces and early diastolic filling.

# ACKNOWLEDGMENTS

I would like to thank my supervisor, Dr. John V. Tyberg for his help and guidance throughout the course of this work. His patience and encouragement were much appreciated. He was always available for discussions and his understanding of my family obligations made it possible for me to finish this thesis. Thank you for having the faith in me to take me on as your student and helping me to fulfill my potential.

I would also like to thank Dr. Rafael Beyar, who was a visiting scientist from the Department of Biomedical Engineering, Technion-Israel Institute of Technology, Haifa, Israel. His enthusiasm for twist mechanics is the reason that this work began. His knowledge, patience and good humour in our many discussions (and E-mail) were greatly appreciated. Thank you for being so encouraging to me (especially when I felt completely inadequate). It has been a real honour for me to have the opportunity to work with you.

Thanks to Dr. Henk ter Keurs for helpful input during the early design days of the optical device. I'd like to acknowledge him, Dr. Merril Knudtson, and Dr. Brian McMahon for serving on my supervisory committee. I'd also like to acknowledge Dr. Ed Shapiro who served as the External Examiner on the thesis defense committee.

Cheryl Meek taught me everything I wanted to know about animal surgery (and lots I didn't!). Thanks for not rolling your eyes too much each time I presented one more thing to attach to the left ventricle, and for pretending to be impressed the first time my carotid cannulation took less than 45 minutes. These experiments would have been impossible without your surgical wizardry. I've appreciated that and your friendship in the last few years. Thanks also to Gerry Groves for lots of lab assistance (you name it- he'll find it!), fatherly advice, and humour (just remember- the bottle design was mine first!).

Sheng-Jing Dong was a good friend in our office-sharing days. Aside from the talks and laughter, he made many helpful suggestions on various aspects of this work. I really appreciate it, Chenner! Thanks also to Jenn, Lisa, and Hui who have put up with a baby stroller (and the perfect child!) in the office more than once. Thanks also to Rosa who's always there when you crash CVSOFT or sigma-plot, and to Dale Bergman who's around when your computer crashes are on a bigger scale!

Others who helped in this study by way of friendship, encouragement, and humour were Warren Fitch (who I still blame for talking me into this in the first place!), Bruce Gordon (one of these days I'll actually make you realize the superiority of science over philosophy), Randy Lauff (a graduate student sympathizer), the Gordons (your teapot runneth over!), Rosanne Kennedy (keep August 12, 2017 open for their wedding!), and BLTNBSG (it took prayer to get me through this one!).

Special thanks to my family who help keep things in perspective. You've

always shown me love and support with every turn my life has taken and I appreciate it. You've also taught me to take life on with a sense of humour and that has served me well. It's nice to know you'll always be there for me!

Thank you to my wonderful (and patient!) husband Ken, who has stood by me through many, many years of studies. I love you. Life will be normal soon. Really!

Love also to my daughter, Sarah, who is still too young to remember the many hours she willingly played at my feet as I ground out plots on the computer.

My great appreciation to the Heart and Stroke Foundation of Canada (Alberta) who supported this work by a grant-in-aid to Dr. Tyberg and by a graduate traineeship to myself.

This is dedicated to my
daughter, Sarah Lynn, and
to her future siblings.
May they know the support,
love, and encouragement that
I have known from my family.
May I teach them to set high
standards for their lives,
because any goal is reachable
with work and the right people
behind you.
I will always try to be there
for you and whatever dreams you
choose to pursue.

# Contents

# List of Tables

# List of Figures

# List of Abbreviations

| | | |
|---|---|---|
| **LV** | - | Left Ventricle |
| **ED** | - | End diastole |
| **ES** | - | End systole |
| **IVC** | - | Isovolumic Contraction |
| **EIVC** | - | End of Isovolumic Contraction |
| **IVR** | - | Isovolumic Relaxation |
| **EIVR** | - | End of Isovolumic Relaxation |
| **VCO** | - | Venae Caval Occlusion |
| **PP** | - | Paired Pacing |
| **SP** | - | Single pacing |
| **LAD** | - | Left anterior descending coronary artery |
| **LCX** | - | Left circumflex coronary artery |

# Chapter 1

# INTRODUCTION

## 1.1 Muscle Fibre Orientation

It is well known that the muscle fibres of the left ventricle (LV) vary in orientation by 100° from the epicardium to the endocardium (Streeter, 1979). While fibres in the LV midwall are mainly oriented circumferentially, the epicardial and endocardial fibres are oriented obliquely with respect to the long axis, forming a right-handed helix in the subendocardium, and making a left-handed helix in the sub-epicardium. Although each myocyte shortens along its own axis, this local shortening is translated into one principal motion observed in the LV. The muscle fibres are "interconnected" by a collagen meshwork which surrounds each myocyte. Waldman et al. (1985) found that the angle of principal shortening varies by approximately 30° through the LV wall, although fibre angles have been shown to change by 100°. This suggests a strong interaction between fibres at different transmural levels via the collagen network. Prinzen et al. (1985) suggest an additional form of global tethering as each myocardial layer responds to the constraints placed on it by the force-developing layers that surround it. Thus, uniaxial shortening of each myocyte is translated into a three-dimensional change in

the LV, as a result of the balance of fibre moments through the ventricular wall. With contraction of the obliquely-oriented fibres, it would be expected that the LV would twist along its long axis. As viewed from the apex, LV twist or torsion is defined as the counter-clockwise rotation of the apex with respect to the base.

The helical distribution of muscle fibres within the LV, along with its associated collagen matrix, provide the substrate for a collective contribution of both active and passive elements which change throughout the cardiac cycle. It is the balance of these moments which result in apical rotation (Ingels et al., 1989). Thus, LV twist may be determined by both active fibre shortening and passive elements.

## 1.2 Fibre Moments and LV Twist

LV twist is a result of the sum of individual muscle fibre moments. The contribution to torque about the long axis by a given fibre is dependent on its circumferential force development (a result of sarcomere length and angle from the ventricular equator) and on the radial location of that fibre (Ingels et al., 1989). Since sarcomere shortening appears uniform through the wall (Arts et al., 1979), the moment of each muscle fibre (its contribution to twist) is dependent on the fibre angle relative to the LV equator. It would not be expected that either the midwall circumferentially-oriented fibres (at 0° to the ventricular equator) or the longitudinal fibres (oriented at 90° to the ventricular equator) would contribute to LV torsion (Ingels et al., 1989). It is therefore likely that fibres oriented at 45° would be able

to contribute the maximal moment to LV twist. Fibres so oriented would be found in the subendocardium and subepicardium. Fibres at opposite angles may counter-balance each other because of an equilibrium of torques (Arts et al., 1979), so the number of fibres (or the volume the fibres occupy) at each orientation is an important determinant of LV twist. Considering a cyclindrical model of the left ventricle, the epicardium is of a larger radius than the endocardium and will, therefore, occupy more cylinder volume than the endocardium (if the thickness of the layers is equal). Assuming fibre density is constant, the epicardial layer will contain more muscle fibres, and these fibres (wrapping over a larger radius) will exert more torque than a similarly-contracting endocardial fibre. Therefore, epicardial fibre moments would dominate and the observed twist would be in a counter-clockwise direction with respect to the base (as viewed from the apex).

The endocardium becomes activated before the epicardium by approximately 1-15 ms (Scher, 1979). In relaxation, the epicardium becomes inactivated before the endocardium, so that the total activation time of the endocardium is greater than the epicardium. Ingels et al. (1989) proposed that during isovolumic contraction, the endocardial fibres are activated before the epicardial fibres, resulting in LV "untwist" (clockwise rotation with respect to the base). As the epicardial fibres become activated, they produce a counter-clockwise torque, which dominates the endocardial fibres because of a greater volume and radius of epicardial fibres. This results in LV twist (counter-clockwise rotation) during ejection. In isovolumic

relaxation, the epicardial fibres begin to relax and lengthen first, while the still-activated endocardial fibres continue to shorten. This results in large and rapid untwist occurring in this period, as endocardial fibres dominate. Hansen et al. (1988) found differences in the amplitude of twist observed between regions of the LV. This may be a result of local differences in fibre orientation within the ventricular wall or in layer thickness (number of fibres within that layer). A thick endocardial layer would oppose twist during contraction (reducing the amount of torsion) but may result in faster and greater untwist during relaxation.

Arts et al. (1979) found that LV torsion is important in equalizing differences in mechanical work across the LV wall by reducing transmural differences in sarcomere shortening and fibre stress. Increased strain and shear in the endocardium over the epicardium has been observed (Feigl and Fry, 1964; Fenton et al., 1978), and is possibly a result of differences in metabolism and coronary perfusion (Feigl, 1983) or a greater wall-thickness-to-radius ratio (Waldman et al., 1985). Using computer modelling, Beyar and Sideman (1986) found that the twisting motion significantly reduced the difference between epicardial and endocardial sarcomere shortening. Twist acted to decrease strain rates at the endocardium and increase rates at the epicardium, with a effect close to 0 at the midwall. This made total strain rate with twist much more uniform through the wall. Beyar and Sideman (1986) also found that the endocardial layers consumed more oxygen than the epicardial layers. This $O_2$ consumption gradient was reduced

when the LV torsion was allowed, indicating that twist can affect oxygen demand distribution. Ohayon and Chadwick (1988) found that normal LV torsion with normal activation delay equalized transmural distribution of fibre external work and lowered myocardial tissue pressure, improving $O_2$ supply.

## 1.3 Apex versus Base Rotation

LV torsion has been shown to increase from base to apex (Buchalter et al., 1990). The base of the heart is well-anchored by the major vessels and thus will rotate very little with contraction. The contraction of obliquely-oriented muscle fibres will cause the portion of the LV distal to these fibres to twist. All the twist created by contracting fibres during systole should be transferred towards the apex, making apical rotation maximal.

Streeter et al. (1969) found that, near the base, the fibre angles (with respect to the circumferential axis) in the lateral wall increased in systole (over the diastolic angle) by approximately 7°, while near the apex, this systolic increase was approximately 19°. This may indicate greater apex rotation than base rotation. Buchalter et al. (1990) studied LV torsion non-invasively using MRI tagging. They also found that torsion (the difference in torsional angles between the base and marker points towards the apex) increased with increasing distance from the base. Further, this increase was not linear. When considering the change in torsion within a "slice" of the LV (between marker sites at different longitudinal levels), a greater

increase in torsion was noted in "slices" near the apex than in "slices" near the base. At the base of the LV, the majority of muscle fibres are oriented circumferentially but, at the apex, the majority of fibres are more oblique in orientation (Greenbaum et al., 1981). Buchalter et al. (1990) suggest this as a possible explanation for the increased apical rotation. Azhari et al. (1992) suggest a conical model of the left ventricle to better describe the nonuniformity of LV twist. This model predicted that the apex should rotate more than the base, implying that LV twist is partly determined by LV geometry.

## 1.4 LV Twist and Restoring Forces

Early ventricular filling is dependent on the atrioventricular pressure gradient which, in turn, is dependent on passive mechanical properties of the ventricle (elastic recoil) and on active properties such as the rate and duration of ventricular relaxation (muscle fibre lengthening) (Nikolic et al., 1988). Tyberg et al. (1970) have demonstrated an active component to early diastolic filling by producing negative LV pressures, or diastolic suction. Caillet and Crozatier (1982) found that increased systolic shortening (and therefore, increased restoring forces) resulted in a greater peak velocity of fibre lengthening (greater relaxation rate), and possibly faster early ventricular filling. Nevo and Lanir (1989) showed that, along with the active contribution of the muscle fibres, the collagen network has a significant passive effect on the overall left ventricular response, and affects elastic recoil.

Relative to the individual muscle fibres, the passive restoring forces may be internal (elastic recoil of individual fibres to their slack length) and external (loading of the network between fibres during systole).

During contraction, counter-clockwise torsion is occurring (in the direction of epicardial fibres but perpendicular to the endocardial fibres). This may "load" the extracellular collagen matrix and space between the epicardium and endocardium like a spring. During relaxation, the fibres cease to be load-bearing, myocardial stiffness decreases, and the elastic elements recoil. This results in potential energy that will be released before and when the mitral valve opens, producing rapid filling (diastolic suction). Because the endocardium remains activated during early isovolumic relaxation while the epicardium does not, the balance of moments shifts in the direction of endocardial fibres, enhancing untwist during this period. Thus, the endocardial fibres may actively contribute to untwisting during the isovolumic relaxation period, and ultimately diastolic suction. If more untwist occurs before the mitral valve opens as in the case of catecholamine administration (Rademakers et al., 1992), there may be greater diastolic suction and faster ventricular filling. Beyar et al. (1989) showed that, while twist and mid-wall fractional shortening were coupled during contraction, they became uncoupled during relaxation, with untwisting occurring before fractional lengthening. Further, much of the untwist occurred during the isovolumic relaxation period with very little lengthening. This supports the suggestion that, in addition to other restoring forces, endocardial

untwisting may act to aid in early diastolic filling.

Thus, the twisting of the LV may be a mechanism which allows the myocardium to store potential energy during ejection, as the collagen matrix would be strained in the radial direction. Upon relaxation, this energy would be released as an untwist in early diastole, possibly aiding in rapid filling of the ventricle. It is believed that LV untwist is governed by a different balance of the same moments which result in twist, i.e., a balance of moments produced by active and passive elements.

## 1.5 Previous Studies

It has long been accepted that the LV exibits torsion during its cardiac cycle. Although this torsion had been documented in both animals (Rushmer et al., 1953) and humans (McDonald, 1970), it had not been quantified until recently. Ingels et al. (1975) implanted tantalum markers into the LV midwall during cardiac surgery and, with radiography, were able to measure systolic LV rotation. They were able to quantify torsion at specific points on the LV and found that the apex and base rotated in opposite directions.

Studies have now been performed to examine and quantify ventricular torsion in both dogs and humans. Arts and Reneman (1980) measured epicardial deformation in dogs using a magnetic-field-generating coil and two sensor coils. One sensor was placed at a distance circumferentially from the magnetic coil, while the other was placed at a distance in the base-to-apex direction. Since the strength

of the field decreases with increasing distance, the amplitudes of the voltages induced in the sensor coils and their phase differences provided data about cireumferential and base-to-apex strains, as well as shear.

Arts et al. (1984) went on to study LV torsional deformation in dogs using two-dimensional echocardiography. Echo-derived transverse cross-sectional projections of the LV were obtained at the levels of the mitral valve and the papillary muscle (anatomical markers). Twist was defined as the difference between the angles of rotation at the two levels in the heart. This study showed that twist was measurable by non-invasive methods. This method is limited by the fact that it cannot detect rapid changes in twist, and because it does not provide information on apical twist.

Buchalter et al. (1990) studied LV twist in humans non-invasively using a Magnetic Resonance Imaging (MRI) technique. With myocardial tagging (produced by radio-frequency pre-excitation), specific areas of the myocardium will appear as black lines that persist for approximately 500 msec. Twist can be detected as the deformation of these lines between end diastole and end systole . Tagging lines fade quickly, however, making this method inadequate to provide information about twist through the entire cardiac cycle. Rademakers et al. (1992) used MRI tagging to study the effects of catecholamines on LV torsion in dogs. Atrial pacing was used to increase heart rate (to an R-R interval of 400 msec) so that a full cardiac cycle could be recorded before the tagging faded, but 20 msec intervals between

measurements may have allowed rapid changes to go unrecorded.

Hansen et al. (1988), Ingels et al. (1989), Yun et al. (1991), and Moon et al. (1994) implanted intramyocardial radiopaque markers into human LV at the time of heart transplantation. By using biplane cineradiography, torsional deformation could be measured by the rotation of these markers through systole. The effects of allograft rejection, moderate volume loading, and inotropic stimulation were examined by this method. These studies are limited by their inability to measure parameters such as LV pressure (due to ethical constraints), making correlations between LV twist and pressure impossible.

Beyar et al. (1989) implanted radiopaque markers and used biplane cineradiography to measure LV twist in dogs. On-line recordings were obtained throughout the cardiac cycle and compared to LV pressure and radial shortening. Using this method, they were able to find a systolic relationship between LV twist and radial shortening, but the complicated set-up and analysis makes the method undesirable to use in the study of beat-to-beat changes from interventions such as preload changes.

Although not measuring LV twist directly, some groups studied myocardial deformation and shear in the canine LV. Changes in the shear angle (longitudinal-circumferential shear strain) are directly related to LV twist (Arts et al., 1982). Waldman et al. (1985), Waldman and Covell (1987), and Waldman et al. (1988) used implanted markers and biplane cineradiography to measure transmural

deformation in the LV. These studies were able to relate measured shear to circumferential, longitudinal, and radial strains. Using a magnetic field-generating coil and two sensor coils, Arts et al. (1982) could measure the change in shear angle during the ejection phase and study the effects of preload on the amplitude of the angle change. As mentioned in previous sections, other groups have used computer modelling to further characterize LV torsion (Arts et al., 1979; Beyar and Sideman, 1984, 1986).

Although all of these methods are useful in describing LV torsion, there was no simple and direct method to measure LV twist that would allow for a full study of interventions such as load changes, contractility, and ischemia.

## 1.6 Aims of these Studies

The first aim of these studies was to develop a new method to accurately and simply measure LV twist. This method had to produce baseline results that would be comparable to other methods and have the ability to be used under many intervention conditions. An optical device was fabricated and used to measure apex-rotation as an index of LV twist. The design and testing of this new twist-measuring method is described in chapter 2. The hypothesis that apex-rotation is sufficient to describe LV twist is also tested in this chapter. Using this method, the next goal was to examine the dynamics of twist throughout the cardiac cycle, particularly during the isovolumic periods, and compare it to parameters such as LV pressure,

LV area index, and LV segment length. These results would be applied to examine the mechanisms of twist and untwist and relate them to the balance of endocardial and epicardial shortening moments. A description of apex-rotation compared to these parameters under control conditions can be found in Chapter 2.

The final aim of this study was to use this method to study the effects of changing preload, afterload, contractility, and ischemia on LV twist and untwist. Since these interventions are known to change fibre shortening and, thus, the balance of epicardial and endocardial moments, it is expected that they will also affect LV apex-rotation. The effects of load and contractility on LV twist are controversial and it is hoped that this method, which allows for beat-to-beat comparison of apex-rotation, can describe the effects more fully than could previous methods. The effects of increased and decreased preload (by volume loading and vena caval occlusion) on apex-rotation are described in Chapter 3. Using these results, a twist-volume relationship at end diastole and end systole is also presented. The effects of increased afterload (by aortic constriction), contractility (by a paired-pacing model and epinephrine injection), and heart rate (by atrial pacing) on apex-rotation are described in Chapter 4.

The effects of ischemia on LV apex-rotation are presented in Chapter 5. Because regional ischemia interferes with the balance of moments between epicardium and endocardium during both systole and relaxation, it is expected that it will also affect apex-rotation throughout the cardiac cycle.

An apex-rotation--shortening relationship is discussed in Chapters 2 (baseline conditions), 3 (effects of preload), 4 (effects of contractility changes), and 5 (effects of ischemia). Because fibre shortening is associated with a change in the balance of moments governing twist, twist is a function of fibre shortening. Further, this relationship changes throughout the cardiac cycle, as the balance of moments change. Therefore, changing load, contractility, and ischemia may affect this twist-shortening relationship.

It is hoped that these studies will provide a clearer understanding of the dynamics and mechanisms of LV twist throughout the cardiac cycle, under conditions not amenable to study by previous methods. Because the method allows for measurement of many haemodynamic parameters, a twist-volume relationship has been established and twist-shortening relationships have been more fully described.

# Chapter 2

# DESIGN OF AN OPTICAL TWIST-MEASURING DEVICE

## 2.1 Abstract

Previous studies on LV twist involved labourious techniques and analysis. To study torsion in a simpler, more direct fashion, it was hypothesized that the dynamics of LV twist would be well-characterized by measurement of apex-rotation, since base-rotation is small. A device was designed to measure apex-rotation on-line continuously throughout the cardiac cycle. It consisted of a light source, a position-sensitive diode, and a small rotating mirror that is coupled to the apex by a wire. As the wire rotated with LV contraction or relaxation, apex rotation (in degrees) was calculated from the position of the deflected light beam on the photo-sensitive diode. Timing of apex-rotation was compared to simultaneous recordings of LV pressure, LV area index (as calculated from short-axis diameters), and segment length. Under control conditions, recordings of apex-rotation were similar to previous results from more labourious methods, confirming that the device is a reliable index of LV twist. Early untwisting was observed during isovolumic contraction, followed by twisting

which peaked before end systole. Rapid untwisting was seen during the isovolumic relaxation (IVR) period, with untwisting nearly complete by the first third of diastolic filling. This device provides precise timing and definition of rapid changes in the isovolumic periods, confirms results by more labourious methods, and provides and easy method to measure the dynamics of apex-rotation continuously during interventions such as load or ischemia.

## 2.2 Introduction

As described in Chapter 1, many methods have been used to describe and quantify LV twist, including magnetic resonance imaging (Buchalter et al., 1990; Rademakers et al., 1992), echocardiography (Arts et al., 1984), and radiopaque markers and biplane cineradiography (Hansen et al., 1988; Beyar et al., 1989; Ingels et al., 1989; Yun et al., 1991; Moon et al., 1994). While these methods had the advantage of being non-invasive (after markers are implanted in the case of biplane cineradiography), they required complicated experimental procedures and labourious analysis. Methods involving MRI tagging and echocardiography did not allow for on-line recordings of twist throughout the cardiac cycle and, in addition, many of the studies involving biplane cineradiography did not record LV pressure for comparison. These methods all measured relative twist between the base and the apex, but a measure of apex-rotation alone may be sufficient to characterize LV twist dynamics since previous studies have shown that the rotation increases

gradually and predictably towards the apex (Buchalter et al., 1990) and that the base of the heart rotates only minimally.

In this chapter, a simple method to measure the dynamics of apex-rotation accurately in open-chest animals is described. Apex-rotation measurements were recorded simultaneously with measurements of ECG, LV pressure, segment length, and diameter. The method was used to describe precisely the pattern of apex-rotation throughout the cardiac cycle and to correlate it with the haemodynamic parameters above. Base-rotation was also measured so support the hypothesis that apex-rotation is sufficient to describe twist.

## 2.3 Methods

### 2.3.1 The Optical Device

The optical twist-measuring device consisted of a light source, mirror, and a light-sensitive photo-diode, which was coupled to the left ventricular apex by a wire. A 15-cm long, 0.5-mm diameter piece of stainless-steel tubing (with the last 1 cm bent to 90°) was attached to the apex (i.e., "hooked" through the sub-epicardium) and sutured securely. The tubing was connected to the device by a tight silastic connector. The mirror (a silver-coated coverslip) was attached to the tubing in such a way that it reflected the light from the source onto the position-sensitive Schottky lateral-effect photo-diode (Fig. 2.1). The tubing rotated with the apex around the LV longitudinal axis with each contraction. This caused the mirror to

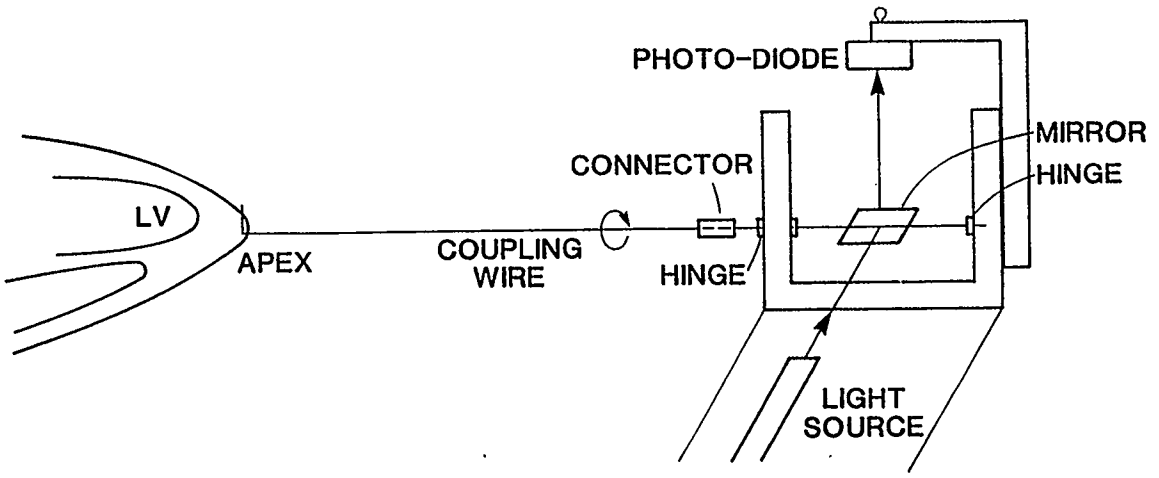


**Figure 2.1**: A schematic diagram of the apparatus as it was used to measure apex-rotation. The left ventricular apex is coupled to the twist-measuring device. The mirror rotates with the apex and deflects the light onto the diode.

deflect the light onto a different position of the diode. Thus, the position of the light on the diode was indicative of the magnitude of LV apex-rotation. The tubing was able to move axially in and out which enabled continuous recording during interventions which caused the size or position of the heart to change slightly (e.g., load effects). The mirror was long enough (1.5 cm) to remain in the path of the incident light beam even when the tubing moved axially by as much as 1 cm. The tubing and silastic connector tubing were slightly flexible which allowed for some lateral movement.

By knowing the calibration deflection distance ($d_{cal}$) on the diode, the corresponding input voltage ($V_{cal}$), and the distance (L) from the diode to the mirror, the voltage signal ($V_{input}$) could be converted into degrees of apex-rotation (AR) by:

$$AR\ (^\circ) = 0.5 \times \arctan\left[(V_{input}) \times (d_{cal} / V_{cal}) / L\right] \qquad (1)$$

The factor of 0.5 accounts for the fact that reflected angle is twice the incident angle. Twisting of the LV, or counter-clockwise rotation of the apex with respect to base (as viewed from the apex), will result in a negative apex-rotation value. Untwisting will produce a positive apex-rotation value.

The deflection mirror was a very light, silver-plated coverslip. Initially, a chopped diode laser source (Draper Linear 1 laser pointer; Draper Shade and

Screen, Spiceland, Indiana) was used (in 4 dogs). A white-light source (Reichert Microscope Light, Model 1177; Reichert Scientific Instruments, Buffalo, New York) was later used. Each light source produced a small point of light on the diode and provided similar results, although the white-light signal produced less noise. The Schottky photo-diode was both intensity- and position-sensitive. The room lights were dimmed and ambient light was kept constant during experiments to eliminate the effects of changes in background light intensity.

Anode currents from the photo-sensitive diode passed through a current-to-voltage converter, and the resultant voltage was fed into a differential amplifier. The difference signal, which reflected the position of the incident light beam, was then fed through a 30-Hz low-pass filter. This filtering caused a 20-msec time delay which was corrected later by directly comparing the filtered signal to an unfiltered signal recorded simultaneously.

A frequency response test was performed on the entire device (i.e., the coupling tubing, mirror, diode, and circuit). A sinusoidal function generator was connected to the input of a pen motor (Gould Model 11-2983-301, Graphics Controls Corp., Cleveland, Ohio) which was coupled to the measuring device with a piece of stainless-steel tubing similar to that used during experiments. This enabled the function generator to control the rate of rotation of the connector wire. The frequency was varied from .5 Hz to 100 Hz. Over this range, virtually no drop was seen in the amplitude of the unfiltered diode output, when compared to the input

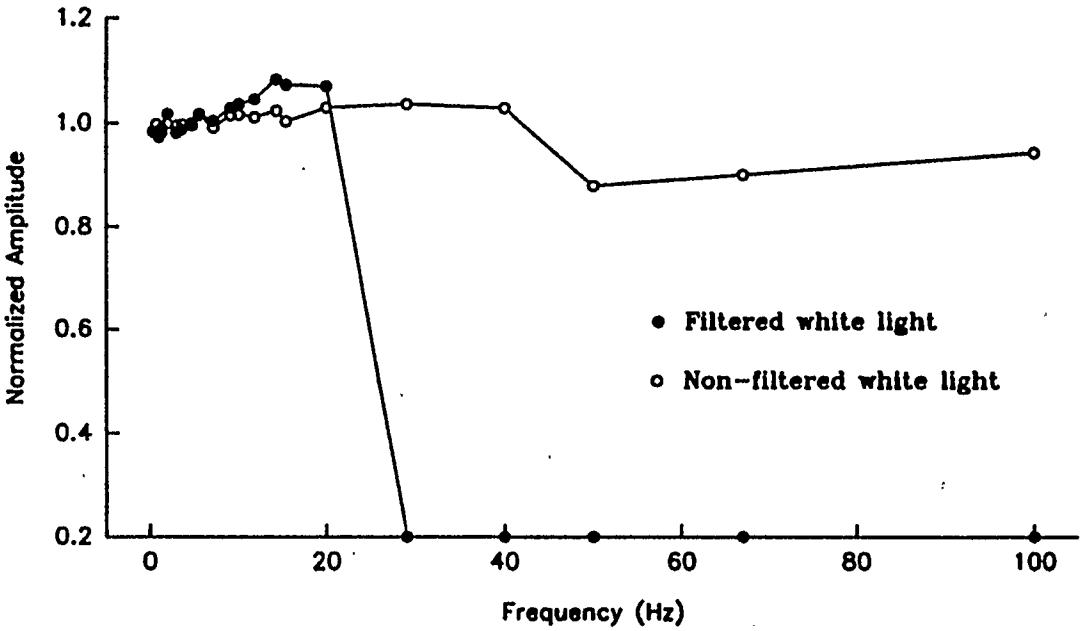


**Figure 2.2**: The frequency response curve of the optical device. The filtered and non-filtered signal are shown as an amplitude ratio of the input signal. Because a 30-Hz filter was used, the filtered signal is not shown beyond 30 Hz.

signal (see Fig. 2.2). Thus, the diode and circuit appear to give adequate results up to at least 100 Hz. The frequency response of the measurement of apex-rotation is therefore far above the typical frequency content of haemodynamic events. The precise timing of apex-rotation can thus be obtained and compared to parallel measurements of ECG, LV pressure, diameter, and segment-length measurements. From this high frequency response, we can also conclude that the weight of the deflecting mirror was not enough to hinder the twisting action of the wire (inertance of the mirror would be seen as a drop in response at all frequency levels).

### 2.3.2 Animal Preparation

Experiments were performed on 8 open-chest, anaesthetized dogs. Anaesthesia was induced using 25 mg/kg IV thiopental and maintained with infusion of a 25 mg/mL solution (100 ml/hr) of fentanyl citrate. The dogs were ventilated with a constant-volume respirator (Model 607, Harvard Apparatus Co., Inc.; Millis, Massachusetts). A trigger connected to the respirator indicated the end of expiration. To allow for successive beats to be recorded without the effects of inspiration, the respirator was turned off for very short periods ($<25$ sec.) at end expiration. The electrocardiogram (ECG) was monitored from limb leads, and body temperature was maintained with a heating pad.

LV pressure was measured by an 8F micromanometer-tipped catheter with a fluid-filled reference lumen (Model PC-480, Millar Instruments, Houston, Texas).

Central aortic pressure was measured by a fluid-filled open-ended catheter connected to a transducer (Model P23ID, Statham-Gould, Oxnard, California). A catheter was also inserted in the jugular vein for infusion of fluid. The pericardium was opened and fashioned into a cradle and LV anterior-posterior and septum-to-free-wall dimensions were measured by sonomicrometry (Model 120, Triton Technology Inc., San Diego, California). A LV area index was defined as the product of these diameters, assuming an elliptical minor-axis cross section. In addition, two pairs of circumferentially oriented sonocrystals (anterior wall and posterior wall at the level of the LV equator) were used to measure LV midwall segment length, to be used as an indicator of LV wall contractile function.

With the heart placed in a pericardial cradle, the apex was free to rotate. Apex-rotation was recorded simultaneously with the ECG, LV pressure, aortic pressure, and length measurements (VR16, Electronics for Medicine/Honeywell, White Plains, New York). The data were digitized at a sampling rate of 200 Hz, using a data acquisition and analysis program (CVSOFT, Odessa Computer Systems, Calgary, Alberta) and a personal computer (IBM, model AT).

To test the hypothesis that the base of the heart does not rotate significantly and, thus, that apex-rotation is sufficient to describe LV twist, rotation of the base of the heart was measured in 8 dogs. Two ties were attached to opposite sides of the base of the heart. These ties were connected to opposite ends of a lever which was suspended over the heart. A wire connected the fulcrum of the lever to the

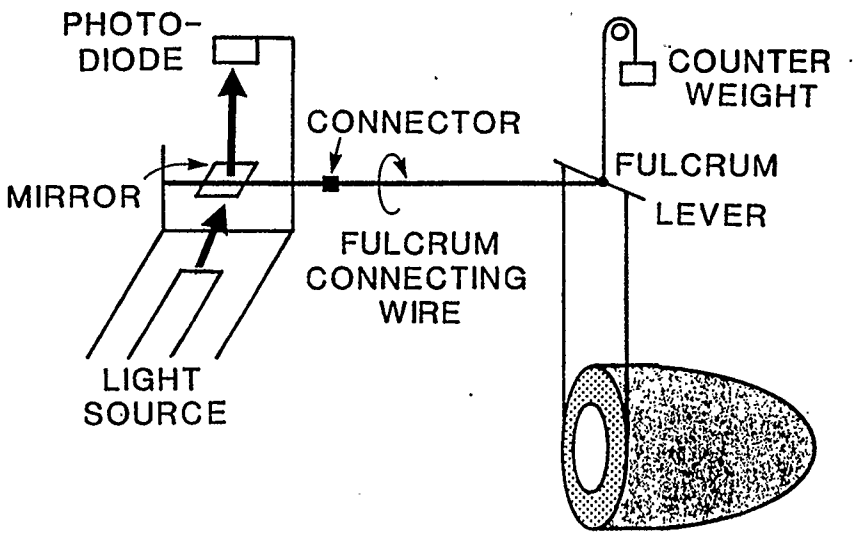


**Figure 2.3**: Schematic diagram of the twist-measuring device as it was used to measure base-rotation.

twist-measuring device (see Fig. 2.3). As the base of the heart rotated, the lever rocked and caused the fulcrum wire to rotate. This rotation was recorded by the measuring device.

### 2.3.3 Experimental protocol

A calibration run was performed at the beginning of the experiment to determine the relation of output voltage to a known distance on the diode. This calibration was repeated several times throughout the experiment to correct for possible slow baseline shifts. These changes have been found to be insignificant. The pressure-apex-rotation loops, LV and aortic pressures, as well as anterior and posterior segment lengths were also monitored continuously throughout the experiment.

Each recording interval lasted 60 sec. After every intervention, haemodynamic parameters were monitored to verify that baseline conditions had been reapproximated.

### 2.3.4 Analysis

Data were analyzed using a computer and CVSOFT software. End diastole (ED) was identified by the peak of the R-wave on the ECG and was defined as the instant immediately preceding the rapid upstroke in LV pressure. End systole, or ES (i.e., end-ejection) was defined as the instant at which aortic (after correction for

the time delay measured by fluid-filled lines) and LV pressure waveforms diverged (at the incisura), and this point was found using CVSOFT by comparing these pressures to the derivative of the aortic pressure. The end of isovolumic contraction was assumed to occur at the local minimum of the corrected aortic pressure and the end of IVR was arbitrarily defined as the time at which LV pressure was 5 mm Hg greater than the preceding ED pressure Raff and Glantz, 1981). For the sake of analysis, data at each of the points defined above were meaned from many dogs, as they were clearly definable in each animal. Means were also calculated at the point of maximal untwist (during IVC), maximal twist (during ejection), peak LV pressure (mid-ejection) and during the diastolic filling phase (i.e., from the end of IVR to ED) which was divided into 3 periods of equal duration.

The raw signal of apex-rotation was converted into degrees using Equation (1) given above. An apex-angle of 0° was defined as the position at ED of the baseline cycles preceding an intervention for a particular run (average ED LV pressure of $7 \pm 3$ mm Hg). Apex-rotation in the counter-clockwise direction (as observed from the apex) was expressed as a negative change.

LV area index was calculated from diameter measurements by :

$$\text{LV Area Index} = \pi\,(D_1/2)(D_2/2) \qquad (2)$$

Pressure--apex-rotation, apex-rotation--LV-area-index, and apex-rotation--

segment-length relations were analyzed. Pressure--apex-rotation loops were averaged and compared for 8 dogs under baseline conditions. These were obtained by finding the mean pressure and apex-rotation values at the times during the cardiac cycle as defined above (as seen in Table 2.1). The mean values were plotted as a continuous loop. A Student's t-test was performed to determine significance of differences between the mean loops at the given time events.

## 2.4 Results

### 2.4.1 Dynamics of Apex-Rotation

Fig. 2.4 shows the dynamics of apex-rotation throughout a cardiac cycle together with LV pressure and LV segment length. Apex position at ED was defined to be 0°. Note the initial untwisting (defined as positive apex-rotation) immediately after ED, followed by twisting during ejection and rapid untwisting during the IVR period. The results from 8 dogs are summarized in Table 2.1. An initial untwist of $3.6 \pm 2.2°$ occurs during the initial part of the isovolumic contraction (IVC) period, confirming the results of others (Hansen et al., 1987; Ingels et al., 1989; Yun et al., 1991;). The LV then begins to twist during the IVC period (to approximately 0° by the end of IVC), and continues during ejection, to a maximal twist of $-15.0° \pm 3.2°$, with almost all of the twist occurring in the first 2/3 of the ejection phase. Under baseline conditions, maximal twist was reached before ES in all dogs. This is followed by rapid untwisting during the IVR period

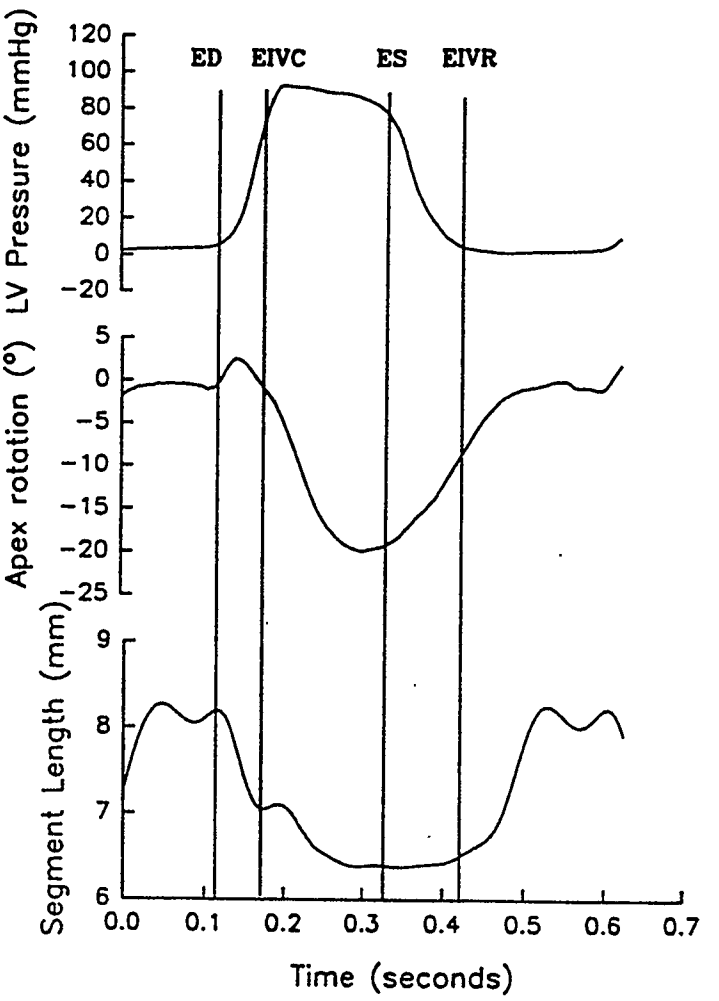


**Figure 2.4:** A typical on-line recording of LV pressure, apical rotation, and segment length through one cardiac cycle. Vertical lines mark end diastole (ED), the end of isovolumic contraction (EIVC), end systole (ES), and the end of isovolumic relaxation (EIVR).

**Table 2.1** - Mean values of LV pressure and LV apex-rotation obtained from 8 dogs under control conditions. Standard Errors are shown. Apex-rotation is arbitrarily set at 0° at end diastole.

| Point in Cycle | LV Pressure (mmHg) | LV Apex-Rotation (°) |
|---|---|---|
| End Diastole | 7.2±4.0 | 0.0±0.0 |
| Maximal Untwist | 21.0±9.2 | 3.6±2.2 |
| End Isovolumic Contraction | 89.6±16.3 | 0.3±5.4 |
| 1/3 Ejection | 116.4±11.8 | -8.8±3.6 |
| 2/3 Ejection | 123.1±17.3 | -14.3±3.2 |
| Maximal Twist | 101.7±18.0 | -15.0±3.3 |
| End Systole | 91.8±16.6 | -12.7±3.2 |
| End Isovolumic Relaxation | 13.4±3.6 | -7.3±2.7 |
| 1/3 Diastolic Filling | 6.5±3.1 | -0.8±2.0 |
| 2/3 Diastolic Filling | 7.3±3.3 | -0.5±1.8 |
| End Diastole | 9.1±3.8 | 0.1±0.1 |

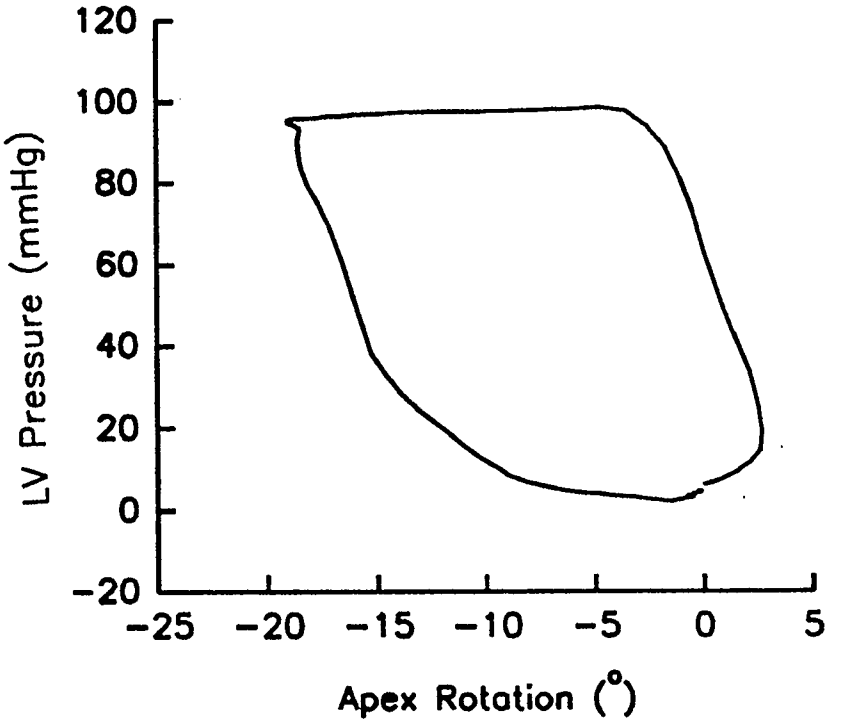


**Figure 2.5:** A typical example of a pressure--apex-rotation loop. ED is arbitrarily set at 0°. The direction of the loop is counter-clockwise.

to -7.3±2.7° by the end of IVR (accounting for almost half of the total untwist). Most of the untwisting (92±10%) is complete before the end of the first 1/3 of diastolic filling (Table 2.1). This results in a plateau in the twist signal in late diastole.

The data was then plotted in terms of an LV pressure--apex-rotation loop (Fig. 2.5). As seen in this example, there is a large change in apex-rotation during ejection, with very little change in pressure. During IVR, both LV pressure and apex-rotation are changing rapidly. The mean values obtained at 11 interval points were then plotted as a mean LV pressure--apex-rotation loop (Fig. 2.6). These baseline loops will be used in later chapters as a control to compare the effects of interventions such as load.

### 2.4.2 Rotation of the Base

A time plot of base-rotation is shown in Figure 2.7, (along with LV pressure). Base position at ED was also defined to be 0°. During the isovolumic contraction period, the base showed a counter-clockwise rotation (twist) to a maximum of -1.3±0.9°, then began to rotate clockwise (untwist), reaching -0.5±0.6° by the end of isovolumic contraction. At ES, the base had untwisted to 1.0±0.8°. A maximum untwist of 1.8±0.3° was reached in the initial portion of IVR. It is interesting to note that the maximal rotation (untwist) of the base occurred after ES (during IVR) rather than during ejection as seen with apex-

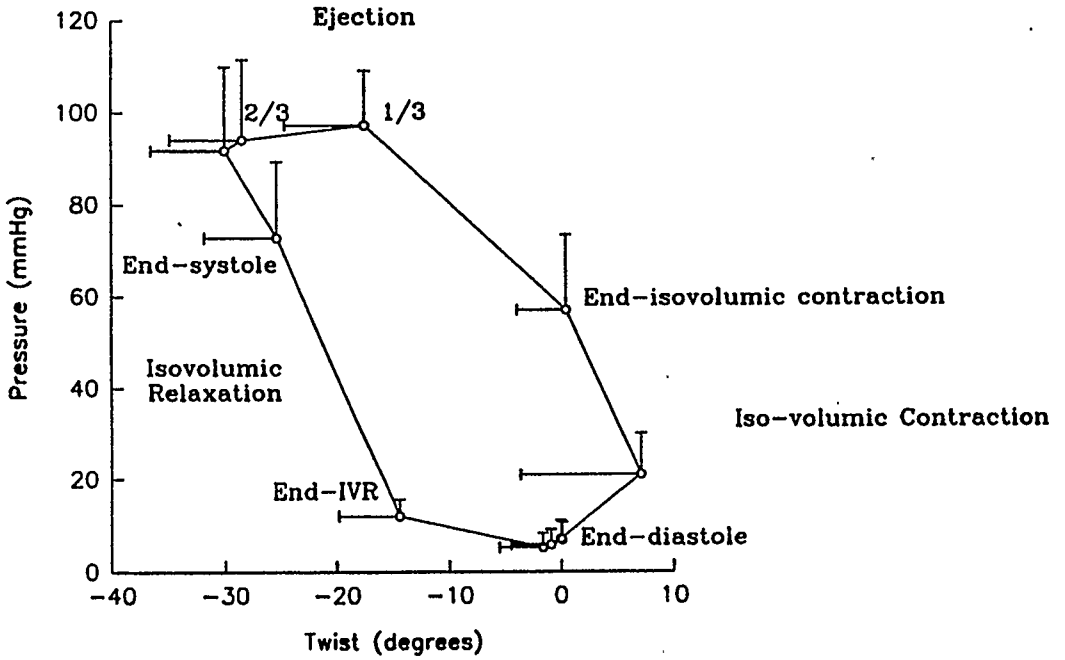


**Figure 2.6**: A mean pressure--apex-rotation loop made from mean data at intervals shown in Table 2.1. End diastole (ED) and end systole (ES) are shown, as well as the end of isovolumic relaxation (EIVR) and the end of isovolumic contraction (EIVC). For the sake of analysis, ejection and diastolic filling were divided into 3 equal time periods. Standard errors are shown.

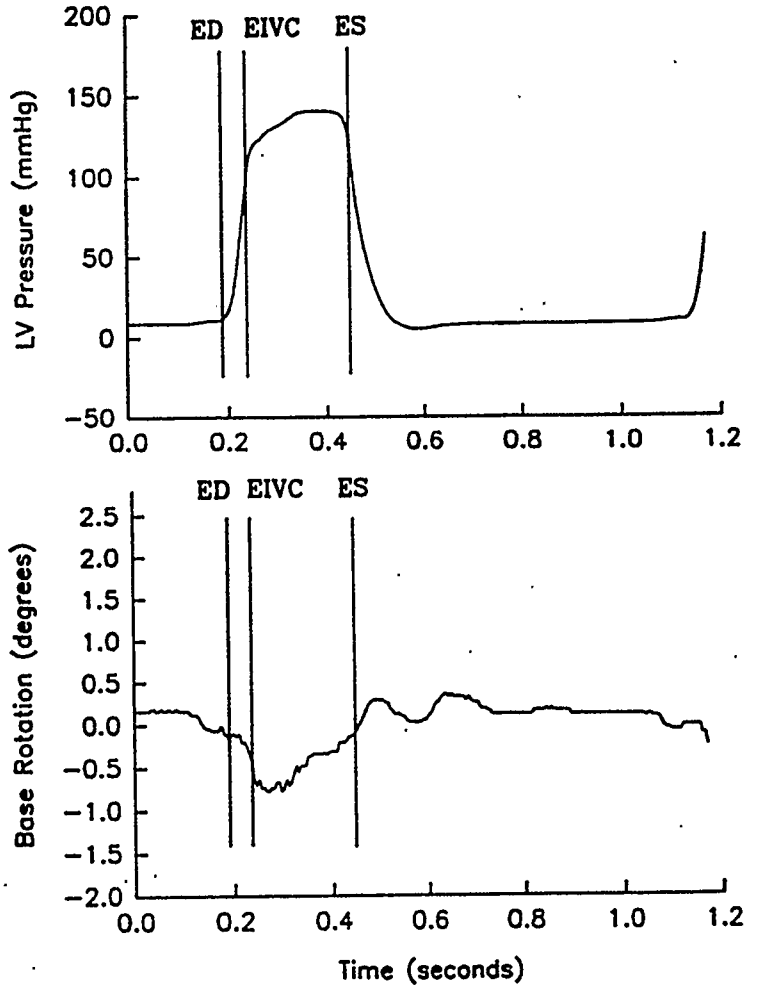


**Figure 2.7:** A typical on-line recording of LV pressure and base-rotation through 1 cardiac cycle. Vertical lines mark end diastole (ED), end systole (ES), and the end of isovolumic contraction (EIVC).

rotation. It should also be noted that, during periods when the apex twisted, the base untwisted, and vice versa. This would indicate that the measure of apex-rotation is a slight underestimation of total LV twist. The relatively small magnitude of base-rotation supports the claim that apex-rotation is a good indicator of LV twist.

### 2.4.3 The Twist-Shortening Relationship

It can be seen in Figure 2.4 that the segment-length signal is very similar in shape to the apex-rotation signal. Apex-rotation was plotted against fractional shortening of a midwall circumferential segment signal (Fig. 2.8). During ejection, it can be seen that the relationship is linear, indicating that apex-rotation and fractional shortening are directly proportional during this period. During diastole, this relationship becomes uncoupled (no longer linear). In IVR, while rapid untwisting is occurring, the relationship is linear with a very steep slope. These linear relationships are shown in Fig. 2.9 by plotting apex-rotation--segment-length points from 8 dogs for the twisting phase (part of isovolumic contraction and ejection) and IVR only. Again, the slope during IVR is much steeper than seen during the twisting phase. In the twisting phase, the mean slope was -119 $\pm$ 47, while during IVR, the mean slope was -461$\pm$205. During the filling period, the relationship is much flatter (very little untwisting occurring with lengthening). This twist-shortening pattern supports results by Beyar et al. (1989) and Moon et al. (1994).

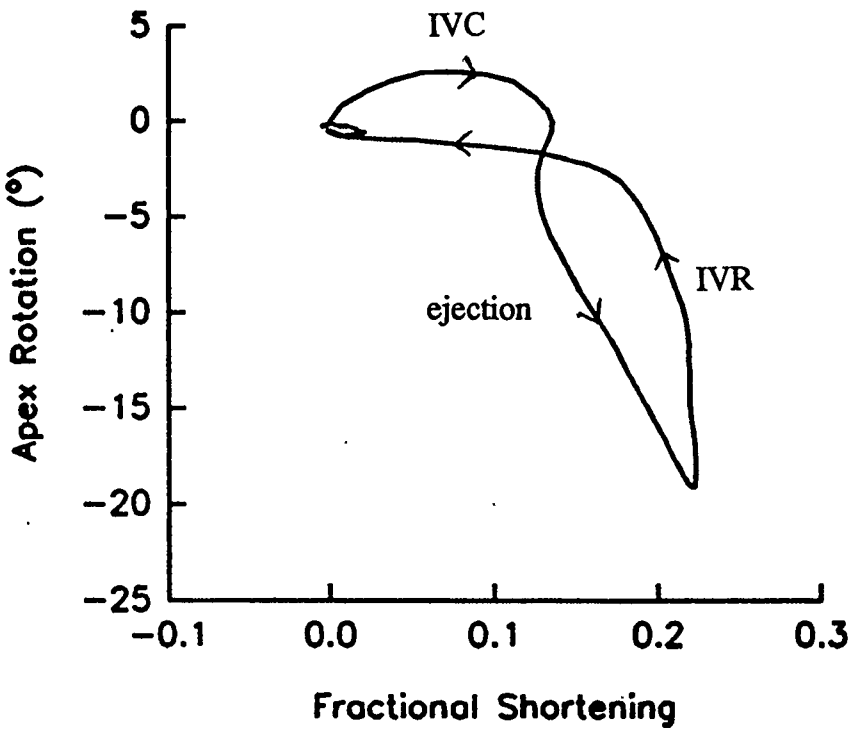


**Figure 2.8**: A typical example of an apex-rotation--fractional shortening loop from one dog. End diastole is set at 0°. Arrows indicate the direction of the loop.

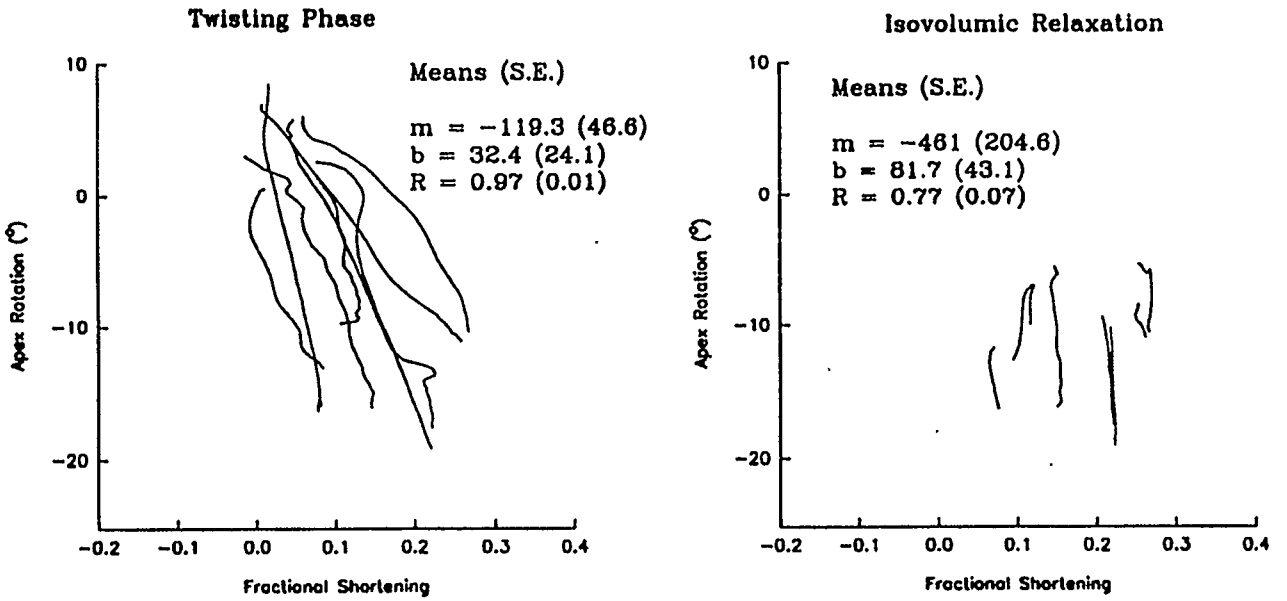


**Figure 2.9**: Apex-rotation--fractional shortening data from 8 dogs shown through (a) the twisting phase (from maximal untwist to maximal twist), and (b) isovolumic relaxation. The regressions from these lines were then meaned and the mean values shown.

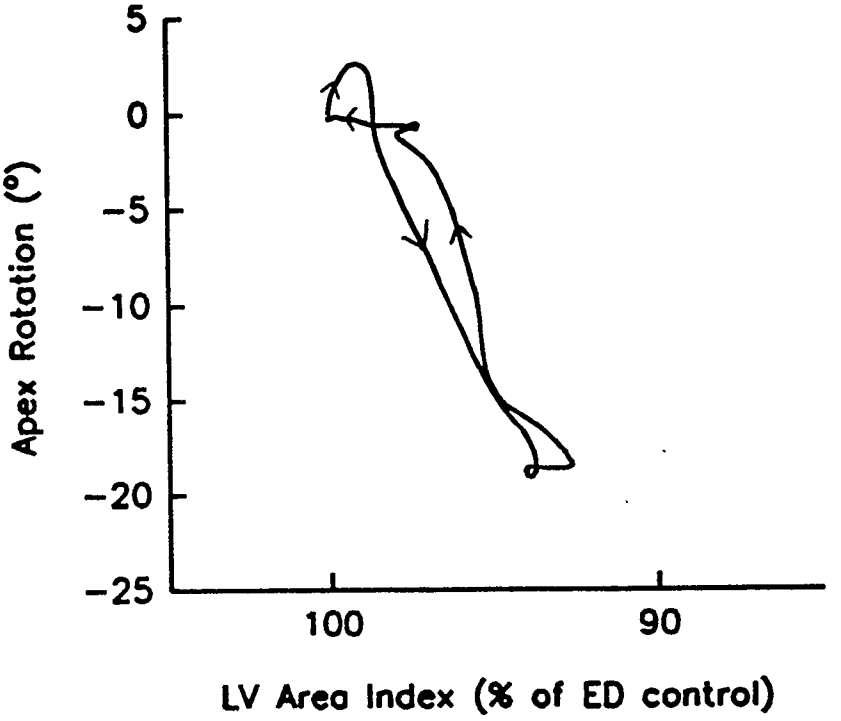


**Figure 2.10:** A typical example of an apex-rotation--area-index loop shown from one dog. End diastole is set at 0°. Arrows indicate the direction of the loop.

Apex-rotation was also plotted against LV area index (calculated as a percent of the ED value). An example from one dog is shown in Fig. 2.10. This relationship was also seen to be linear during the ejection period, and remained relatively linear during diastole, in contrast to the twist-shortening relationship.

## 2.5 Discussion

In this chapter, a device has been described which measures the apex-rotation dynamically. It provides an on-line output, allowing apex-rotation to be related precisely and accurately to haemodynamic parameters. Similar to what has been shown previously with more labourious non-invasive methods (Arts et al., 1984; Beyar et al., 1989; Hansen et al., 1987; Waldman et al., 1988), it was demonstrated that the apex of the LV continuously rotates during isovolumic contraction and ejection, and untwists rapidly during the IVR. It was also shown that there is an initial rapid untwisting during isovolumic contraction period, verifying previous findings (Ingels et al., 1989; Yun et al., 1991).

### 2.5.1 The optical device

The major rationale to use such an approach measuring apex-rotation only is based on the observation that the amount of rotation at different ventricular levels has been shown to increase from base to apex and that the base of the heart rotates only minimally (Beyar et al., 1989; Buchalter et al., 1990). Measurements of base-

rotation (Fig. 2.7) indicate that the apex-rotation measurements found with this device may underestimate absolute LV twist by no more than 1 to 2°. Therefore, absolute measurements of the apex-rotation provide valuable information regarding the dynamics and magnitude of the torsional deformation of the left ventricle. The device is unique relative to the other methods in its ability to provide an on-line signal representing the dynamics of torsion, and therefore, the results of different interventions can easily be assessed during the experiment and simply analyzed afterward. The other methods (i.e., multiple markers, MRI, or echocardiography) require different modalities of image analysis that are complex and do not provide on-line analysis. In addition, methods such as biplane cineradiography using multiple-marker tagging (Hansen et al., 1991) that have been used to study load interventions were limited to steady-state interventions and, because of ethical considerations, could not be used to study the dynamics of transient perturbations, such as load interventions (Chapter 3). This device should also be valuable in the study of coronary occlusions (Chapter 5). The frequency response of the mechanical components of this device (i.e., flat to 100 Hz) makes it theoretically superior to other approaches, which are limited by a slower image frame rate.

### 2.5.2 The Dynamics of Apex-rotation

The apex-rotation values reported were slightly higher than previously reported by other methods in dogs (Arts and Reneman, 1980; Rademakers et al., 1992) and in humans (Hansen et al., 1987; Hansen et al., 1988; Ingels et al., 1989.

The greater systolic twist seen in these experiments ($15 \pm 3°$) as compared to that observed using biplane cineradiography ($13.3 \pm 6.0°$)(Hansen et al., 1988) and that using magnetic resonance imaging techniques ($11.2 \pm 1.3°$)(Buchalter et al., 1990) may be due to the fact the present measurements of rotation are made at the apex, where it is maximal, rather than at a position near the apex. In fact, it has been predicted using a mechanical model of the LV (Azhari et al., 1992) that twist increases towards the apex in a non-linear fashion. This method serves to confirm results found by more labourious non-invasive techniques.

It has long been recognized that the twisting motion of the heart about its long axis results from the distribution of the helically oriented muscle fibres that vary in angle across the LV wall (Lower, 1669 in Gunther, 1932; Streeter et al., 1969; Streeter, 1979). The torsional moments generated by the muscle fibres result in the observed torsional deformation. Throughout ejection, epicardial moments dominate those of the endocardium (Azhari et al., 1992; Ingels et al., 1989) and the LV twists in a counterclockwise direction, as viewed from the apex. However, since activation of the endocardium occurs first (Durrer et al., 1970), during the initial part of the isovolumic contraction, the moments contributed by endocardial fibres predominate and should cause untwist (Yun et al., 1991).

In this study a consistent rapid untwisting during the IVR period ($40 \pm 17\%$ of total untwist) was observed. This result is in agreement with Beyar et al. (1989) and with Rademakers et al. (1992) who measured the twist using information from

the entire ventricle (48±20% and 44% of total untwist during IVR, respectively). The latter authors found that this untwist was markedly faster and larger with the use of catecholamines. This may an effect of activation patterns on fibre moments. The epicardial fibres are inactivated before the endocardial fibres during IVR. This produces decreased "twisting" moments while "untwisting" moments still remain. This would result in rapid untwisting during the IVR period. As discussed in Chapter 1, early diastolic filling is dependent on myofilament relaxation, left atrial pressure and passive left ventricular compliance. Twist, or torsional deformation of the left ventricle, may be associated with storage of elastic energy in some of the myocardial passive elements. With the rapid fall in active force during myocardial relaxation, this elastic energy is released and leads to rapid untwisting. This may suggest that the rapid diastolic untwisting is a reflection of the effectiveness of the relaxation process and also that rapid untwisting and rapid filling are tightly linked.

A twist-shortening relationship has been shown under control conditions, verifying previous results (Beyar et al., 1989; Moon et al., 1994) and again, showing apex-rotation to be a reliable index of LV twist. A linear relationship was shown between twist and shortening during ejection and during IVR (the latter being a much steeper relation). The effects of interventions such as load or ischemia may affect these relationships by changing the balance of moments that determine them.

Much of the apex-rotation data in the following chapters will be presented in the form of LV pressure--apex-rotation loops, similar to the often-used pressure-

length or pressure-volume loops. The latter are well-accepted and are a simple way to express the correlation between segment-length or volume and LV pressure. From Fig. 2.5, apex-rotation and segment-length and volume appear to be related and, thus, it would be appropriate to plot apex-rotation in a similar manner. Further, this method allows for beat-to-beat shifts in apex-rotation with interventions to be easily seen. Baseline data established in this chapter will be used as a comparison control when studying the effects of load (Chapter 3), contractility (Chapter 4), and ischemia (Chapter 5).

### 2.5.3 Summary

In conclusion, an on-line device that produces a continuous analog signal and measures the dynamics of apex-rotation was developed and used in dogs. Confirming previous observations, an initial untwisting during the beginning of the isovolumic contraction period was shown, with twisting during the remainder of isovolumic contraction and ejection, and rapid untwisting during the IVR period. Using this relatively simple methodology, the effects of load manipulation, contractility, and heart rate on the dynamics of apex-rotation can now be characterized. This methodology can also be used to study interventions of clinical importance such as ischemia. The method may be limited, however, by the fact that the procedure is invasive (to have an unimpeded connection between the apex and device requires a large, wide opening). It is known that the apex-rotation values

obtained by this method are a slight underestimation of LV torsion since base-rotation is not measured simultaneously.

# Chapter 3

# THE EFFECTS OF PRELOAD ON APEX-ROTATION

## 3.1 Abstract

The effects of preload on LV torsion in 12 open-chest dogs was studied using the optical device discussed in Chapter 2. The advantage of this method is the ability to measure dynamic changes accurately throughout the cardiac cycle, even with large preload changes. Using results from venae cavae (VC) occlusion and volume loading, a linear ED relationship between apex-rotation and normalized LV area index was established (slope = $0.61 \pm 0.06$, intercept = $-132 \pm 24.9$, $n=10$) which was different from the ES relationship (slope = $1.36 \pm 0.27$, intercept = $-60.1 \pm 6.2$; $p<0.005$). Venae cavae occlusion (preload and afterload decrease) caused a slight increase in amplitude of apex-rotation, with maximal apex-rotation occurring earlier in the cycle. In contrast, acute volume loading caused a small decrease in apex-rotation amplitude and twist relaxation was delayed into the IVR period. A twist-shortening relationship is shown which is linear during the twisting phase and linear (but with a steeper slope) during IVR. The relationship during

twisting is essentially unaffected by preload changes, but delayed untwisting with volume loading appeared to affect the relationship during IVR. In summary, LV twist at both ED and ES is primarily a function of volume. A decrease in preload caused early untwisting, while preload increases caused delayed untwisting. The optical device has been shown to be a useful tool in the study of dynamic changes with load interventions.

## 3.2 Introduction

As discussed in Chapter 2, an optical measuring device has been designed which allows for the dynamic measurement of apex-rotation throughout the cardiac cycle. The advantages of the current on-line system are the ability to directly and continuously relate apex-rotation to simultaneous haemodynamic parameters and to characterize the dynamics of twist during interventions such as preload changes.

Because twist is directly related to fibre shortening and is a function of the balance of moments between muscle fibres (Ingels et al., 1989), a twist-shortening relationship may exist. Beyar et al. (1989) have shown that twist and shortening are directly related during ejection, but become uncoupled during relaxation. Yun et al. (1991) and Moon et al. (1994) have confirmed these results. Because fibre shortening is affected during preload changes, the twist-shortening relationship may also be affected.

Since LV volume and fibre shortening are closely related, a relationship may

also exist between LV volume (as measured by the minor-axis index of cross-sectional area) and twist. ED and ES LV volume is dependent on preload and fibre shortening. Thus, by changing preload, it may be possible to establish a relationship between apex-rotation and LV volume using this device.

Load dependency of ventricular twist is controversial. Some studies (Hansen et al. 1991) seem to imply that LV torsion is essentially unaffected by changes in preload or afterload. Moon et al. (1994) also suggested that systolic LV twist is unaffected by pressure and volume loading in human patients, but found that early diastolic untwisting (elastic recoil) was decreased with volume loading. These studies would indicate that LV volume is not an important factor determining LV twist. These methods, however, do not allow for a shift in ED angular rotation to be observed, since they arbitrarily set this point to be zero at the onset of each cycle. Although, these methods allow for the amplitude of twist to be measured throughout the cycle, a comparison of successive cycles cannot be made adequately. The use of the optical device for measuring apex-rotation provides a way to describe LV twist throughout the cardiac cycle, and the effects of changing preload on twist dynamics.

The aim of this chapter was, therefore, to establish a possible relationship between apex-rotation and LV volume for both the active (systole) and passive (diastole) states, by changing preload. Furthermore, the dynamics of apex-rotation over a wide range of preload conditions will be studied, utilizing the advantages of

the optical device. The twist-shortening relationship and the effects of changing preload will also be examined. Venae caval occlusion and volume-loading are imposed in the open-chest canine model and apex-rotation was measured continuously.

## 3.3 Methods

Experiments were performed to study the effects of changing preload on 12 open-chest, anaesthetized dogs. As well as measuring apex-rotation, the effects on base-rotation of volume loading (3 dogs) and venae caval occlusion (8 dogs) were also noted. Animal preparation and the use of the optical device is fully described in Chapter 2. In addition to this outlined procedure, 12- to 16-mm pneumatic occluders (IVM, Healdsburg, California) were placed around the superior and inferior venae cavae to transiently reduce preload when inflated.

A calibration run was performed at the beginning of the experiment to determine the relation of output voltage to a known distance on the diode. This calibration was checked several times throughout the experiment to correct for possible slow baseline shifts. These changes were found to be insignificant. The pressure--apex-rotation loops, LV and aortic pressures, as well as the segment-lengths were monitored throughout the experiment. A recording interval lasted 60 sec. After each intervention, time was allowed for the haemodynamic parameters to return to baseline conditions.

To study the effects of reduced LV preload, the superior and inferior venae cavae were transiently occluded to impede venous return to the heart. Only the first 20 beats were analyzed to minimize the effects of reflex changes. Recordings of apex- and base-rotation were obtained under reduced LV preload conditions.

To study the effects of increased LV preload, volume loading was performed. Saline was added at a rate of 500 mL/min through a catheter in the jugular vein into the superior venae cava until the LV ED pressure reached 15 mm Hg. The volume infusion usually lasted approximately 40 sec. In three dogs, base-rotation was also measured during volume loading. Venous blood was withdrawn to return the dog to normal haemodynamic conditions.

Pressure--apex-rotation, pressure--segment-length, and apex-rotation--LV area-index relationships were analyzed. Average loops for 9 dogs were compared under baseline and intervention conditions. Averages (mean $\pm$ SE) were obtained by finding the mean pressure and apex-rotation values at the times during the cardiac cycle as defined in Chapter 2. The mean points were then plotted as a continuous loop. A Student's t-test was performed to determine the significance of differences in rotation at specific times in the cardiac cycle between control and intervention conditions. The p-values were uncorrected for multiple comparisons and were used for descriptive purposes rather than for the purpose of confirmation.

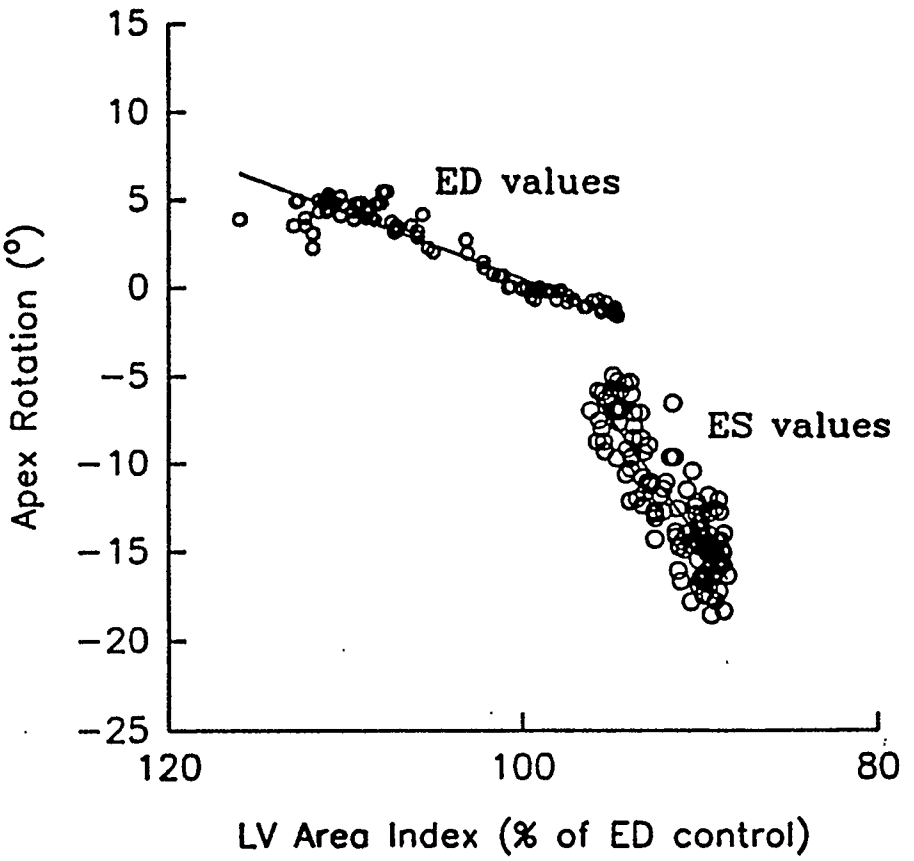


**Figure 3.1** - A scatter plot showing end diastolic and end systolic points from one dog during a vena caval occlusion and a volume load. Regression lines are shown for end diastole and end systole.

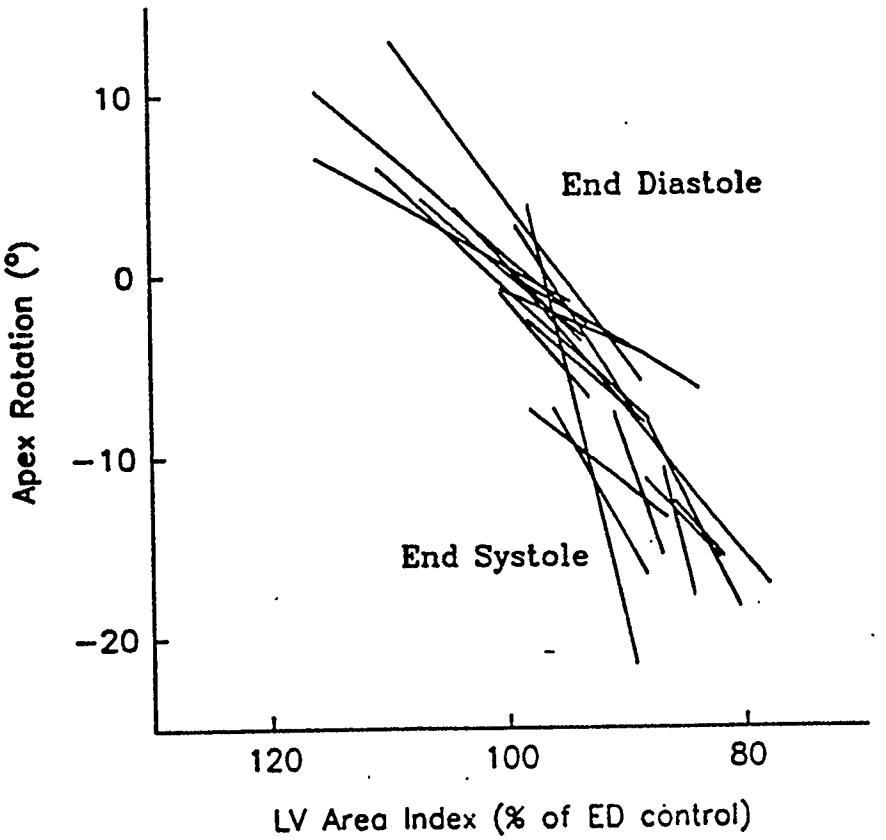


**Figure 3.2** - A plot showing end-diastolic and end-systolic regression lines from vena caval occlusion and volume loading from 10 dogs. The regressions slopes and intercepts were then meaned and compared for significant differences.

## 3.4 Results

### 3.4.1 The Twist-Volume Relationship

Preload was decreased by performing a transient venae caval occlusion (VCO) and increased by volume loading in 11 dogs. With decreased preload, ED volume decreased and apex-rotation values became more negative, indicating that the LV was in a more twisted state. With volume loading, ED volume increased and apex-rotation values became more positive, indicating that the LV was less twisted at ED. When ED apex-rotation values were plotted against normalized LV area-index values (assuming control values at ED to be 100%), a linear relationship was observed (Fig. 3.1). For 10 dogs, the mean value of the slope (m) of the regression lines at ED was $0.61 \pm 0.06$, while the y-intercept (b) was $-60.1 \pm 6.2$ and the R-value was 0.28 (Fig. 3.2). When ES values were plotted in the same fashion, a different relationship was observed (Fig. 3.1), with a mean slope calculated from the regressions lines of $1.36 \pm 0.27$ and a y-intercept of $132.5 \pm 24.9$ (Fig. 3.2).

When multiple comparison tests were performed, these values are significantly different from those found at ED ($p < 0.03$). Significantly different slopes were again obtained for ED and ES even when the x- and y- axes were reversed (to account for regression assumption of error in the y-direction only). Significant differences were also noted between end-diastolic and end-systolic relationships when individual dogs were studied.

**Table 3.1** - Standard haemodynamic parameters averaged for animal groups under control, VC occlusion, and volume loading conditions.

| Parameters | Control | VC Occ. | Control | Volume |
|---|---|---|---|---|
| Heart Rate | 108±34 | 116±30 | 90±14 | 102±13 |
| End-diastolic Aortic pressure | 67±16 | 44±12 | 57±5 | 66±6 |
| End-systolic Aortic pressure | 87±20 | 49±14 | 83±4 | 78±5 |
| End-diastolic LV area index | 2400±320 | 2160±250 | 2272±113 | 2611±220 |
| End-systolic LV area index | 2080±370 | 2010±240 | 2034±93 | 2299±156 |
| End-diastolic Segment length | 11.2±0.6 | 9.2±0.7 | 10.1±0.9 | 10.8±0.9 |
| End-systolic Segment length | 10.0±0.6 | 9.0±0.7 | 8.9±0.9 | 9.0±0.9 |

Data is meaned from dogs used in each intervention group. Standard errors are shown. VC occlusion is abbreviated as VC Occ. The volume loading intervention is indicated as volume.

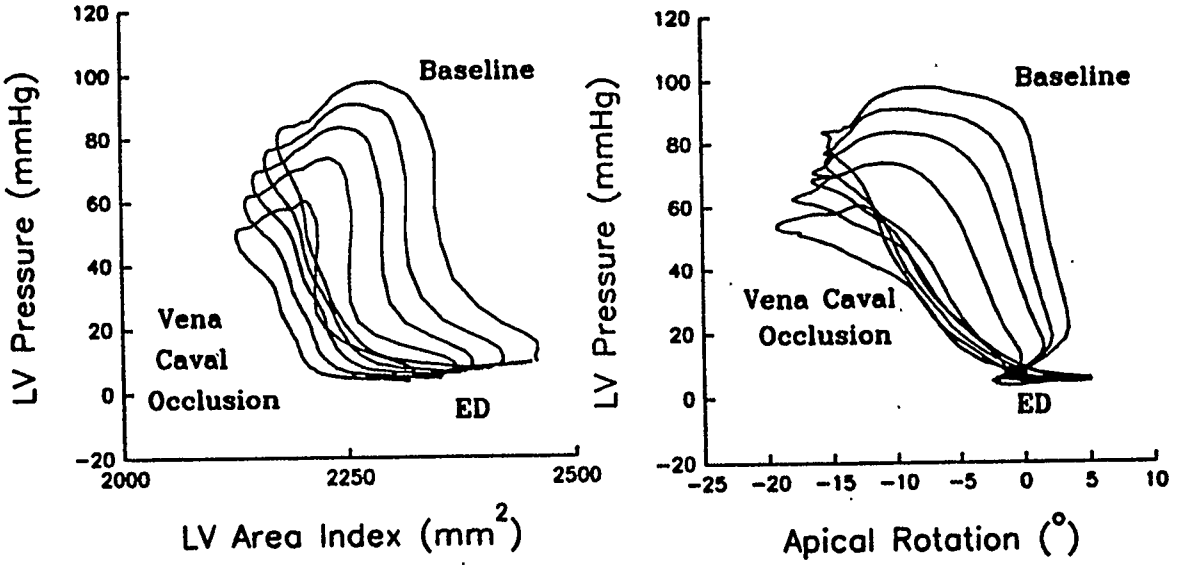


**Figure 3.3**: Typical LV pressure-area loops (left) and LV pressure-apical rotation loops (right) shown for a baseline cycle and during venal caval occlusion (every fourth beat is shown, up to the 20th beat of occlusion). ED marks end diastole.

### 3.4.2 The Effects of Venae Caval Occlusion on Apex-Rotation

Preload was decreased by a transient occlusion of both the superior and inferior venae cavae. This acute preload decrease is associated with secondary reduction in aortic pressure as well, and cannot be considered as a pure preload intervention (Table 3.1). During the first 20 beats of the occlusion, there was an increase in heart rate of only 6.4±4.5% (Table 3.1), suggesting that reflex-mediated increases in contractility were trivial. The LV pressure--apex-rotation relationship as well as the LV pressure--area-index relationship during the first 20 beats of occlusion are shown in Fig. 3.3. The LV pressure--apex-rotation loops gradually shifted leftward and became more diagnonally oriented. Mean values for 8 dogs were calculated at 10 intervals throughout the cycle (Table 3.2) and used to form mean pressure--apex-rotation loops seen in Fig. 3.4. With reduced load, we noted a leftward shift of the pressure--apex-rotation loops (ED apex-rotation values of -2.6±7.0° compared to control values of 0°). ED apex-rotation values were more negative (LV more twisted at ED) with VC occlusion as a direct result of decreased LV volume as shown in section 3.3.1. During isovolumic contraction, maximal untwist was reached earlier with VC occlusion, with more twisting then able to occur in this period. A greater fraction of the total twist occurred during isovolumic contraction with VC occlusion (46% vs. 20% for control; $P<0.05$).

Maximal apex-rotation occurred earlier in the ejection phase and was increased to -17.9±4.0°. During VC occlusion, a greater fraction of the untwisting

**Table 3.2** - Mean apex-rotation and LV pressure values at different phases throughout the cardiac cycle for baseline and VC occlusion-conditions for 8 dogs.

| Point in Cycle | Baseline Apex-Rotation | Baseline LV pressure | VC Occ. Apex-Rotation | VC Occ. LV Pressure |
|---|---|---|---|---|
| End diastole | 0.0±0.0 | 7.2±4.0 | -2.6±7.0 | 3.5±2.7 |
| Maximal untwist | 3.6±2.2 | 21.0±9.2 | 0.9±4.4 | 6.7±1.8 |
| End isovolumic contraction | 0.3±5.4 | 89.6±16.3 | -7.6±2.3 | 38.1±12.2 |
| 1/3 ejection | -8.8±3.6 | 116.4±11.8 | -15.6±2.0 | 66.7±15.3 |
| 2/3 ejection | -14.3±3.2 | 123.1±17.3 | -16.8±4.1 | 63.2±16.4 |
| Maximal twist | -15.0±3.3 | 101.7±18.0 | -17.9±4.0 | 62.0±15.2 |
| End systole | -12.7±3.2 | 91.8±16.6 | -13.6±5.6 | 44.8±12.0 |
| End isovolumic relaxation | -7.3±2.7 | 13.4±3.6 | -5.7±4.3 | 8.4±3.3 |
| 1/3 diastolic filling | -0.8±2.0 | 6.5±3.1 | -0.5±4.3 | 2.6±3.0 |
| 2/3 diastolic filling | -0.5±1.8 | 7.3±3.3 | -1.4±3.0 | 2.7±3.0 |
| Subsequent end diastole | 0.1±0.1 | 9.1±3.8 | -1.5±3.6 | 3.6±2.7 |

Values are means ± standard errors for 8 dogs and are expressed in degrees. End diastole is defined as 0° rotation. VC occlusion is marked as VC Occ. and represents the 20th beat into the intervention.

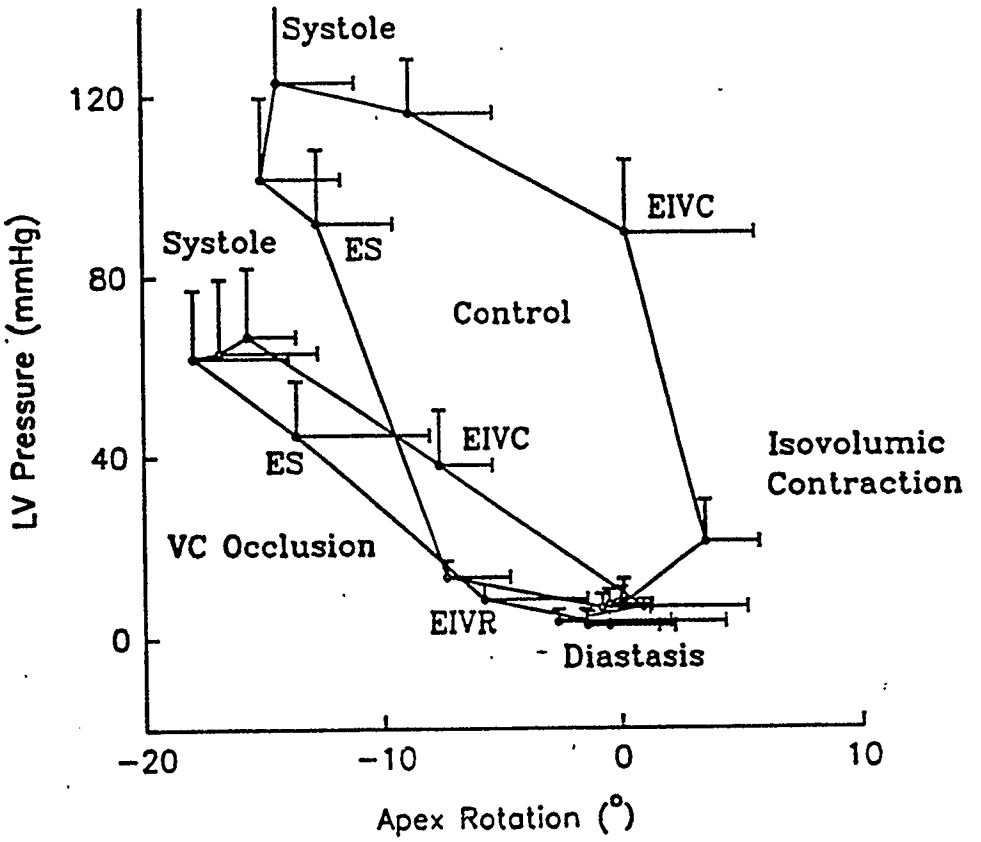


**Figure 3.4** - A mean plot of pressure--apex-rotation under control conditions and for venae caval occlusion (after 20 beats). Means are obtained at 11 points through the cycle, with these points connected to make the loops. Standard errors are indicated. End of isovolumic contraction and relaxation are indicated by EIVC and EIVR respectively. End systole and end diastole are shown by ES and ED, respectively. n=8.

occurred before the end of IVR than was seen under control conditions (76% vs. 55% for control, $P<0.05$). More apex-rotation was occurring during the isovolumic contraction period and more of the untwist was occurring in the IVR period, resulting in the pressure--apex-rotation loop with VC occlusion being more diagonally-oriented (Fig. 3.4). During diastolic filling, the LV appears to untwist early and then twist again (overshoot). This may be a result of still-activated endocardial fibres shortening to produce untwist.

Base-rotation also changed during VC occlusion in 8 dogs. The LV pressure--base-rotation loops were seen to shift rightward. The amplitude of base-rotation decreased slightly under these conditions, and the maximal untwist was seen to occur earlier in ejection. Again, because base-rotation amplitudes were small (approximately 1-1.3°), measurements of apex-rotation were a reasonable index of LV twist (although a slight underestimation).

Because measurements of base-rotation during VC occlusion show a rightward shift of the loops, while apex-rotation showed a leftward shift, there is not a rotation of the LV as a whole during VC occlusion, but a change in its "twist state" at ED.

### 3.4.3 The Effects of Volume Loading on Apex-Rotation

LV preload was increased by volume-loading in 8 mongrel dogs. A 10% increase in volume at 25 sec of volume infusion and more than a 25% increase after

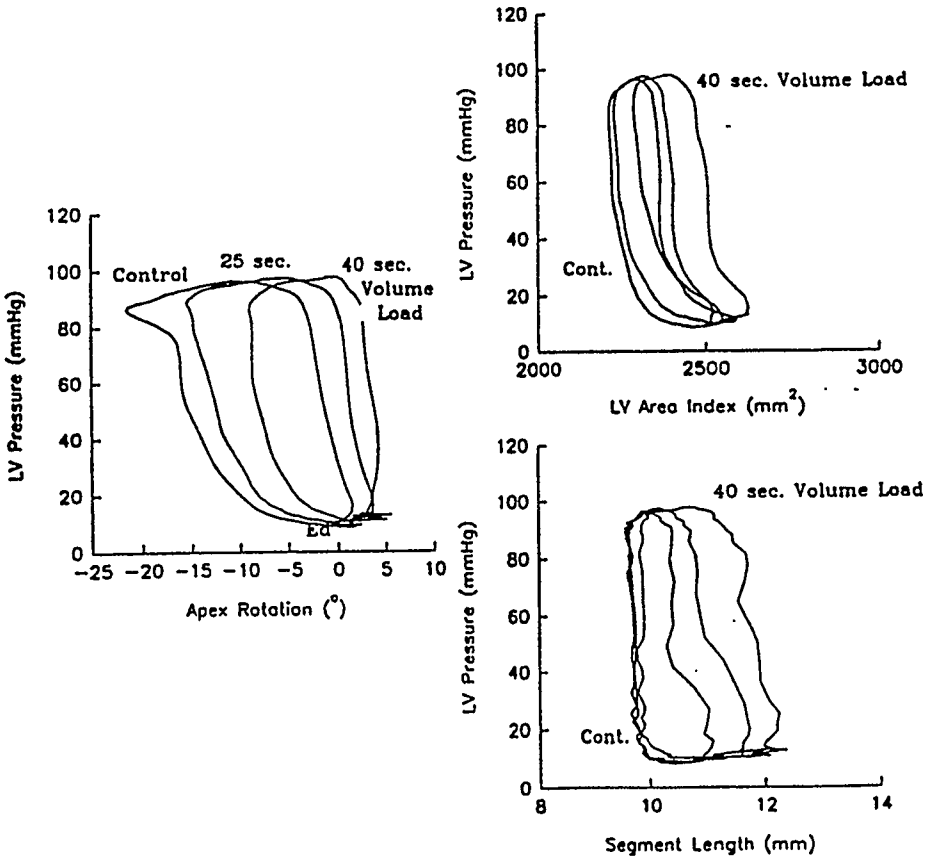


**Figure 3.5** - A typical on-line recording from one dog of LV pressure, apex-rotation, LV area index, and segment length during a volume loading intervention. Data is presented in the form of pressure-apex-rotation, pressure-area, and pressure-length loops. Loops (cycles) are shown for control, after 25 sec of volume infusion, and after 40 sec of volume infusion.

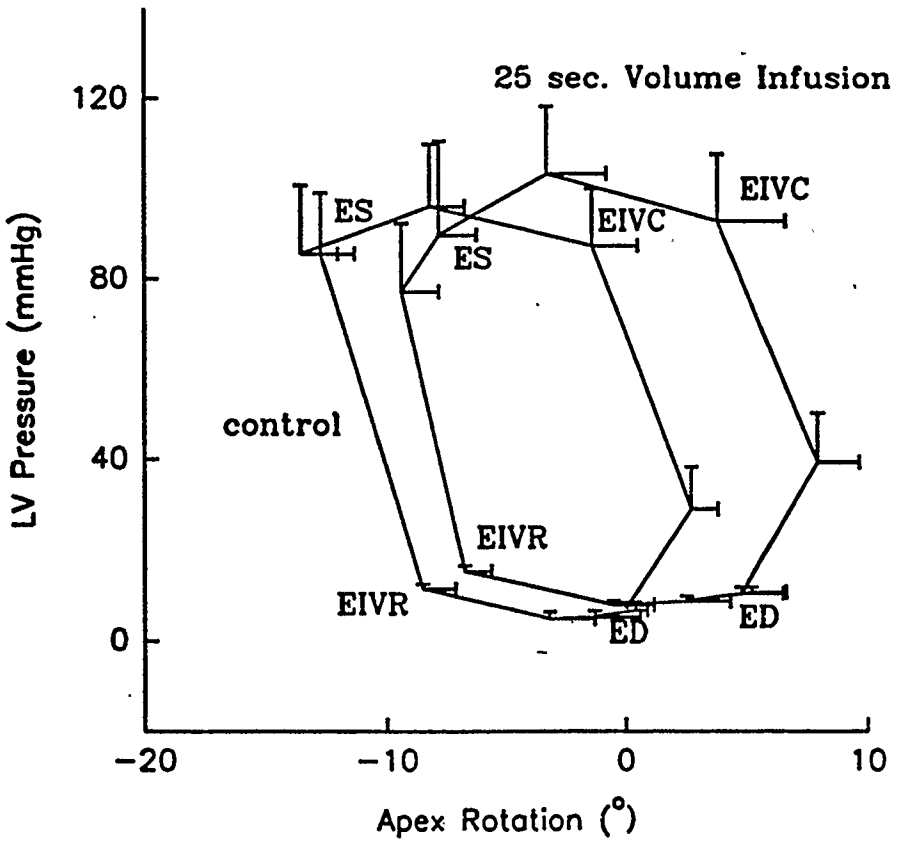


**Figure 3.6** - A mean plot of pressure-apex-rotation during a volume infusion. One loop shows control conditions, and the other is after 25 seconds of volume infusion. Points are obtained by meaning values at 11 set points in the cycle. These points are connected to show mean loops. n=8. Other abbreviations as in Figure 3.4.

**Table 3.3** - Mean apex-rotation and LV pressure values at different phases throughout the cardiac cycle for baseline and volume loading conditions for 8 dogs.

| Point in Cycle | Apex-rotation Baseline | Apex-rotation 25 sec. Volume Load | Apex-rotation 40 sec. Volume Load |
|---|---|---|---|
| End diastole | 0.0±0.0 | 4.9±1.7 | 5.1±1.3 |
| Maximal Untwist | 2.8±1.1 | 8.0±1.7 | 7.7±2.4 |
| End isovolumic Contraction | -1.4±1.9 | 3.9±2.8 | 4.6±2.7 |
| Peak LV pressure | -8.2±1.5 | -3.3±2.5 | -0.4±1.1 |
| Maximal twist | -13.5±1.5 | -9.4±1.6 | -6.3±2.7 |
| End systole | -12.7±1.4 | -7.8±1.6 | -4.2±2.7 |
| End isovolumic Relaxation | -8.5±1.4 | -6.7±1.1 | -3.8±2.4 |
| 1/3 diastolic filling | -3.2±1.9 | -0.5±1.7 | 0.8±1.4 |
| 2/3 diastolic filling | -1.3±0.9 | 2.6±1.8 | 3.1±0.8 |
| End diastole | 0.4±0.5 | 5.3±1.4 | 5.1±1.1 |

| Point in Cycle | LV pressure Baseline | LV pressure 25 sec. Volume Load | LV pressure 40 sec. Volume Load |
|---|---|---|---|
| End diastole | 7.1±1.3 | 10.5±1.3 | 14.2±3.7 |
| Maximal untwist | 29.1±9.2 | 39.4±10.8 | 39.9±9.1 |
| End isovolumic contraction | 87.5±12.7 | 93.0±14.8 | 107.2±28.7 |
| Peak LV pressure | 96.3±13.7 | 103.5±14.8 | 118.9±30.5 |
| Maximal twist | 85.7±15.3 | 72.2±20.8 | 87.0±43.9 |
| End systole | 85.7±13.5 | 89.9±15.3 | 104.9±29.4 |
| End isovolumic relaxation | 11.5±1.1 | 15.4±1.3 | 19.2±4.0 |
| 1/3 diastolic filling | 4.9±1.5 | 7.9±1.0 | 10.9±3.2 |
| 2/3 diastolic filling | 5.3±1.3 | 8.7±1.1 | 11.2±3.1 |
| End diastole | 6.8±1.8 | 10.7±1.1 | 14.2±4.1 |

Means are averaged for 8 dogs and standard errors are shown.

End diastole under baseline conditions is defined as 0°. Volume loading was done by saline infusion into the jugular vein, and values are shown for 25 and 40 sec of infusion.

40 sec of loading was noted in most cases. An example of pressure--apex-rotation and pressure--area-index loops obtained from one dog is shown in Fig. 3.5. Mean values obtained at 10 intervals in the cycle were used to produce a mean pressure--apex-rotation loop shown in Fig. 3.6. The volume-loading resulted in significantly increased ED and peak pressures (Table 3.3). In addition, there was a significant increase in heart rate (Table 3.1). With increased preload, the ED apex-rotation value was seen to increase from 0.0° (control) to 4.9±1.7° at 25 sec of volume loading to 5.1 ± 1.3° at 40 sec ($p<0.02$). This would indicate that volume loading results in a rightward shift of the pressure--apex-rotation loops (Fig 3.6), and again shows the dependence of apex-rotation on LV volume at ED. While the amount of untwist in the isovolumic contraction period remained relatively similar, the increased ED rotation values caused the maximum untwist values during this period to be higher (from 2.8±1.1° control to 7.7±2.4° with volume load $P<0.006$). The maximum apex-rotation during systole was seen to decrease with volume-loading from -13.5±1.5° under control conditions to -9.4±1.6° at 25 sec of volume to -6.3±2.7° at 40 sec of volume ($p<0.003$). In part, this is a result of the rightward shift of the pressure--apex-rotation loops (positive ED apex-rotation values), but the 40-sec volume-load loop shows an overall small, statistically insignificant change in the amplitude of apex-rotation (of approximately 2°). With volume-loading, the maximum apex-rotation occurred during the IVR period (much later than seen with control cycles). With volume loading, only 18% of the untwist

occurred in the IVR period, and only 60% by the end of the first third of diastole (compared to 47% and 76% for the same periods under control conditions). Similar results were seen after 40 sec of volume load. This could be because the maximum apex-rotation occurs after ES, indicating that the apex is still twisting during part of IVR, and that apex-rotation is delayed at high volumes. Because relatively less twist/untwist is occurring in the isovolumic periods, the pressure--apex-rotation loop is less sloped than the control loop (Fig 3.6).

In three dogs, base-rotation was measured during a period of volume loading. The base of the heart rotates clockwise (i.e., untwist) during systole, opposite to the apex-rotation. The ED base-rotation values do not change significantly with volume loading, but do show a trend towards clockwise rotation relative to control. After 40 sec of volume loading, the base of the heart rotates clockwise at ED by only 0.5° relative to the control ED position. At ES, the base of the heart rotates in the clockwise direction one degree more than control. Since the values of base rotation are more than an order of magnitude smaller than apex-rotation, the measured apex-rotation here indeed reflects ventricular twist and torsion.

### 3.4.4 The Twist-Shortening Relationship

With VC occlusion, the shape of the apex-rotation--fractional shortening loop changed very little. There was a small downward and rightward shift of the loops (Fig. 3.7), but the relationship remained linear during ejection and IVR, with slopes

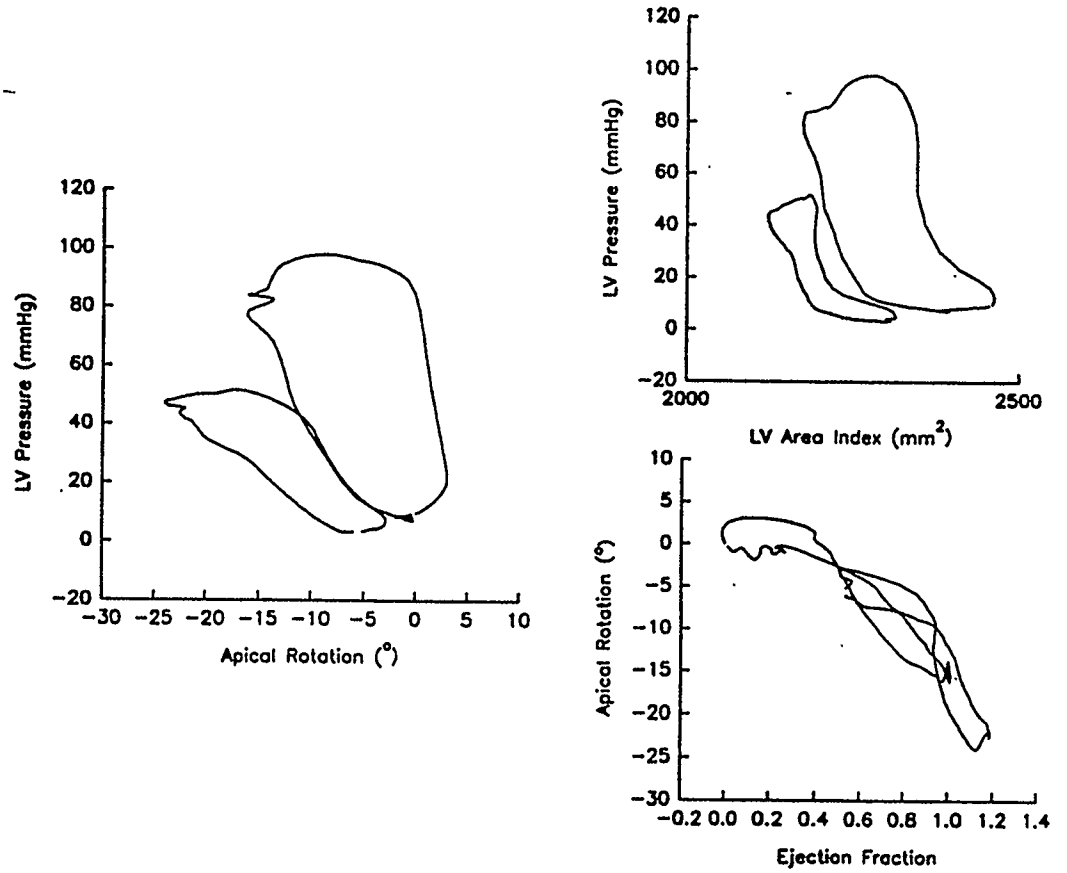


**Figure 3.7:** A typical example of pressure--apex-rotation loops (a), and apex-rotation--fractional shortening loops under control conditions and with VC occlusion (after 20 beats). Arrows indicate the direction of the loops.

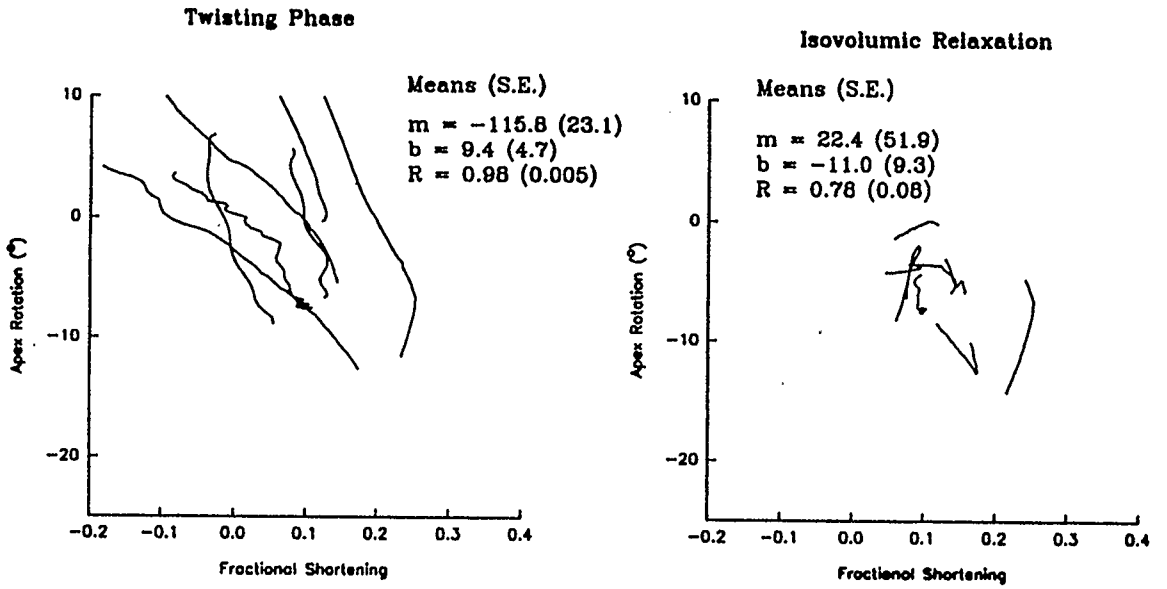


**Figure 3.8**: Apex-rotation--fractional shortening data shown for 7 dogs through the twisting phase (a) and during isovolumic relaxation (b) after 40 sec of volume loading. The regressions of these lines were used to calculate the means shown.

similar to those presented in Chapter 2. During the twisting phase, the mean slope with VC occlusion was -151±23 (compared to -119±47 for control) and during IVR, the slope was -401±138 (compared to -461±205 for control). These differences were not significantly different.

With volume loading, the apex-rotation--fractional shortening loops were shifted slightly upward and leftward. They were similar in shape to control with the exception of IVR, where the linearity previously described was less well-defined (Fig. 3.8). During the twisting phase, the mean slope from 8 dogs was -116±23 (very similar to control slope of -119±47). During IVR, there is no strong trend among dogs toward a linear relationship. This may be a result of delayed maximal twist into the IVR period. A change in the balance of endocardial and epicardial moments may be reflected in the twist-shortening relationship as a loss of linearity in the IVR period.

## 3.5 Discussion

In this study, the optical method for on-line measurement of apex-rotation was used to study the effects of changing preload on the dynamics of LV apex-rotation. A twist-volume relationship was established, showing that twist is primarily determined by LV volume at ED and ES. As shown in Chapter 2, measurements of apex-rotation obtained under baseline conditions with the optical measuring device were comparable to those from previous studies which used other

methods (Arts and Reneman, 1980; Rademakers et al, 1992; Hansen et al., 1987; Hansen et al., 1988; Hansen et al., 1991; Ingels et al.,1975; Moon et al., 1994). Further, it has been shown that the base of the heart rotated minimally (at most, 1-2°) under control conditions, making apex-rotation measurements a good indication of LV twist. Thus, dynamic changes observed with this device during changing preload accurately reflect changes in LV twist. Again, because the base rotates in a clockwise direction (opposite to the apex) during systole, the values of apex-rotation obtained by the measuring device slightly under-estimate the actual LV twist.

### 3.5.1 The Twist-Volume Relationship

Using load manipulations, we have established statistically different linear relationships between apex-rotation and LV volume for ED and ES (Fig. 3.2). Even though large changes were not seen in the total amplitude of twist with changes in preload, the use of the optical device allows for beat-to-beat comparisons with on-line recordings. Thus, a shift in the ED or ES apex-rotation values with load interventions can be observed. In the analysis of some other methods involving MRI (Buchalter et al., 1990; Beyar et al., 1989), cineradiography (Ingels et al., 1989; Hansen et al., 1988; Hansen et al., 1991) or echocardiography (Arts and Reneman, 1980), the ED twist value is arbitrarily made zero for every beat, and shifts in ED twist cannot be observed. Although these methods are adequate to

study changes in the total amplitude of twist during a cycle, the changes in apex-rotation at ED as a result of various interventions cannot be measured over successive cycles. Since these methods determine twist values at other times in the cycle (e.g. ES) by comparing them to the ED value, beat-to-beat shifts seen in the ES twist are also not seen. Similarly, values of volume were expressed in terms of normalized ejection fraction in these studies (Hansen et al., 1988; Ingels et al., 1989, Beyar et al., 1989; Moon et al., 1994) and beat-to-beat changes in volume could also not be seen. Hansen et al. (1991) and Moon et al. (1994) suggested that LV twist was relatively insensitive to preload and afterload changes. In contrast to the results of these studies, the data in this chapter suggest that changes in LV dimensions at ED and ES are sufficient to explain the changes in apex-rotation that were observed. The twist-volume relationship results in a leftward shift of pressure--apex-rotation loops with decreased preload, and a rightward shift of the pressure--apex-rotation loops with volume loading.

### 3.5.2 The Effects of Decreased Preload on Twist Dynamics

Hansen et al. (1991) studied the effects of increased preload on human implanted hearts using implanted midwall markers. In their study, no significant difference in LV torsion was observed with volume load. Our study imposed both a VC occlusion, which is a manoeuvre that changes both preload and afterload, and volume loading, which has a lesser effect on afterload. An increase in heart rate of

6.4±4.5 during the first 20 beats of VC occlusion indicates some sympathetic response and a possible modest change in contractility. Based on the data to be presented in Chapter 4, however, it is not likely that a modest increase in contractility is sufficient to account for the changes seen in apex-rotation values.

The results show that apex-rotation is significantly affected by decreased preload and afterload. Under these conditions (VC occlusion), the pressure--apex-rotation loop is shifted to the left with both the ED and ES apex-rotation values being more negative. This is a direct result of the twist-volume relationship we have previously established. Load pertubations cause changes in the dynamics of twist in addition to the shift of the loops. More twist/untwist occurred during the isovolumic periods and maximum apex-rotation occurred earlier in systole with VC occlusion than under control conditions (Fig. 3.4). Total ES to ED twist amplitude remained relatively unchanged with VC occlusion however (15.0° under control conditions compared with 15.3° for VC occlusion). With reduced load, the LV empties more completely and achieves a smaller ES volume (Fig. 3.3). This increased shortening may lead to more potential energy being stored in the myocardial passive elements, which leads to much faster untwisting once the myocardial active force starts to relax.

During diastolic filling, the LV appeared to untwist to -0.5±2.8° and then retwist to -1.5±3.6° with VC occlusion. During this period, the epicardial fibres are inactivated but the endocardial fibres are still activated and shortening.

Endocardial moments would dominate and active untwisting would occur (in addition to the untwist resulting from elastic recoil of the loaded collagen network). With reduced load, untwisting occurred faster and earlier in the cycle, so that the still-activated endocardial fibres may "overshoot" the normal ED state. When these fibres are inactivated and begin to lengthen, the LV returns to its "optimal" twist state as determined by the twist-volume relationship.

The results also indicate that VC occlusion and volume loading also affect the timing and length of contraction at the endocardial and epicardial layers.

### 3.5.3 The Effects of Increased Preload on Twist Dynamics

With increased preload by volume-loading a rightward shift of the pressure-twist loops is apparent (Figs. 3.5, 3.6), with positive apex-rotation values at ED and less negative values at ES. This is a direct result of the twist-volume relationship discussed above. The ED to ES twist amplitude did not change ($13.5 \pm 1.5°$ under control conditions vs. $13.3 \pm 3.3°$ and $11.4 \pm 4.0°$ after 25 and 40 sec of volume infusion, respectively). Therefore, the data emphasizes that, while large differences in twist/untwist pattern are seen with load manipulation, they are still consistent with the results of Hansen et al. (1991), i.e., that twist amplitude is relatively insensitive to load.

Volume loading caused less untwist to occur during the IVR period (47% of total untwist at baseline to 18% with volume infusion, $P < 0.03$). In addition, the

maximal apex-rotation occurs after ES with volume loading, indicating that the apex is still rotating during the IVR period. It is well-accepted that the torsion observed in the left ventricle is a result of the distribution of obliquely-arranged muscle fibres within the ventricular wall (Streeter et al., 1969; Streeter, 1979) and the balance of these fibre moments (Ingels et al. 1989). With increased preload, the balance of endocardial and epicardial moments may change, and this new balance of moments may result in maximal apex-rotation being achieved during the IVR period.

Combining the above data on preload manipulations leads to the conclusion that LV untwist is delayed under conditions associated with a larger ES volume (volume load) and enhanced by conditions associated with small ES volumes (VC occlusion).

### 3.5.4 The Effects of Load on Restoring Forces

With delayed torsion and delayed relaxation due to volume loading, as well as changed contraction timing of the endocardial and epicardial layers, restoring forces and early diastolic filling may be affected. Data presented in this study are consistent with the measurements of Rademakers et al. (1992) who used open-chest atrial-paced dogs and found that untwisting occurred mainly in IVR before filling occurred and that the resulting restoring forces allowed for rapid early filling. Since restoring forces attributed to the collagen matrix are a function of LV ES volume, the data supports the concept that untwisting is probably related to the magnitude of

these restoring forces. With decreased fibre shortening due to volume loading, there may be less potential energy stored in the passive elements of the myocardium. This may lead to slower untwisting of the LV during IVR due, in part, to less elastic recoil and reduced restoring forces. Therefore, slower early diastole filling is likely. With VC occlusion, there may be more potential energy stored in the collagen matrix of the myocardium due to increased fibre shortening against decreased load. Upon release of this potential energy, more elastic recoil would be expected and greater early diastolic filling.

### 3.5.5 The Twist-Shortening Relationship

Beyar et al. (1989) described the twist-shortening relationship as linear during ejection but uncoupled during relaxation. Moon et al. (1994) confirmed these results and found that volume loading decreased early IVR untwisting. This would result in a decrease in the slope of the twist-shortening relationship during IVR. Because their method arbitrarily set ED to 0° each beat (essentially normalizing twist) and used normalized ejection fraction, no shift in the twist-shortening loops with volume loading could be observed. In our study, it was shown that VC occlusion resulted in a rightward and downward shift of the loops, while volume loading resulted in a leftward and upward shift.

As in previous studies (Beyar et al., 1989), the twist-shortening relationship during the twisting phase (from mid-isovolumic contraction to maximal twist) was

shown to be linear, and this linearity remained during both VC occlusion and volume loading. The linear relationship observed during IVR was not significantly affected by VC occlusion but with volume loading, the linearity was less well-defined. This may be a result of the changing balance of moments that result in delayed maximal twist into the IVR period with volume loading. This uncoupling of the twist-shortening relationship during IVR may result in less early diastolic filling, as IVR untwisting was slower (as noted by Moon et al., 1994).

### 3.5.6 Summary

This optical device has been shown to be a simple and direct method to measure apex-rotation, which allows for the study of dynamic changes in LV torsion with changes in preload. With this device, changes to LV torsion under load conditions have been demonstrated that were previously undocumented. Not only are on-line measurements possible throughout the cycle (the IVR period in particular), but shifts in the angular rotation at specific points in the cycle (ED, for example) can be measured on successive cycles during an intervention. It has been shown that the angular position of the apex at ED is determined by the volume of the left ventricle. This linear ED relationship is significantly different from the linear relationship established for ES. While changing load altered the dynamics of twist within the cardiac cycle, the amplitude of LV twist remained relatively unchanged. Decreased load resulted in a leftward shift of the LV pressure--apex-

rotation loops, while increased load resulted in a rightward shift of these loops. With decreased load, maximal twist occurred earlier in ejection and more twisting/untwisting occurred in the isovolumic periods. With increased load, maximal twist was delayed into IVR, with less untwist occurring in this period. The rate of untwisting during IVR is a balance between the restoring forces and the torque moments at that moment. In general, the lower the ES volume the higher the stored elastic energy and larger is the IVR untwist. The twist-shortening relationship may also play a role in determining early diastolic filling. With VC occlusion, there was a rightward and downward shift of the loops with no significant change in the linear relationships during either ejection or IVR. With volume loading, however, there was a loss of the linear twist-shortening relationship (uncoupling) during IVR, corresponding to delayed maximal twist and slow IVR untwisting.

# Chapter 4

# THE EFFECTS OF AFTERLOAD, CONTRACTILITY AND HEART RATE ON APEX-ROTATION

## 4.1 Abstract

Using the optical device, the effects of afterload (1-beat aortic constrictions), contractility (paired pacing model and epinephrine injection) and heart rate (atrial pacing model) on apex-rotation was studied in 12 open-chest dogs. The twist-volume relationship (established in Chapter 3) was further examined under these intervention conditions. Contractility, afterload, and heart rate had little or no independent effect on this twist-volume relationship as the variance in twist seen with these interventions could be explained by the change in volume. Apex-rotation--area index points obtained at ED and ES with these interventions fell within the range found by changing preload. Increased afterload caused a slight decrease in apex-rotation amplitude, with maximal apex-rotation delayed into IVR. Increased contractility by paired pacing increased the total amplitude of apex-rotation 42% and caused a delay in untwisting into IVR. Epinephrine injection increased apex-rotation

amplitude but did not delay maximal twist into the IVR period.

An increase in heart rate to over 150 bpm resulted in a significant decrease in the amplitude of apex-rotation with a similar delay of twist relaxation into the IVR period. In summary, changes in afterload, contractility, and heart rate, resulted in changes in apex-rotation amplitude and in the twist relaxation patterns, as determined by the optical device. These interventions had no independent effect of the twist-volume relationship, however.

## 4.2 Introduction

In Chapter 3, it was shown that the optical-measuring device was useful in measuring the dynamic changes in apex-rotation with preload interventions, as it directly and continuously related apex-rotation to various haemodynamic parameters.

By changing preload, a direct, linear relationship between apex-rotation and LV volume was established for both ED and ES. Some groups (Hansen et al., 1991; Moon et al., 1994), however, suggest the LV torsion is sensitive to variation in contractility, but relatively insensitive to changes in preload or afterload. MacGowan et al. (1992) found that LV twist is still substantial during isovolumic contractions (extreme afterload). Unlike data shown in Chapter 3, these studies would indicate that LV volume is not as important as contractility in determining LV twist. While increased contractility is known to increase twist and augment the untwisting rate (Rademakers et al., 1992; Moon et al., 1994), other investigators

(Arts et al., 1984) claim this observation is only secondary to a change in volume and shortening. Thus, it is not clear yet whether the effect of contractility on twist is a primary effect or a secondary result of altered volumes. In this study, it will be determined whether shifts in apex-rotation are largely due to changes in LV volume or whether other independent effects, such as variation in contractility or afterload, play a role.

Since contractility also affects fibre shortening, the effects of increased contractility on the twist-shortening relationship will be examined. Moon et al. (1994) found that dobutamine injection increased twist amplitude and early IVR untwist. Their method normalized ejection fraction, however, so that no right or left shifts in the relationship could be observed. In addition, since this method arbitrarily sets the ED torsion value at 0° each beat, no upward or downward shifts in the relationship could be observed between beats.

Hansen et al. (1991) examined the effects of pharmacologic pressure loading and found no change in LV torsion. This method may have led to secondary changes in LV volume as well as reflex-mediated changes. Using the optical method (open-chest) allows for the study of afterload by aortic one-beat aortic constrictions, which eliminate any reflex-mediated effects. No studies have been performed to examine the effects of heart rate on LV twist, although Rademakers et al. (1992) studied the effects of catecholamines while atrial pacing the heart at 150 bpm. With reduced contraction and relaxation time at higher heart rates, both

LV volume and fibre shortening would be affected. Since LV twist is dependent on both fibre shortening and LV volume (as shown in Chapter 3), it is likely that LV twist dynamics would be affected by increased heart rate.

The aim of this chapter was to establish if changing afterload, contractility and heart rate affected the twist-volume relationship established in Chapter 3. The effects of contractility on the twist-shortening relationship were also examined. Using the optical device, the effects of variation in afterload (by aortic constriction), contractility (paired-pacing model and epinephrine injection), and heart rate (atrial pacing) on apex-rotation dynamics were examined throughout the cardiac cycle.

## 4.3 Methods

Experiments were performed to study the effects of variation in afterload, contractility, and heart rate on apex-rotation in 12 open-chest, anaesthetized dogs. The effects of afterload on base-rotation was also examined in 5 dogs.

The animal preparation and the use of the optical device was as described in Chapter 2. In addition to this outlined procedure, a tie was placed around the aorta as close to the base of the heart as possible. A plastic tube was placed over the tie which could be pushed down (while pulling up on the tie) to allow for quick occlusion of the aorta.

To study the effects of heart rate and contractility, pacing leads were placed on the right atrium and the right ventricle, with an indifferent electrode connected

to thoracic muscle. Using a stimulator (Grass S88; Quincy, Massachusetts), the atrium was paced at heart rates varying from 90 beats per minute (bpm) to 180 bpm (1.5 - 3.0 Hz). To study the effect of increased contractility, the heart was single-paced or pair-paced (Ross et al., 1965) via the right ventricle. With a proper delay between the twin pulses (second pulse arriving immediately following the refractory period and producing a minimal increase in pressure late during the IVR period), it was possible to augment ventricular performance (Ross et al., 1965).

A calibration run was performed at the beginning of the experiment to determine the relation of output voltage to a known distance on the diode. This calibration was checked several times throughout the experiment to correct for possible slow baseline shifts. These changes were found to be insignificant. The pressure--apex-rotation loops, LV and aortic pressures, as well as the segment-lengths were monitored throughout the experiment. A recording interval lasted 60 sec. After each intervention, time was allowed for the haemodynamic parameters to return to baseline conditions.

To study the effects of increased LV afterload, short systolic aortic constrictions were performed. The aorta was manually occluded for one-beat intervals by rapidly pulling up the tie placed at the base of the aorta. LV pressures could be seen to rise up to pressures of 250 mm Hg. Many occlusions could be done in a single run, usually with 5-10 sec between occlusions. Data for a single aortic constriction beat was only used if the preceding and following beats were

normal.

To study the effects of increased contractility, a paired-pacing model was used. The heart rate was set at 90 bpm (RV pacing). Starting from a pulse interval of approximately 600 msec, the delay of the second stimulus was decreased until a visible increase in pressure was seen. This normally occurred at approximately 400 msec delay. The advantage of paired-pacing was that the heart rate and the length of the cardiac cycle remained stable, even when contractility changed. For comparison, the effects of increased contractility were studied in 3 dogs using IV epinephrine (1:10,000 dilution, administered to effect (approximately 0.3 mL)). In contrast to the paired-pacing model, the changes in contractility in the epinephrine model are accompanied by changes in heart rate and are therefore difficult to interpret.

Atrial pacing was used to study the effects of heart rate with the frequency of pacing varied from 90 bpm (1.5 Hz) up to 180 bpm (3 Hz).

## 4.4 Results

### 4.4.1 The Twist-Volume Relationship

The effects of contractility on the twist-volume relationship (established in Chapter 3 by VC occlusion and volume loading) was examined using the paired-pacing model. The apex-rotation--normalized-LV-area-index values for ED were

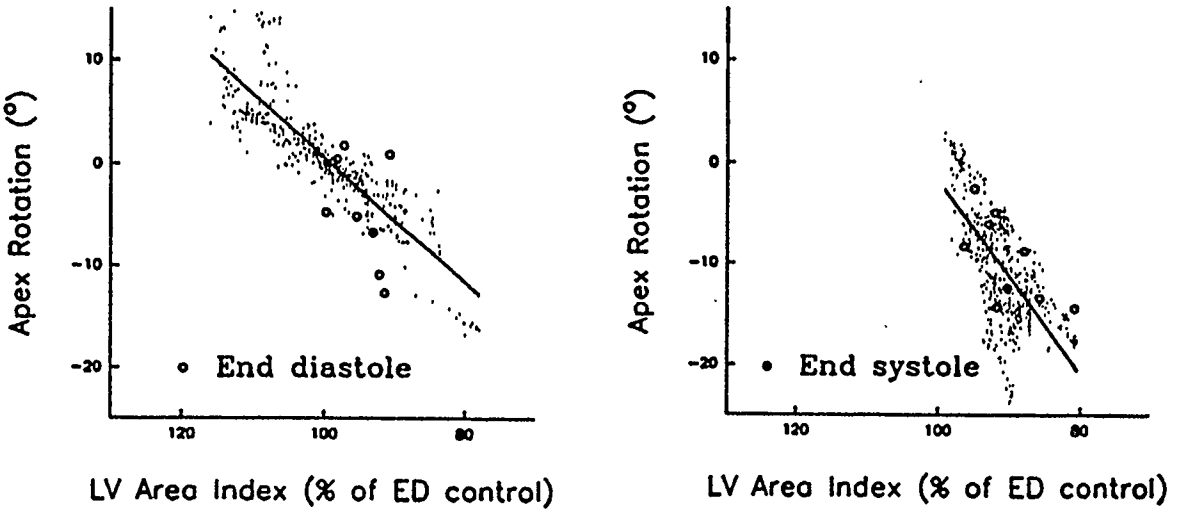


**Figure 4.1** - A plot showing end-diastolic and end-systolic apex-rotation-LV area index values for volume loading and VC Occlusion in 10 dogs as single points. The regression line for these points is shown. ED (open circles) and ES values (closed circles) for contractility changes are shown.

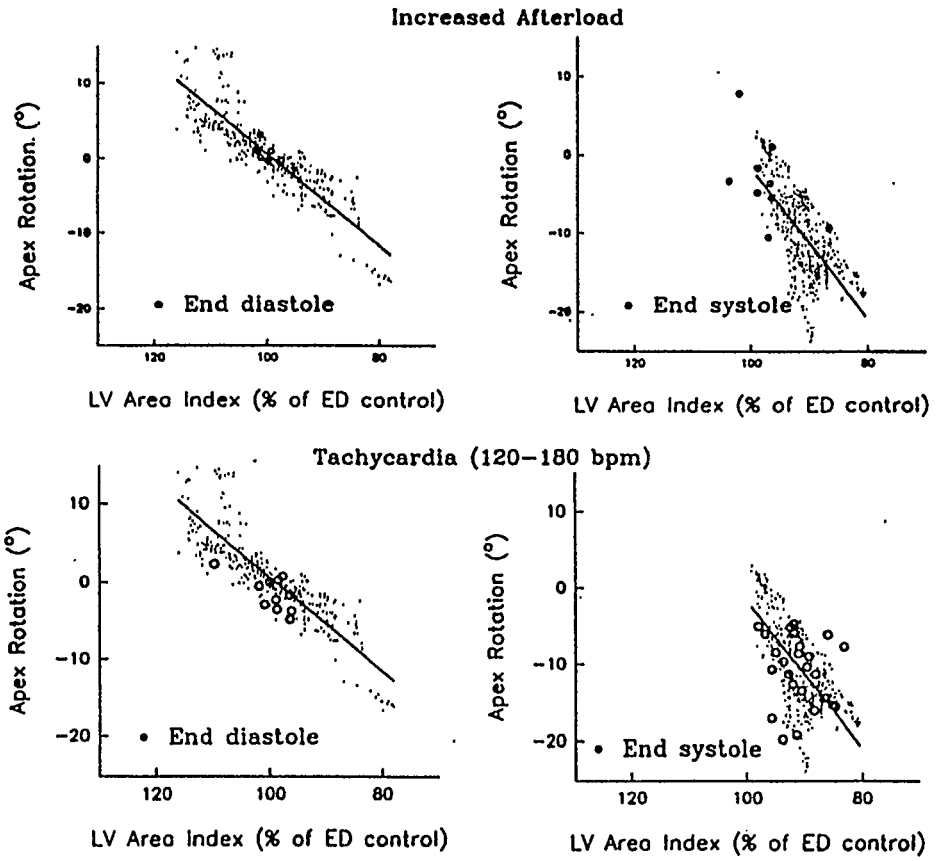


**Figure 4.2**: Plots showing end-diastolic (left) and end-systolic (right) apex-rotation--area-index values for volume loading and VC occlusion in 10 dogs as single points. The regression line for these points is shown. ED (left) and ES values (right) are shown as open circles for aortic constriction (A) and heart rate changes (B).

superimposed on the relationship established with changing preload (Fig. 4.1). Both ED and ES paired-pacing values fell within the confidence intervals of the ED and ES-relationships defined by preload alterations. This indicates that increased contractility had no independent effect on twist in that all the variance in twist was explained by the change in volume. When individual dogs were examined, the paired pacing point was found to again fall within the confidence intervals of the apex-rotation--area-index points established by VCO and volume loading for that particular animal, again indicating no independent effect of contractility on these relationships. Because of small sample size (1 data point per dog), no statistical analysis can be done at this time, but, rather, these results strongly suggest that there is no independent effect of contractility on the end-diastolic and end-systolic apex-rotation--area-index relations.

Likewise, the apex-rotation-normalized LV area index values were superimposed on the relationship under conditions of increased afterload (by aortic constriction) and heart rate changes (by atrial pacing). Again, the points for ED and ES for both aortic constriction and heart rate alteration fell within the confidence intervals of the relationships established by changing preload, without any trends or shifts observed (Fig. 4.2). This would indicate that changing afterload and heart rate has no independent effect on twist, as again, all the variance in twist is explained by the change in volume. Again, no significant shifts or changes were noted when results from individual dogs were examined.

**Table 4.1** - Standard haemodynamic parameters meaned for animal groups under baseline conditions and with contractility, afterload, and heart rate changes.

| Parameters | Single-paced (control) | Paired-paced (increased contractility) |
|---|---|---|
| Heart rate | 100 | 100 |
| ED aortic pressure | 82±5 | 97±7 |
| ES aortic pressure | 99±7 | 123±11 |
| ED LV area index | 2470±175 | 2495±172 |
| ES LV area index | 2290±202 | 2281±172 |
| ED segment length | 11.5±0.7 | 11.7±0.7 |
| ES segment length | 10.3±0.6 | 9.9±0.7 |

| Parameters | Baseline | Aortic Constriction |
|---|---|---|
| Heart Rate | 79±5 | 82±7 |
| ED aortic pressure | 80±6 | 83±8 |
| ES aortic pressure | 110±6 | 81±5 |
| ED LV area index | 2324±116 | 2313±113 |
| ES LV area index | 2194±168 | 2361±165 |
| ED segment length | 10.5±0.5 | 10.5±0.6 |
| ES segment length | 8.7±0.4 | 9.8±0.5 |

| Parameters | Baseline (90 bpm) | Increased Heart rate 180 bpm |
|---|---|---|
| Heart Rate | 90 | 180 |
| ED aortic pressure | 91±6 | 81±16 |
| ES aortic pressure | 114±9 | 96±14 |
| ED LV area index | 2257±136 | 1969±118 |
| ES LV area index | 2099±158 | 1810±142 |
| ED segment length | 11.7±0.8 | 9.9±0.7 |
| ES segment length | 10.1±0.7 | 9.0±0.7 |

Standard errors are shown. ED and ES represent end diastole and end systole respectively.

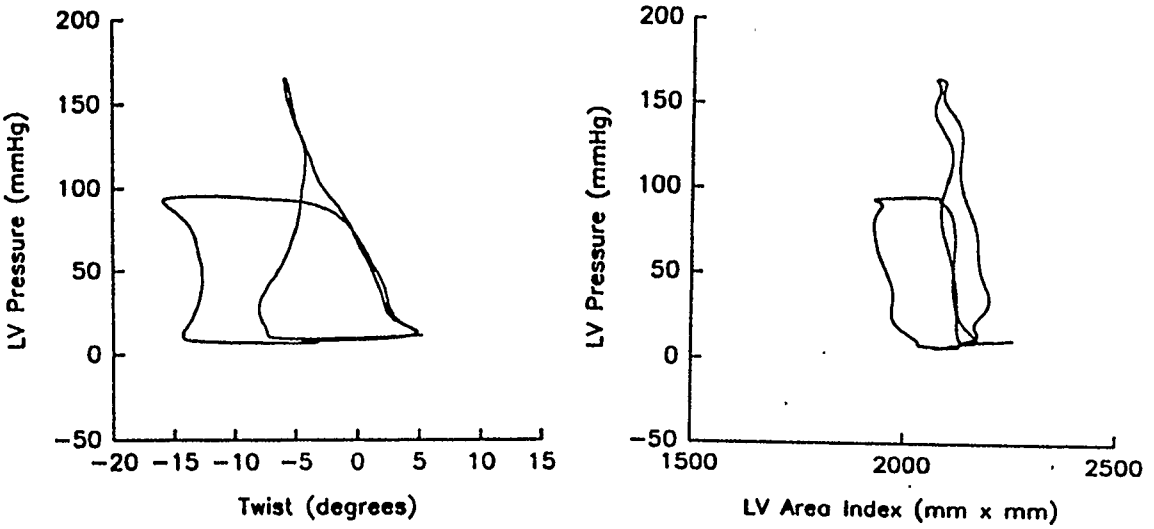


**Figure 4.3:** A typical example of pressure--apex-rotation (a) and pressure--area-index (b) loops shown under control conditions and for aortic constriction.

**Table 4.2** - Mean apex-rotation and LV pressure values under baseline and aortic constriction conditions for 9 dogs.

| Point in Cycle | Apex-rotation Baseline | Apex-rotation Moderate Aortic Const. | Apex-rotation Maximal Aortic Const. |
|---|---|---|---|
| End diastole | 0.0±0.0 | -1.0±1.2 | 0.0±0.6 |
| Maximal untwist | 2.8±3.4 | 4.9±1.4 | 4.2±1.0 |
| End isovolumic Contraction | -1.4±1.9 | -4.8±1.7 | -3.3±1.6 |
| Peak LV pressure | -8.2±1.5 | -6.6±2.7 | -3.2±1.7 |
| Maximal twist | -13.3±1.5 | -10.0±2.1 | -6.8±1.1 |
| End systole | -12.7±1.4 | -4.9±2.9 | -2.6±1.9 |
| End isovolumic Relaxation | -8.5±1.4 | -9.1±3.7 | -6.3±1.1 |
| 1/3 diastolic filling | -3.2±1.9 | -6.3±3.8 | -3.1±1.1 |
| 2/3 diastolic filling | -1.3±1.9 | -3.0±2.2 | -1.5±1.1 |
| End diastole | 0.4±0.5 | 3.3±1.9 | 1.3±0.9 |

| Point in Cycle | LV pressure Baseline | LV pressure Moderate Aortic const. | LV pressure Maximal Aortic const. |
|---|---|---|---|
| End diastole | 7.1±1.3 | 7.4±0.8 | 9.2±1.0 |
| Maximal untwist | 29.1±9.2 | 32.3±10.8 | 43.4±12.5 |
| End isovolumic contraction | 87.5±12.7 | 153.7±16.5 | 188.2±14.1 |
| Peak LV pressure | 96.3±13.7 | 160.6±16.5 | 195.9±14.0 |
| Maximal twist | 85.7±15.3 | 75.9±25.3 | 115.7±23.3 |
| End systole | 85.7±13.5 | 152.5±16.4 | 187.5±14.3 |
| End isovolumic Relaxation | 11.5±1.1 | 11.9±0.9 | 14.0±1.0 |
| 1/3 diastolic filling | 4.9±1.5 | 6.0±0.7 | 8.4±1.3 |
| 2/3 diastolic filling | 5.3±1.3 | 6.6±0.7 | 8.9±1.2 |
| End diastole | 6.8±1.8 | 8.2±0.8 | 10.5±1.2 |

End diastole under control conditions is defined as 0° rotation. Data for moderate and maximal 1-beat aortic constriction is shown. Means are averaged for 9 dogs and standard errors are shown.

### 4.4.2 The Effects of Afterload on Apex-Rotation

Increased afterload was produced by constricting the ascending aorta for 1-beat intervals. Two levels of aortic constrictions were achieved. The moderate aortic constriction had LV pressures which peaked at 161±17 mm Hg (compared with 96±6 mm Hg control) and the maximal aortic constriction had LV pressure which peaked at 196±17 mm Hg. As expected, aortic constrictions caused an increase in the ES LV area-index and segment-length (Table 4.1).

A sample of the data collected during a constriction in one dog is shown in Fig. 4.3. Since no constriction had been applied during the previous ejection, no significant difference was seen in ED apex-rotation values or with the amount of untwist seen in the isovolumic contraction period. Mean values for 9 dogs (Table 4.2) were calculated at 10 set points in the cardiac cycle (as discussed in Chapter 2) and plotted in the form of an LV pressure--apex-rotation loop (Fig. 4.4). Maximum apex-rotation decreased from -13.3±1.5° under control conditions to -10.0±2.1° with a moderate aortic constriction to -6.8±1.1° with a maximal aortic constriction ($p<0.02$; Table 4.2). In contrast to control conditions, the maximum apex-rotation occurred after ES (indicating that apex-rotation is delayed). With the moderate aortic constriction, only 7% of the untwist occurred during the IVR period and only 28% by the end of the first third of diastole (compared to 37% and 78% respectively for control cycles). Fairly similar results were seen for the maximal aortic constriction (6% and 46% respectively; $p<0.04$). With aortic constriction,

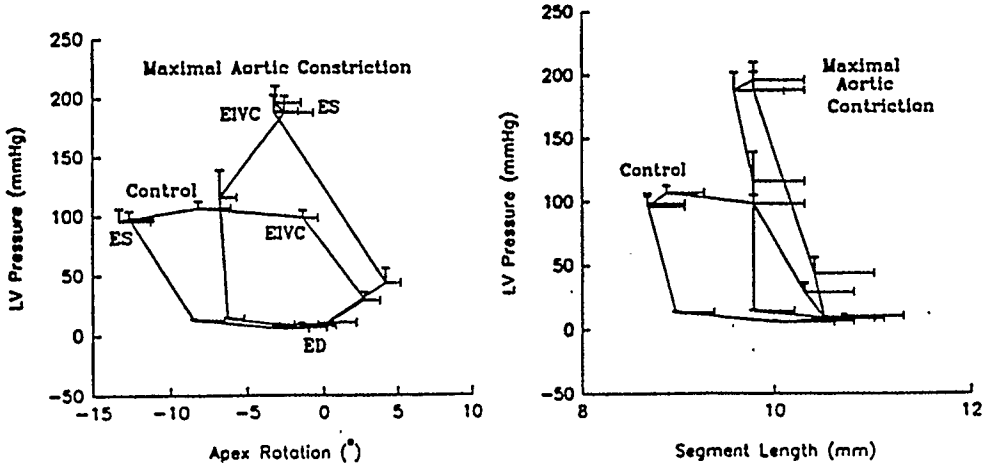


**Figure 4.4:** Mean plots of pressure-apex-rotation and pressure-segment length under normal conditions and during a maximal aortic constriction. n=8.

the isovolumic contraction and relaxation periods were longer but less apex-rotation occurred in these periods. Very little rotation occurs in the absence of ejection and apex-rotation is delayed under these conditions, with the maximum apex-rotation occurring well into the IVR period. The LV shows a short period of untwist after reaching peak pressure and before ES with aortic constrictions (Fig 4.4). This untwist period disappears in subsequent beats and appears to be a result of the increased afterload.

Measurement of rotation of the base of the heart was also done during aortic constrictions in 5 dogs. The total amount of rotation during the cardiac cycle is decreased slightly (from 1 to 1.5° to less than 1°), and there is a slight leftward shift of the base-rotation-pressure loops (approximately 0.5°).

### 4.4.3 The Effects of Increased Contractility on Apex-Rotation

Heart rate was set at approximately 1.7 Hz (100 beats per minute) when the paired-pacing model was used to study contractility effects. Paired-pacing generates alternating high and low contractility beats. Pressure--apex-rotation loops for one dog are shown in Fig. 4.5. Mean values (9 dogs) at 10 intervals in the cycle were used to form mean pressure--apex-rotation loops (Fig. 4.6). With paired-pacing, the LV peak pressure increased from $101 \pm 5$ mm Hg to $130 \pm 7$ mm Hg (Table 4.3). Aortic pressures were also seen to rise and fibre shortening increased (Table 4.1). With paired-pacing, the pressure--apex-rotation loops were much larger than seen

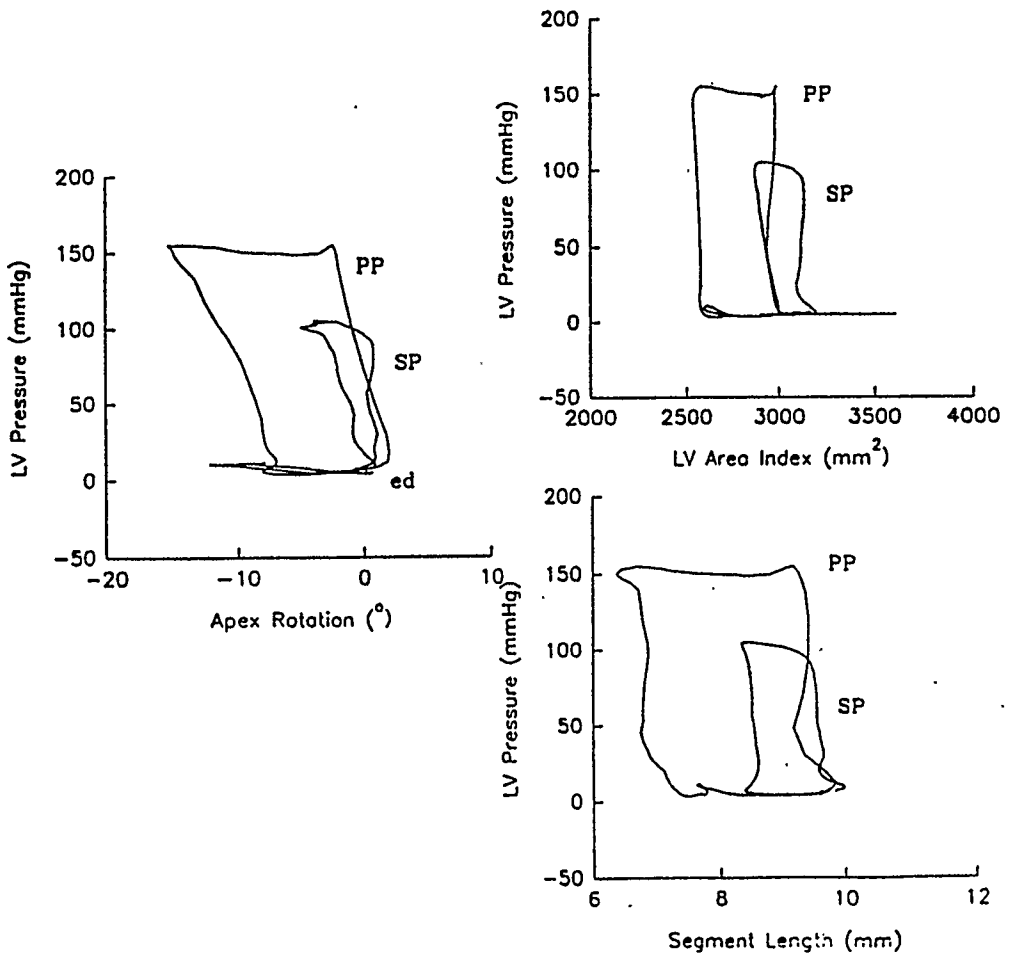


**Figure 4.5**: A typical on-line recording from one dog of contractility changes in apex-rotation, LV pressure, LV area index, and segment length with paired pacing. Loops marked by SP are single paced loops, while those marked by PP are paired-paced.

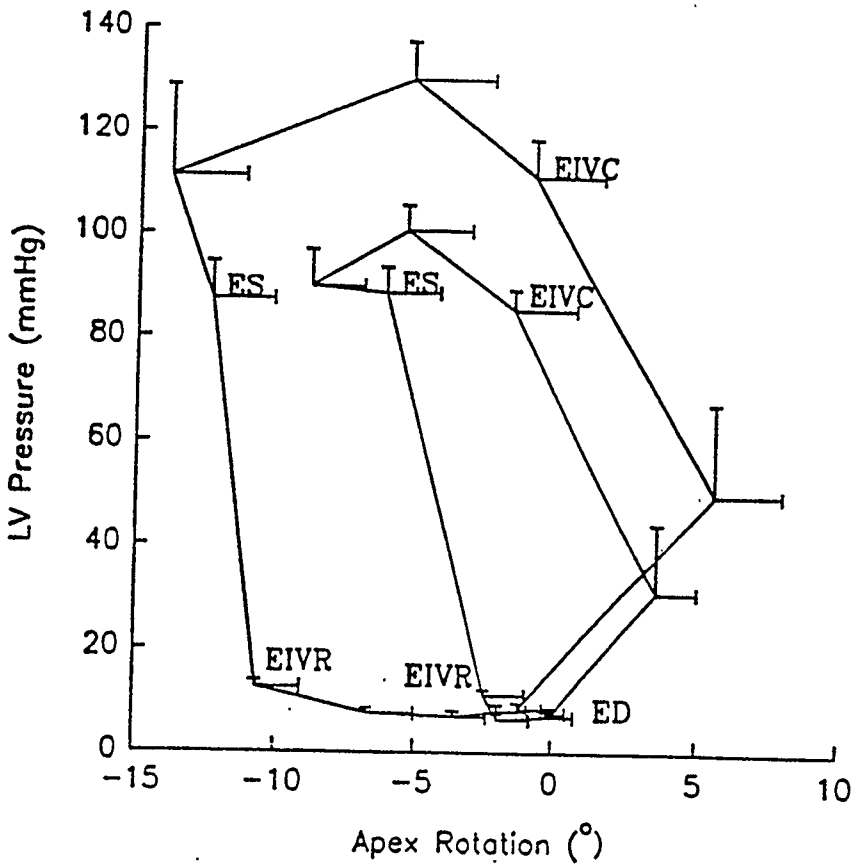


**Figure 4.6**: A mean plot of pressure-apex-rotation for contractility changes by the paired pacing model. n=8. Other abbreviations as shown in Figure 3.4.

**Table 4.3** - Mean apex-rotation and LV pressure values for baseline and increased contractility (paired pacing model) for 9 dogs.

| Point in Cycle | Apex-rotation Single- paced | Apex-rotation Paired-paced | LV pressure Single-paced | LV pressure Paired-paced |
|---|---|---|---|---|
| End diastole | 0.0±0.0 | -1.3±0.9 | 7.4±1.1 | 8.4±1.3 |
| Maximal untwist | 3.6±1.4 | 5.6±2.4 | 30.9±13.3 | 49.9±17.6 |
| End isovolumic contraction | -1.6±2.3 | -0.9±2.5 | 85.3±3.6 | 111.3±7.3 |
| Peak LV pressure | -5.5±2.3 | -5.4±2.9 | 100.7±5.0 | 130.2±7.3 |
| Maximal twist | -8.9±1.9 | -13.9±2.6 | 89.9±7.0 | 87.4±17.6 |
| End systole | -6.2±1.9 | -12.4±2.2 | 88.6±5.0 | 111.3±7.2 |
| End isovolumic relaxation | -2.5±1.5 | -10.7±1.6 | 11.1±1.0 | 12.5±1.2 |
| 1/3 diastolic filling | -2.0±1.5 | -6.7±1.7 | 6.4±1.1 | 7.5±1.1 |
| 2/3 diastolic filling | -0.1±1.0 | -3.6±1.2 | 6.9±1.2 | 6.9±1.2 |
| End diastole | -0.1±0.6 | -2.0±1.1 | 7.6±1.1 | 8.1±1.2 |

End diastole under baseline conditions is defined as 0° rotation. Changes in contractility are achieved by using the paired pacing model. Values are shown for either single paced or paired paced (increased contractility). Means are from 9 dogs and standard errors are shown.

with single pacing (Fig. 4.6). A very small leftward shift of the ED point of the pressure--apex-rotation loop occurred with paired-pacing (-1.3±0.9° at ED), corresponding to very little change in the LV area index. The maximum untwist in the isovolumic contraction period increased with paired-pacing from 3.6±1.4° (single-paced) to 5.6±2.4° ($p<0.05$; Table 4.3, Figure 4.6). Maximum apex-rotation in systole increased significantly from -8.9±1.9 (single-paced) to -13.9±2.6° with paired-pacing ($p<0.02$). With single pacing, more untwist occurred during systole than with paired-pacing. By the end of the IVR period, the LV was 72% untwisted in the single-paced model. With paired-pacing, the LV was only 27% untwisted by the end of IVR ($p<0.002$). In general, the pressure--apex-rotation loop under paired-pacing conditions was larger than the single-paced loops with greater twist/untwist occurring and greater pressures being achieved. The LV showed more untwist in the isovolumic contraction period with paired-pacing and remained in its twisted state longer into the diastolic period than seen with single pacing (Fig 4.6). This may be a result of delayed endocardial relaxation.

The effects on apex-rotation of epinephrine (which has both a positive inotropic and chronotropic effect) was studied in 3 dogs. Heart rate increased significantly (Table 4.1). There was a 20% increase in maximum apex-rotation with an injection of epinephrine, corresponding to a 25% increase in peak LV pressure. There was no significant change in the amount of untwist during the isovolumic contraction period between control and epinephrine conditions (Table 4.4). Also,

**Table 4.4** - Mean values for apex rotation and LV pressure from 3 dogs for control and epinephrine injection.

| Point in Cycle | Apex-rotation Baseline | Apex-rotation Epi. Inj. | LV pressure Baseline | LV pressure Epi. Inj. |
|---|---|---|---|---|
| End diastole | 0.0±0.0 | 1.1±0.5 | 6.7±3.2 | 8.4±4.0 |
| Maximal untwist | 2.2±0.8 | 3.3±2.5 | 19.4±6.4 | 34.5±10.8 |
| End isovolumic contraction | -2.5±1.8 | -1.0±2.1 | 84.5±9.4 | 110.9±15.4 |
| Peak LV pressure | -2.5±5.5 | -7.9±4.2 | 92.5±10.7 | 115.3±16.6 |
| Maximal twist | -20.2±2.5 | -24.3±3.2 | 72.5±14.3 | 94.6±18.8 |
| End systole | -14.7±2.4 | -23.0±3.6 | 82.1±9.1 | 100.4±14.6 |
| End isovolumic relaxation | -8.2±2.3 | -10.8±2.3 | 10.5±3.2 | 13.0±3.8 |
| 1/3 diastolic filling | 0.3±4.5 | -1.0±2.8 | 5.5±5.4 | 5.4±3.7 |
| 2/3 diastolic filling | -1.9±1.4 | -1.8±0.8 | 5.6±3.5 | 6.2±3.9 |
| End diastole | 0.0±0.6 | 0.0±0.7 | 5.7±3.2 | 7.5±4.3 |

Baseline end diastole is defined as 0° rotation. Data is shown for control and epinephrine injection (increased heart rate and contractility) (epi. inj.). Means are for 3 dogs and standard errors are shown.

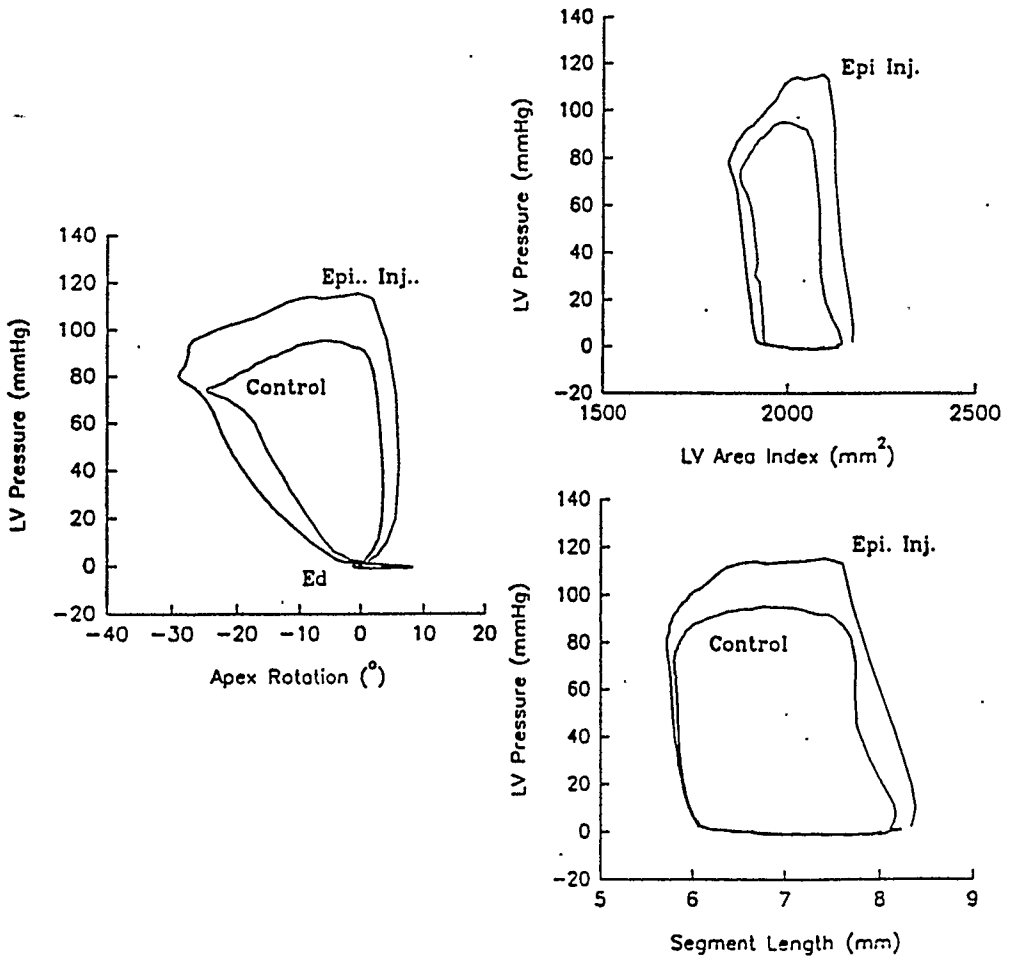


**Figure 4.7:** A typical on-line recording from one dog of LV pressure, apex-rotation, LV area index, and segment length during an epinephrine injection. Cycles are shown in the form of loops.

there was no notable difference between control and epinephrine conditions when examining the changes in IVR. With epinephrine injection, 55% of the untwist occurred during IVR (compared with 59% for control), and 96% of the untwisting had occurred by the first third of diastole (as opposed to 99% for control). The pressure--apex-rotation loop after epinephrine injection, however, was much larger (Fig 4.7). The amplitude of apex-rotation seen during the cardiac cycle with epinephrine increased to approximately 28° compared to 22° for control. Both maximum untwist (during isovolumic contraction) and maximum apex-rotation (during systole) were greater with epinephrine than seen under control conditions. With epinephrine, the LV remained in a twisted state for more prolonged period. At ES, the apex-rotation value for epinephrine state was still -23°, compared with -14.7° for control. The very small sample size must be taken into consideration when studying these results.

### 4.4.4 The Effects of Increased Contractility on the Twist-Shortening Relationship

The apex-rotation--fractional shortening loops from one dog are shown under control conditions and with an epinephrine injection (Fig. 4.8). With increased contractility due to epinephrine, there is more fractional shortening and greater apex-rotation, which results in a much larger twist-shortening loop. In control and epinephrine cases, the twist-shortening relationship remains linear in both the

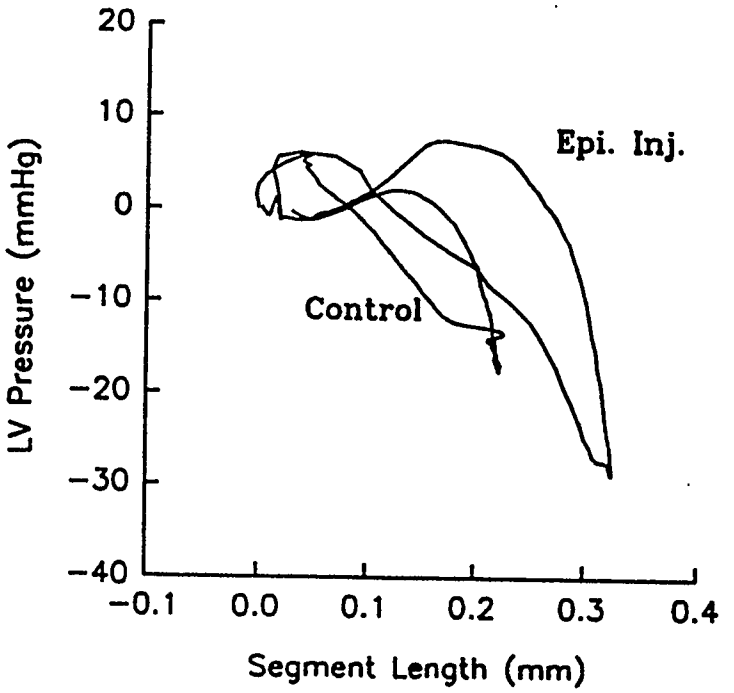


**Figure 4.8**: A typical example of apex-rotation--fractional shortening loops under control conditions and with epinephrine injection from one dog. Arrows indicate the direction of the loops.

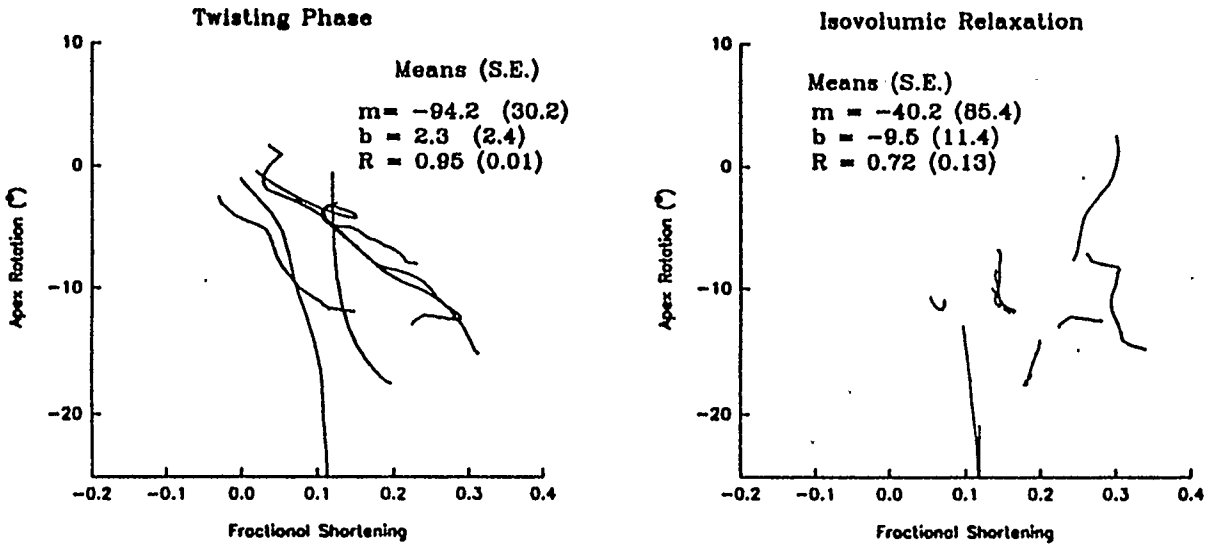


**Figure 4.9**: Apex-rotation--fractional shortening data shown from 8 dogs through the twisting phase and during isovolumic relaxation during paired-pacing (increased contractility). Regressions of these lines were used to calculate the means shown.

twisting and IVR phases. During the IVR phase, the slope of the relationship appears to be slightly steeper with epinephrine due to an increased rate of early untwist, but this change is not significantly different. Likewise, the slope of the twist-shortening relationship during the twisting phase was not significantly different than the slope seen under control conditions, due to a concomitant increase in twist with shortening under conditions of epinephrine injection.

With paired-pacing, the twist-shortening relationship does not appear to change significantly during the ejection phase (relatively similar slopes). During IVR, however, the twist-shortening relationship loses its defined linearity (Fig. 4.9). As with volume loading, maximal twist with paired-pacing was delayed into the IVR period (likely due to ventricular pacing changing the activation pattern). As seen with volume loading, the relationship appears uncoupled in IVR.

### 4.4.5 The Effects of Heart Rate on Apex-Rotation

Heart rate was controlled by atrial pacing, and varied between 90 and 180 beats per minute. Average values obtained at intervals throughout the cycle in 9 dogs and shown in Table 4.5. An example of pressure--apex-rotation loops for one dog is shown in Fig. 4.10. There was a leftward shift and narrowing of pressure--apex-rotation loops with increasing heart rate corresponding to a leftward shift and narrowing of both pressure-volume loops and pressure-segment-length loops with increasing heart rate (Fig 4.10). With increasing heart rate, ED LV area index

**Table 4.5** - Mean Values for apex-rotation and LV pressure from 9 dogs for baseline and changing heart rate (90-180 bpm).

| Point in cycle | Apex-rotation 90 bpm | Apex-rotation 120 bpm | Apex-rotation 150 bpm | Apex-rotation 180 bpm |
|---|---|---|---|---|
| End diastole | 0.0±0.0 | -0.7±1.1 | -4.9±1.6 | -7.0±2.2 |
| Maximal untwist | 4.0±0.9 | 3.8±1.5 | -1.0±1.7 | -2.8±2.5 |
| End isovolumic contraction | -0.7±1.5 | -1.0±2.0 | -5.8±2.3 | -7.4±3.0 |
| Peak LV pressure | -6.9±2.2 | -6.9±1.6 | -10.1±1.7 | -9.1±2.8 |
| Maximal twist | -9.8±1.5 | -11.3±1.3 | -13.2±1.2 | -14.2±1.3 |
| End systole | -8.2±1.8 | -10.0±1.5 | -11.9±1.6 | -13.0±2.0 |
| End isovolumic relaxation | -8.4±1.7 | -7.2±2.1 | -8.9±1.9 | -10.6±2.4 |
| 1/3 diastolic filling | -5.3±1.3 | -5.5±1.9 | -8.0±1.9 | -9.9±2.3 |
| 2/3 diastolic filling | -3.3±0.8 | -3.5±1.4 | -7.2±1.7 | -8.9±2.2 |
| End diastole | -1.2±0.4 | -0.9±0.8 | -5.3±1.8 | -7.7±2.1 |

| Point in cycle | LV pressure 90 bpm | LV pressure 120 bpm | LV pressure 150 bpm | LV pressure 180 bpm |
|---|---|---|---|---|
| End diastole | 10.0±1.2 | 8.8±1.1 | 9.1±1.1 | 11.3±1.2 |
| Maximal untwist | 33.8±11.0 | 43.9±13.2 | 46.7±12.7 | 49.1±17.1 |
| End isovolumic contraction | 101.9±7.6 | 107.3±6.1 | 102.7±7.1 | 101.8±7.4 |
| Peak LV pressure | 115.4±8.9 | 116.9±7.1 | 110.8±7.5 | 107.2±7.2 |
| Maximal twist | 105.9±9.5 | 104.8±9.9 | 99.6±8.2 | 87.0±10.0 |
| End systole | 105.8±8.2 | 106.9±7.1 | 99.9±7.66 | 96.2±7.0 |
| End isovolumic relaxation | 15.4±1.3 | 13.7±1.1 | 13.7±0.9 | 15.8±1.2 |
| 1/3 diastolic filling | 8.1±1.4 | 6.9±1.0 | 8.8±1.3 | 19.7±9.6 |
| 2/3 diastolic filling | 8.5±1.4 | 7.1±1.1 | 7.4±1.2 | 18.4±10.0 |
| End diastole | 9.8±1.3 | 8.0±1.1 | 7.6±1.0 | 18.5±9.9 |

Baseline end diastole is defined as 0° rotation. Heart rate was changed from 90 beats per minute to 180 beats per minute by atrial pacing. Values are meaned for 9 dogs and standard errors are shown.

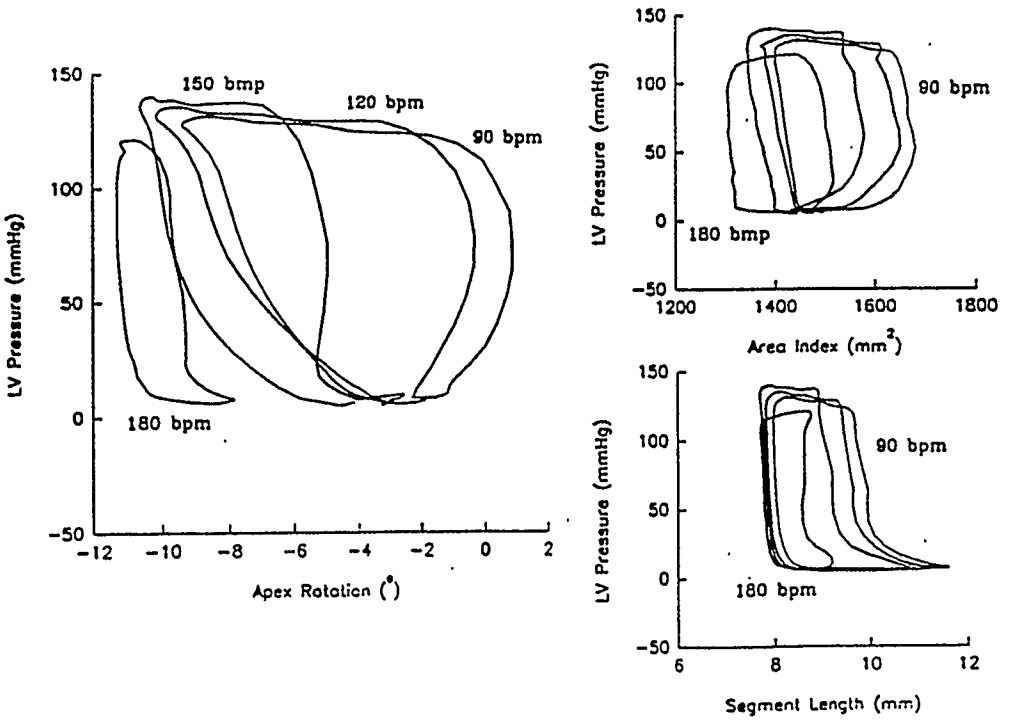


**Figure 4.10:** A typical on-line recording of LV pressure-apex-rotation, LV pressure-LV area index, and LV pressure-segment length with atrial pacing (heart rate changes from 90 to 180 beats per minute (1.5-3.0 Hz).

decreased, and apex-rotation became more negative (indicating that the LV is more twisted at ED). This is again consistent with the twist-volume dependence previously described. There was no significant difference between the averaged pressure--apex-rotation relationship at 90 beats per minute (bpm) and 120 bpm (see Table 4.5). Maximum apex-rotation values increased slightly at 120 bpm (from -9.8$\pm$1.5° to -11.3$\pm$1.3°).

At 150 bpm, the ED apex-rotation value shifted leftward to -4.9$\pm$1.6° ($p<0.008$). A leftward shift of the pressure--apex-rotation loop was noted, which could, in part, be due to the decreased volume of the heart at higher rates. During the IVR period, 53% of the untwist occurred (compared to approximately 40% for lower heart rates). At 180 bpm, the pressure--apex-rotation loop was further shifted leftward. At ED, the apex-rotation value is -7.0$\pm$2.2° (compared to 0 at 90 bpm; $p<0.005$). This indicates that the heart is in a more twisted state in diastole at higher heart rates. Maximum apex-rotation in systole is -14.2$\pm$1.3° ($p<0.004$) which is not only shifted left but shows a decrease in the amount of actual apex-rotation occurring. Total change in apex-rotation at 180 bpm was only 7.2° compared with 10.5° at lower heart rates (total apex-rotation for dog shown is even less). The amount of untwist in IVR is 55% (close to values found at 150 bpm). The maximum apex-rotation occurs during the IVR period rather than during systole as was seen at the lower heart rates and when the heart was unpaced.

## 4.5 Discussion

In this chapter, the optical device was used to study the effects of afterload, contractility, and heart rate on the dynamics of apex-rotation and on the twist-volume relationship. Although a slight underestimation, apex-rotation is a reliable index of LV twist, as baseline measurements remain comparable to previous studies (Hansen et al., 1988; Ingels et al., 1989; Beyar et al., 1989; Moon et al., 1994). The method's ability to measure angular shifts in consecutive beats allows for better study of the effects of afterload, contractility, and heart rate on LV twist.

### 4.5.1 The Twist-Volume Relationship

In the previous chapter, direct, linear relationships between LV twist and LV volume were established at both ED and ES which were significantly different from one another.

Hansen et al. (1988) suggest that LV twist is dependent on contractile strength and the same group later suggested (Hansen et al. 1991; Moon et al. 1994) that LV twist was relatively insensitive to preload and afterload changes. In contrast to these studies, the data presented here suggest that LV twist is independent of contractility (Fig. 4.1), as the changes in apex-rotation associated with increased contractility can be attributed to the change in LV volume (indexed by the cross-sectional area) under these conditions (no shift in the twist-volume relationship was seen with increased contractility). In addition, changes in afterload and heart rate

have no independent effect on the twist-volume relationship, as the changes in ED and ES dimensions under these conditions were sufficient to explain the changes in twist that were observed (Fig. 4.2).

### 4.5.2 The Effects of Afterload on Twist Dynamics

Hansen et al. (1991) performed pressure loading (increasing ED aortic pressure by methoxamine) on patients with cardiac allografts. They found no change in LV torsion with these interventions and concluded that altering afterload had no effect on ventricular twist. In the current study, only afterload was altered by performing one-beat occlusions of the aorta. Clearly, the magnitude of twist was reduced (more positive ES apex-rotation values) with afterload increase. However, the experimental conditions are not comparable to those of Hansen et al (1991), where changes in afterload by methoxamine may lead to secondary changes in LV ED volume. The single-beat occlusions have the advantages of not allowing time for reflex changes as well as having controlled ED volume. It was also found that with increased afterload, the maximal apex-rotation occurs after ES. Similar to the preload interventions discussed in Chapter 3, the delayed maximal apex-rotation may be a result of a significant change in the balance of epicardial and endocardial moments with aortic constriction. With less fibre shortening and a higher ES volume during aortic constriction, it may also indicate that less potential energy is stored in the myocardial passive elements, allowing for slower untwisting in the IVR

period. The amount of untwist that had occurred at the end of the IVR period with increased afterload was significantly reduced when compared to baseline. Again, as seen with increased preload, the restoring forces would be reduced and early diastolic filling would be affected with increased afterload.

### 4.5.3 Effects of Increased Contractility on Twist Dynamics

Hansen et al. (1991) found that inotropic stimulation increased LV torsion in a heterogeneous and regional fashion. Rademakers et al. (1992) found that catecholamines increased the amount of LV untwist seen during the IVR period. In this study, a paired ventricular pacing model was used to increase contractility without affecting heart rate (and therefore, length of the cardiac cycle). In addition, the effect of adrenaline on the dynamics of twist was also studied. The shape of the apex-rotation recording was different from that seen under unpaced conditions. This may be a result of pacing from the ventricle, as the patterns of excitation are different. This may result in changes to the balance of moments that produce the typical apex-rotation tracing.

Increased contractility resulted in greater untwist occurring in the isovolumic contraction period as well as greater apex-rotation occurring during systole. In addition, with paired-pacing-induced increases in contractility, the LV remained in its twisted state for a longer period and less untwisting occurred during the IVR period with paired-pacing than was seen with single pacing. Consistently, results

from epinephrine injection show that the apex-rotation values for epinephrine injection at ES are much smaller (more twisted) than seen at baseline. Similar to the paired-pacing data, the heart remained in a twisted state for a longer period of time and less twisting during the IVR period was noted. While the increase in twist with contractility is consistent with previous results (Moon et al., 1994; Hansen et al., 1991) the data regarding twist relaxation are in contrast to results by Rademakers et al. (1992) who found that untwisting rate was enhanced by increased contractility. This may be a direct result of different drug interventions and the use of a pacing model for contractility (pacing may delay the untwisting action). The increased speed of untwisting they observed in their study may also be a direct result of increased heart rate. The larger total apex-rotation observed in the present study with paired-pacing-induced increased contractility would result in greater restoring forces to aid in diastolic filling. Again, the effects of contractility on twist is probably secondary to the changes in ES volume.

### 4.5.4 The Effects of Increased Contractility on the Twist-Shortening Relationship

With increased contractility, there is increased fibre shortening and increased LV torsion. Because these both increased concomitantly, there is little change in the twist-shortening relationship with epinephrine injection. The relationship remained linear during the twisting phase, and was linear (but with a steeper slope) during

IVR. The slopes of the relationships in both these periods were not significantly different than what was seen under control conditions. Thus, as with the twist-volume relationship, increased contractility does not have a large effect on the twist-shortening relationship.

With paired-pacing, the twist-shortening relationship during IVR became less defined (more uncoupled). This could be a result of pacing via the right ventricle. Different activation patterns produce a different balance of epicardial and endocardial moments, which result in delayed maximal twist into the IVR period. As seen with volume loading, delayed maximal twist into IVR was associated with an uncoupling of the twist-shortening relationship in IVR.

### 4.5.5 Effects of Changing Heart Rate on Twist Dynamics

Hansen et al. (1988) noted a mild inotropic effect of tachycardia on the torsional deformation observed in their human subjects. In this study, the heart was atrially paced and heart rate increased from 90 bpm to 180 bpm. With this increase, there was a leftward shift of the pressure--apex-rotation loops, as a result of the twist-volume relationship established with preload changes. With increased heart rate, significantly less untwisting occurred during the IVR periods. A smaller LV volume as well as more negative ED apex-rotation values are characteristic for larger rates. At 180 bpm, the total apex-rotation decreases significantly and the maximal apex-rotation occurs during the IVR period (indicating significant delay in

apex-rotation). As heart rate increases, there is decreased activation time, and possibly earlier epicardial relaxation. As discussed previously, less fibre shortening and higher ES volume could reduce restoring forces, slow untwisting during IVR and reduce early diastolic filling. Consistent with the findings for other interventions, ED and ES apex-rotation values could also be attributed here to changes in the corresponding LV volumes.

### 4.5.6 Summary

By use of the optical apex-rotation measuring device, relationships between twist and LV volume at ED and ES have been shown. They were found to be independent of contractility, afterload, and heart rate. The effects of these interventions on twist dynamics throughout the cardiac cycle have also been documented.

Delayed twist and reduced amplitude of twist was observed with increased afterload and increased heart rate. Heart rate itself has complicated effects on twist dynamics, which are likely secondary to changes in LV volumes and dynamics of contraction. Total apex-rotation was seen to increase with increased contractility. The twist-shortening relationship remained linear during twisting and IVR with epinephrine injection with slopes in these periods similar to control, as both fibre shortening and twist increased concomitantly.

In general, with lower the ES volume (increased fibre shortening) as with increased contractility, there is more stored elastic energy, restoring forces are greater, and there is larger IVR untwist. This pattern was shown to be true for epinephrine injection. Twist pattern with the paired-pacing model may have varied due to different activation patterns (ventricular pacing).

With higher ES volume produced by increased afterload or increased heart rate, there is less stored elastic energy, smaller restoring forces, and slower IVR untwist. The observed changes in LV twist with changing afterload, contractility, and heart rate are a result of a changing balance between epicardial and endocardial moments.

# Chapter 5

# THE EFFECTS OF ISCHEMIA ON APEX-ROTATION

## 5.1 Abstract

Because LV twist is a result of the balance of epicardial and endocardial moments, and is determined by fibre shortening, interventions such as ischemia are likely to affect torsion. The effects of both left anterior descending coronary artery (LAD) occlusion and circumflex (LCX) coronary artery occlusion was studied in 16 open-chest dogs with the optical device. After 10 sec of LAD ischemia, a pronounced increase in apex-rotation was noted. This may be a possible result of decreased endocardial fibre shortening in early ischemia. Less endocardial "untwisting" torque would produce greater apex-rotation amplitude. At 10, 30, and 50 sec of ischemia, the maximal apex-rotation is delayed into the IVR period, probably as a result of changing fibre moments. At 30 and 50 sec of ischemia, a paradoxical untwisting/ twisting/ untwisting pattern was observed during IVR. At 50 sec of occlusion, there was a decrease in apex-rotation amplitude. Circumflex ischemia resulted in similar results to LAD ischemia. Maximal apex-rotation was

delayed into the IVR period and the untwisting/ twisting/ untwisting pattern was observed in IVR. No increase in apex-rotation amplitude was observed after 10 sec of circumflex occlusion, however, and no decrease in amplitude was observed after 50 sec. This may be due to the domination of subendocardial ischemia. Although the LV apex is generally fed by the LAD artery, occlusion of the circumflex artery caused similar ischemic effects, since apex-rotation is a result of torque moments translated to the apex from all levels of the LV.

The twist-shortening relationship is affected by ischemia, as the relationship appears less linear during both ejection and IVR. In summary, ischemia has a strong effect of fibre shortening and fibre moments that govern LV twist. This may, in turn, affect restoring forces and early diastolic filling.

## 5.2 Introduction

By providing on-line measurement of apex-rotation (by the optical method) simultaneously with various haemodynamic parameters, the direct relationship of twist to ventricular mechanics and haemodynamics can be easily achieved with rapidly changing parameters such as ischemia.

Using this method, it was possible to study the effects of load, contractility, and heart rate on both the amplitude and dynamics of LV apex-rotation in Chapters 3 and 4. These results helped to show that, as the balance of moments between endocardial and epicardial fibres are altered with changing load or contractility,

there is a significant change in LV twist. Since local transient ischemia has been shown to alter fibre shortening in the ischemic area, it seems likely that LV twist would also be altered, as the balance of fibre moments would be changed.

Because many of the previous studies (Buchalter et al., 1990; Hansen et al., 1988; Ingels et al., 1989; Yun et al., 1991) were done non-invasively or performed on humans, little is known about the effects of ischemia on LV twist. It has been established that, with transient ischemia produced by coronary artery occlusion, blood flow and metabolic processes are more affected in the subendocardium than in the subepicardium (Bache et al., 1977; Prinzen et al., 1984). Prinzen et al. (1986) used an inductive technique in dogs and found that, with coronary arterial stenosis, fibre shortening in the inner layers decreased more than in the outer layers. Further, they found that this decrease occurred earlier in the subendocardium (after 5 sec. of ischemia) than in the subepicardium (after 30 sec. of ischemia). These results would indicate that the balance of fibre moments between the epicardium and the endocardium is indeed changed with ischemia. Thus, it is likely that local, transient, ischemia affects both the amplitude and the dynamics of twist.

Hansen et al. (1987) studied the effect of acute human allograft rejection on LV torsion using intramyocardial markers. They found that both LV torsion amplitude and rate are sensitive to these rejection episodes. Using the same method, Yun et al. (1991) found that the amount of LV untwisting in early diastole is reduced with allograft rejection, with possible effects on restoring forces and early

diastolic filling, but found no effect on systolic twist dynamics.

When studying the effects of ischemia on LV twist, the use of the optical device has the advantage of continuous on-line recordings of LV twist throughout the ischemic episode, and the open-chest experimental set-up allows us to easily control the extent of ischemia. In this study, ischemia was produced by pulling up on a snare around a coronary artery. Depending on where the snare was placed and how long the snare was held for, the ischemia could be well-controlled. For comparison, snares were placed in two positions on the left anterior descending (LAD) coronary artery. The more distal snare produced a smaller, ischemic zone. A snare was also placed on the left circumflex (LCX) coronary artery. In this way, comparison of ischemic effects from both ischemic zones could be made. This may be important since, in general, the LV apex is fed by the LAD artery.

In Chapter 3, ED and an ES twist-volume relationships were established. It was shown that these relationships were unaffected by changes in afterload, contractility, and heart rate. Since local transient ischemia is known to affect muscle fibre shortening in the ischemic zone, and because LV twist is closely correlated with fibre shortening, it seems likely that these ED and ES twist-volume relationships may also change. Beyar et al. (1989) showed that the relationship between twist and shortening was linear during systole but became uncoupled during early diastole. This was again shown by Yun et al. (1991). Because fibre shortening, and possibly twist, is affected by ischemia, this apex-rotation--segment-

length relationship will also be studied under control and ischemic conditions.

The aim of this chapter was, therefore, to examine the dynamic changes in LV apex-rotation with local transient ischemia using the optical device. Changes in amplitude and rate will be noted, particularly in the IVR period. Further, a comparison will be made between a large LAD ischemic zone (proximal snare) and a smaller LAD ischemic zone (more distal tie). In addition, the effects of LAD and LCX ischemia on LV apex-rotation will be studied and compared. The effects of ischemia on the ED and ES twist-volume relationships as well as the ischemic effects on the apex-rotation--segment-length relationship are studied here.

## 5.3 Methods

The effects of ischemia on LV apex-rotation were studied in 16 open-chest dogs. The effects on base-rotation of LAD ischemia in 6 dogs was also noted. Animal preparation and the use of the optical device was as described in Chapter 2.

To study the effects of ischemia, snares were placed around both the LAD and the LCX coronary arteries. Snares were placed at 2 positions on the LAD artery, a proximal position just after the branching of the LAD and LCX arteries, and a more distal position below the first major branch of the LAD artery. The anterior segment-length sonocrystal was placed so that it was in the ischemic zone of both of these snares. The snare over the LCX artery was positioned just after the

branching of the LAD and LCX arteries. A small piece of tubing was placed over the snare and pushed against the artery during the ischemic periods. This allowed for easy maintenance of the artery occlusion without movement or restriction of the heart (particularly for the LCX occlusions).

Apex-rotation was recorded simultaneously with the ECG, LV pressure, aortic pressure, and segment-length measurements. A calibration run was performed at the beginning of the experiment to determine the relation of output voltage to a known distance on the diode. This calibration was checked several times throughout the experiment to correct for possible slow baseline shifts. These changes were found to be insignificant. The LV pressure--apex-rotation loops, LV and aortic pressures, and segment-lengths were monitored throughout the experiment. A recording interval lasted 60 sec. After each intervention, time was allowed for the haemodynamic parameters to return to baseline conditions.

To study the effects of the LAD coronary occlusion, either the distal or proximal snare was pulled tight to occlude the vessel (the distal ischemia was produced first). The occlusion was held for approximately 1 min. Longer runs were also performed in some of the dogs to study the further effects, if any, of a longer ischemic period. Following this, the dog was allowed to recover, with ongoing recording of the recovery period. The occlusion was also performed while measuring base-rotation in 6 dogs.

Similarly, occlusions of the LCX coronary occlusion, using the snare were

also held for periods of approximately 1 min. Again, in some dogs, the occlusion was held for a longer period to observe further effects. Following the release of the ocelusion, the dog was allowed to recover fully between runs, with the recovery period being recorded. All measurements were compared to control cycles measured at the beginning of each run.

## 5.4 Results

### 5.4.1 The Effects of LAD Ischemia on LV Apex-Rotation

The effects of LAD occlusion on apex-rotation was studied in 9 dogs. An example of typical time plots for LV pressure, apex-rotation, and ischemic-zone segment-length under control and ischemic (10 and 30 sec) conditions are shown for one dog in Fig. 5.1. No significant change was seen in either LV pressure or segment-length after 10 sec of LAD coronary artery occlusion. Interestingly, however, there was a notable increase in the amplitude of the LV apex-rotation signal after 10 sec of occlusion. This would indicate a possible change in the balance of moments between endocardial and epicardial muscle fibres in favour of the epicardial moments. After 30 sec of LAD occlusion, both the LV pressure and segment-length signals were showing a typical ischemic response. IVR was prolonged (shown in a more gradual decrease in LV pressure in this period). The segment-length had increased at ED, indicating that the ischemic wall was more stretched than under control conditions. The amplitude of the segment-length signal

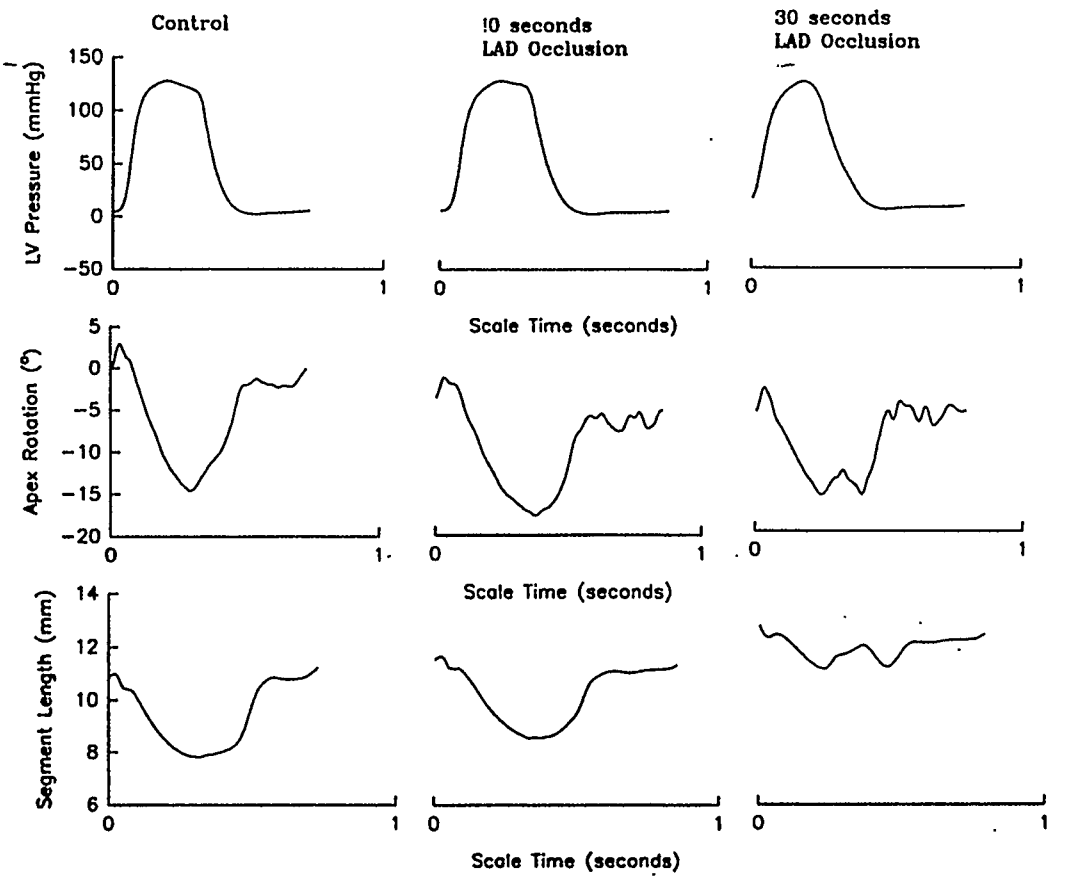


**Figure 5.1**: A typical on-line recording of LV pressure, apex-rotation, and segment length through one cardiac cycle under control conditions (a), 10 sec of LAD occlusion (b), and 30 sec of proximal LAD occlusion.

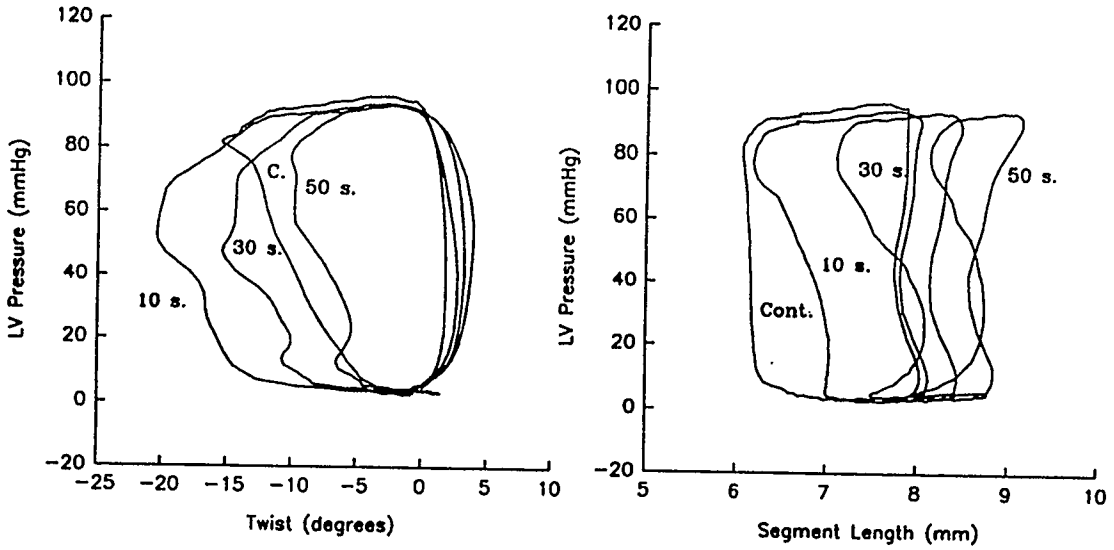


**Figure 5.2**: A typical example of pressure--apex-rotation loops (a) and pressure--segment-length loops under control conditions and after 10, 30, and 50 sec of proximal LAD occlusion.

had decreased significantly with ischemia. There was fibre shortening during systole and initial lengthening in the IVR period, followed by IVR shortening with subsequent relengthening to ED.

Likewise, the apex-rotation signal also changed during the IVR period. Maximal twist occurred after ES (rather than during ejection as in control), followed by untwisting during IVR. This was then followed by a period of IVR twisting, before untwisting to ED values. It is interesting to note that the shape of the apex-rotation and segment-length signals are very similar under control conditions. At 10 sec of occlusion, the apex-rotation signal increased in amplitude without a similar increase in segment-length. At 30 sec of occlusion, the segment-length and apex-rotation signals are again similar, with both showing a period of shortening/twisting in the IVR period during which there is normally only lengthening/untwisting. This may indicate early endocardial relaxation with ischemia. During the recovery period, LV pressure, apex-rotation, and segment-length rapidly returned to control values (within 1 to 2 min).

Figure 5.2 shows typical LV pressure--apex-rotation loops and pressure--segment-length loops from a single animal at baseline and 10, 30, and 50 sec of LAD ischemia. The pressure-segment-length loops show a typical ischemic response. The loops shifted rightward as occlusion time progressed, and the shape of the loops changed from rectangular to a figure-eight shape. Again, there was a period of fibre shortening during the IVR period.

**Table 5.1** - Mean Values for apex-rotation and LV pressure from 9 dogs for baseline and 10, 30, and 50 seconds of LAD artery occlusion.

| Point in Cycle | Apex-rotation Baseline | Apex-rotation 10 sec ischemia | Apex-rotation 30 sec ischemia | Apex-rotation 50 sec ischemia |
|---|---|---|---|---|
| End diastole | 0.0±0.0 | -3.4±1.2 | -2.4±1.5 | -1.6±2.2 |
| Maximal untwist | 4.7±1.1 | 2.0±1.5 | 3.1±2.2 | 2.2±1.8 |
| End isovolumic contraction | 0.2±1.6 | -2.8±1.5 | -2.4±1.8 | -3.0±1.8 |
| Peak LV pressure | -8.1±1.4 | -10.5±2.0 | -10.6±2.5 | -9.2±1.9 |
| Maximal twist | -15.9±2.0 | -17.1±2.2 | -16.8±2.5 | -13.8±2.0 |
| End systole | -14.4±2.0 | -15.0±2.4 | -14.4±2.5 | -11.4±2.5 |
| Mid isovolumic relaxation | -11.8±2.0 | -15.2±3.0 | -10.8±3.2 | -6.8±2.2 |
| End isovolumic relaxation | -9.3±1.9 | -14.1±1.9 | -11.2±2.6 | -8.7±1.7 |
| 1/3 diastolic filling | -2.8±1.4 | -7.8±2.1 | -6.4±1.1 | -5.5±1.2 |
| 2/3 diastolic filling | -2.3±1.2 | -6.3±1.6 | -5.2±1.2 | -4.7±1.3 |
| End diastole | -0.9±0.6 | -4.0±1.1 | -3.0±1.4 | -2.3±1.4 |

| Point in Cycle | LV pressure Baseline | LV pressure 10 sec ischemia | LV pressure 30 sec ischemia | LV pressure 50 sec ischemia |
|---|---|---|---|---|
| End diastole | 9.0±0.9 | 8.9±1.0 | 10.2±1.0 | 11.1±1.0 |
| Maximal untwist | 38.3±7.6 | 32.6±9.2 | 41.4±9.9 | 43.7±8.3 |
| End isovolumic contraction | 93.4±5.4 | 92.1±5.6 | 92.6±5.6 | 91.2±5.7 |
| Peak LV pressure | 104.1±6.7 | 102.1±6.6 | 104.1±7.3 | 101.9±6.2 |
| Maximal twist | 96.2±7.2 | 61.9±9.3 | 67.1±11.2 | 66.5±14.2 |
| End systole | 90.6±6.6 | 89.9±6.3 | 93.4±7.4 | 91.5±6.6 |
| Mid isovolumic relaxation | 44.4±2.3 | 42.0±2.1 | 48.7±3.7 | 52.9±4.5 |
| End isovolumic relaxation | 13.6±0.8 | 14.2±0.8 | 15.6±1.0 | 16.5±1.1 |
| 1/3 diastolic filling | 6.4±1.1 | 6.4±1.0 | 7.0±1.0 | 8.7±1.3 |
| 2/3 diastolic filling | 6.6±1.0 | 6.8±0.9 | 7.7±0.9 | 9.2±1.0 |
| End diastole | 8.2±0.9 | 8.2±1.0 | 9.5±0.9 | 11.2±1.1 |

Baseline end diastole is defined as 0° rotation. LAD Ischemia was produced by occluding the LAD artery for up to one minute. Values are meaned for 9 dogs and standard errors are shown.

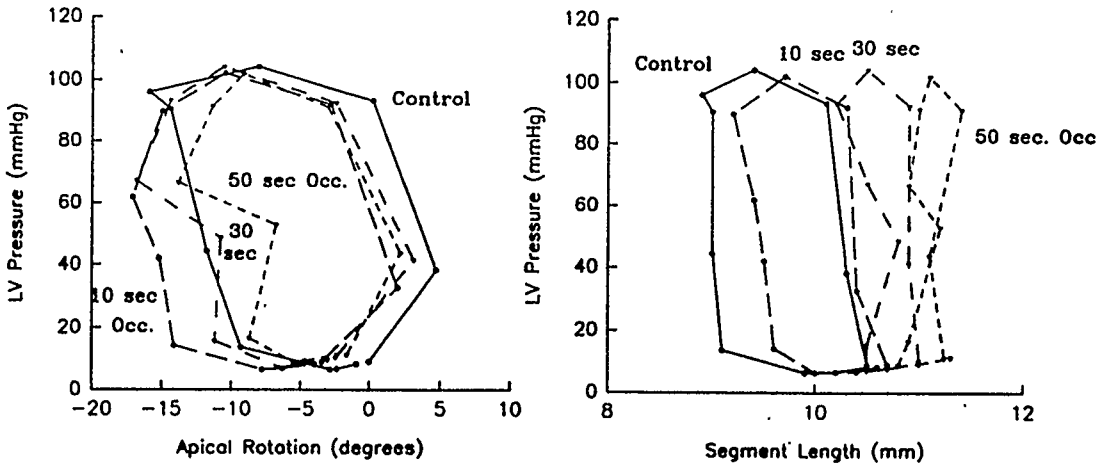


**Figure 5.3**: Mean plots of pressure--apex-rotation and pressure--segment-length under normal conditions and after 10, 30, and 50 sec of proximal LAD occlusion. Mean values are shown in Table 5.1.

The control LV pressure--apex-rotation loop was similar to results reported in earlier chapters. After 10 sec of LAD occlusion, the pressure--apex-rotation loops was much wider (a result of greater apex-rotation amplitude). Maximal apex-rotation was delayed into the IVR period. At 30 and 50 sec of ischemia, the loops decreased in width (decreased apex-rotation amplitude) and showed the untwisting/ twisting/ untwisting pattern in IVR. Maximal apex-rotation again occurred in the IVR period rather than during ejection.

Results from 9 dogs were then meaned at 11 defined points through the cardiac cycle (see Table 5.1). These points were then plotted in the form of pressure--apex-rotation loops, with mean pressure--segment-length loops for comparison in Fig. 5.3. The mean pressure--segment-length loops again show the typical ischemic response with a rightward shift and distortion of the loops.

At 10 sec of ischemia, the mean pressure-apex-rotation loop was shifted leftward ($p < 0.02$). As shown in individual examples, the total amplitude of apex-rotation was increased, with maximal apex-rotation occurring in the IVR period rather than during ejection. This would indicate a change in the balance of fibre moments within the ischemic wall. Delayed untwisting during IVR may affect the rapid elastic recoil and early diastolic filling. At 30 sec and 50 sec of LAD ischemia, loops remain shifted leftward and maximum apex-rotation was again delayed into IVR period. This was followed by a pattern of IVR untwisting/ twisting/ untwisting, again indicating a change in the balance of endocardial and

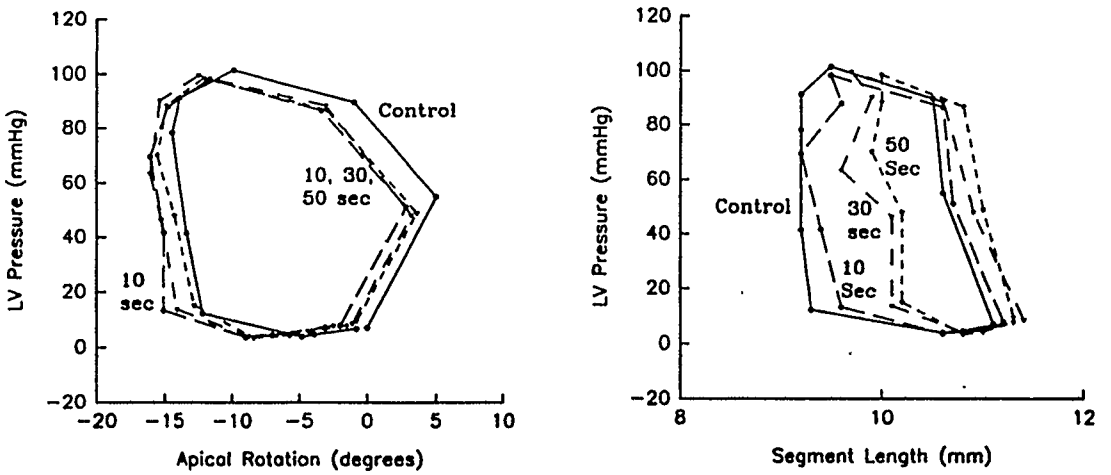


**Figure 5.4:** Mean plots of pressure--apex-rotation and pressure--segment-length under control conditions and after 10, 30, and 50 sec of a distal LAD occlusion.

epicardial moments with ischemia. The total amplitude of apex-rotation at 50 sec of LAD ischemia has decreased.

To estimate the effect of the size of the ischemic zone on twist dynamics, a smaller LAD ischemic zone was induced by occluding the LAD coronary artery at a more distal position. In this case, there was no early transient increase in twist as noted for the large LAD ischemia (Fig. 5.4). The pressure--segment-length loops showed a slight rightward shift with some distortion, but the effect was mild (loops did not change to a figure-eight shape). The ischemic pressure--apex-rotation loops at 10, 30, and 50 sec all showed a leftward shift of approximately 2°, but no significant change in the total amplitude of apex-rotation was noted. In all 3 ischemic loops, maximal apex-rotation was delayed into the IVR period. Further, no paradoxical twisting pattern (untwisting/ twisting/ untwisting) was noted in the IVR period.

The effects of LAD ischemia on base-rotation was measured in 6 dogs. An example of a time plot for LV pressure, base-rotation, and segment-length is shown in Fig. 5.5. Total base-rotation amplitude was approximately 1° under control conditions, and this amplitude decreased with ischemia. The dynamics of base rotation was a mirror image of the apex rotation. The base showed an initial counter-clockwise rotation followed by clockwise rotation in the isovolumic contraction period. The base rotated clockwise to a maximum value during ejection. This was followed by anti-clockwise rotation which continued into the IVR period.

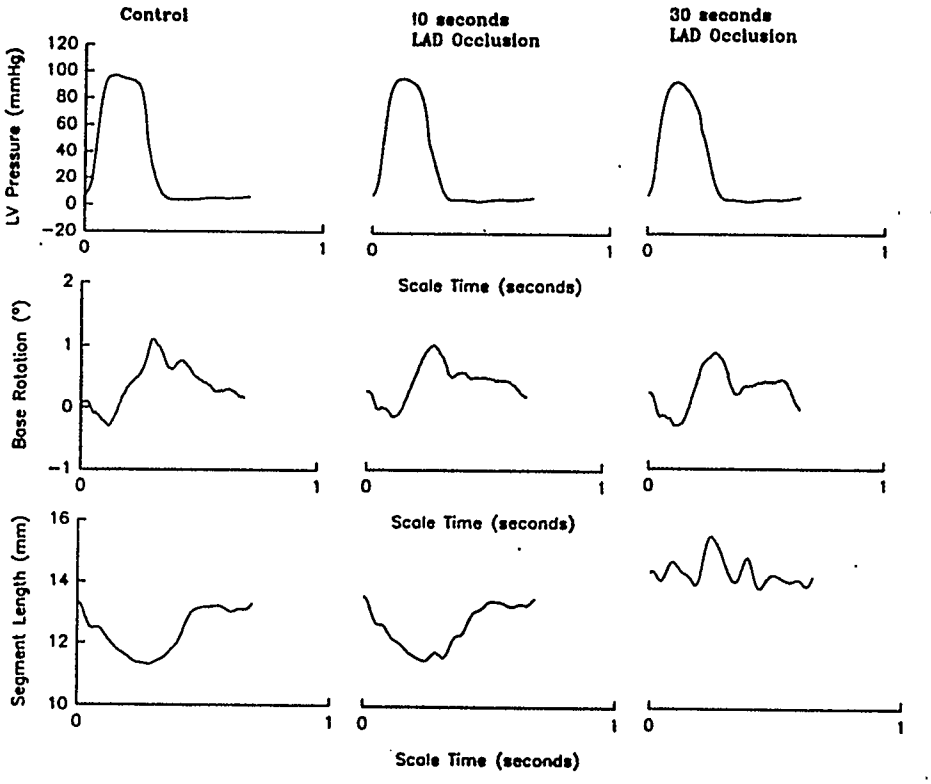


**Figure 5.5**: A typical on-line recording of LV pressure, base-rotation, and segment length through one cardiac cycle under control conditions and after 10 and 30 sec of an LAD occlusion.

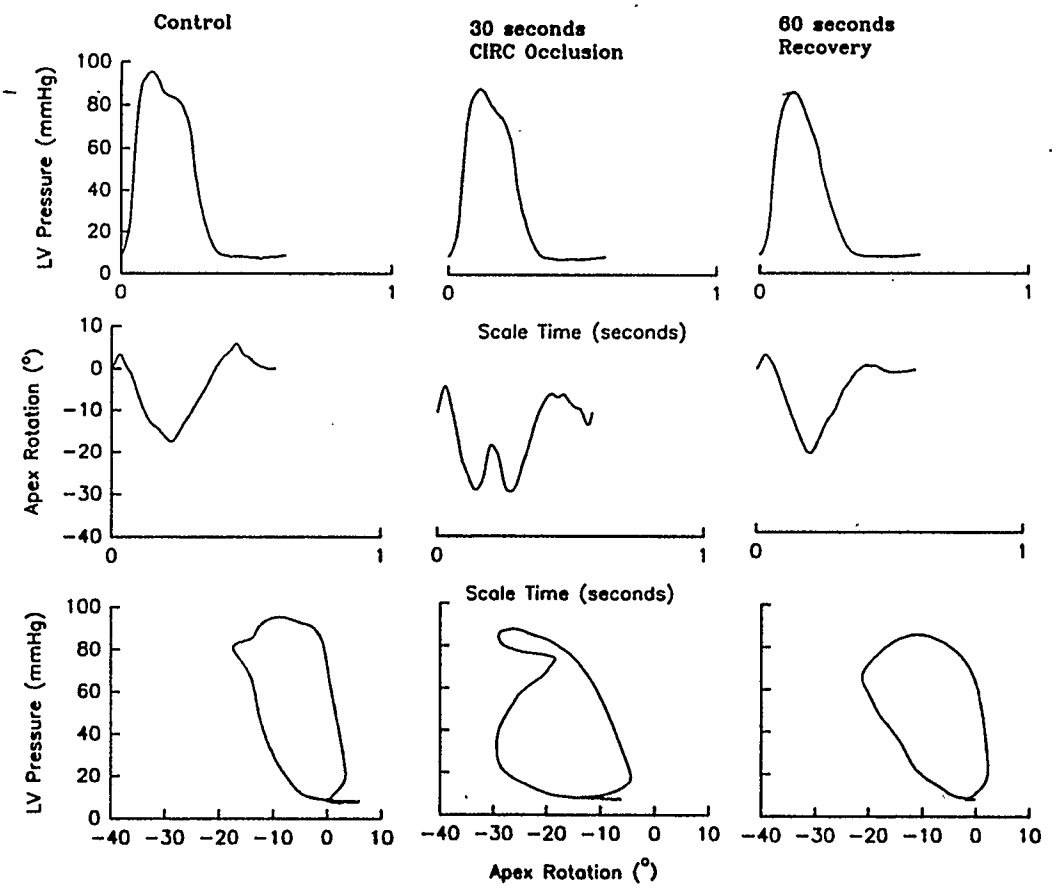


**Figure 5.6:** A typical on-line recording of LV pressure and apex-rotation through one cardiac cycle under control conditions, after 30 sec of a circumflex occlusion, and after 60 seconds of recovery. These data are also shown in the form of pressure--apex-rotation loops.

With ischemia, this maximal clockwise rotation value was delayed into the IVR period. Since base-rotation values are quite small during control conditions and decrease with ischemia, these results support the fact that measurement of apex-rotation by the optical device is a good indicator of the dynamics of LV twist throughout the cardiac cycle, particularly in the case of ischemia.

### 5.4.2 The Effects of Circumflex Ischemia on LV Apex-Rotation

The effects of LCX coronary occlusion on apex-rotation was measured in 8 dogs. Figure 5.6 shows an example of time plots of LV pressure and apex-rotation, as well as pressure--apex-rotation loops at control, 30 sec LCX occlusion, and after 60 sec of recovery. At 30 sec of LCX occlusion, there was a shift of the apex-rotation signal towards a more twisted state, resulting in a leftward shift of the pressure--apex-rotation loops. As with LAD ischemia, maximal apex-rotation was delayed into the IVR period, with the ischemic pattern of untwisting/ twisting/ untwisting occurring in this period.

Values at 11 points in the cardiac cycle were then averaged for 8 dogs (Table 5.2). The mean pressure-apex-rotation loops and the mean pressure--segment-length loops for control and LCX ischemia are shown in Fig. 5.7. The pressure--segment-length loops show a typical ischemic response (Tyberg et al., 1974). After 10 sec of LCX ischemia, the pressure--apex-rotation loop had shifted leftward but did not increase in amplitude as seen in LAD occlusion. Maximal apex-rotation was

**Table 5.2** - Mean Values for apex-rotation and LV pressure from 8 dogs for baseline and 10 sec, 30 sec, and 50 sec of a circumflex artery occlusion.

| Point in Cycle | Apex-rotation Baseline | Apex-rotation 10 sec ischemia | Apex-rotation 30 sec ischemia | Apex-rotation 50 sec ischemia |
|---|---|---|---|---|
| End diastole | 0.0±0.0 | -4.4±1.6 | -1.0±2.7 | -0.2±3.5 |
| Maximal untwist | 6.0±1.1 | 1.7±1.9 | 5.9±3.6 | 5.5±3.7 |
| End isovolumic contraction | -0.2±2.0 | -5.6±2.8 | -2.0±4.3 | -2.8±4.1 |
| Peak LV pressure | -9.7±2.5 | -13.1±3.0 | -10.0±3.0 | -10.1±2.7 |
| Maximal twist | -13.4±2.1 | -16.8±2.5 | -15.2±2.2 | -14.7±2.1 |
| End systole | -12.2±1.8 | -15.2±2.8 | -11.0±1.4 | -11.0±1.0 |
| Mid isovolumic relaxation | -11.7±2.2 | -14.8±1.8 | -9.6±2.1 | -6.6±5.5 |
| End isovolumic relaxation | -11.5±3.0 | -15.7±2.6 | -13.7±2.1 | -9.8±3.7 |
| 1/3 diastolic filling | -7.1±3.2 | -9.8±2.7 | -10.2±2.5 | -8.9±1.8 |
| 2/3 diastolic filling | -5.3±1.9 | -8.3±1.9 | -6.6±1.1 | -5.5±1.5 |
| End diastole | -2.7±1.1 | -5.6±1.5 | -2.5±2.4 | -1.1±3.3 |

| Point in Cycle | LV pressure Baseline | LV pressure 10 sec ischemia | LV pressure 30 sec ischemia | LV pressure 50 sec ischemia |
|---|---|---|---|---|
| End diastole | 8.8±1.3 | 8.8±1.4 | 10.0±1.7 | 11.1±1.7 |
| Maximal untwist | 44.0±9.1 | 40.6±7.2 | 43.4±7.7 | 42.2±8.0 |
| End isovolumic contraction | 104.5±12.1 | 104.5±12.4 | 101.6±12.0 | 100.8±11.8 |
| Peak LV pressure | 113.8±12.7 | 109.2±12.4 | 109.8±12.2 | 108.9±11.8 |
| Maximal twist | 106.4±12.1 | 52.7±11.8 | 54.5±14.9 | 72.8±17.7 |
| End systole | 97.5±16.5 | 105.7±12.6 | 102.7±12.3 | 93.7±8.0 |
| Mid isovolumic relaxation | 50.9±6.0 | 49.5±5.9 | 54.5±9.2 | 58.2±7.6 |
| End isovolumic relaxation | 14.5±1.4 | 14.5±1.4 | 16.0±1.3 | 16.6±1.8 |
| 1/3 diastolic filling | 6.1±1.1 | 6.4±1.2 | 7.3±1.4 | 7.7±1.5 |
| 2/3 diastolic filling | 6.3±1.2 | 6.7±1.3 | 7.6±1.4 | 8.0±1.5 |
| End diastole | 7.9±1.3 | 8.6±1.3 | 9.7±1.5 | 10.3±1.7 |

Baseline end diastole is defined as 0° rotation. Circumflex ischemia was produced by occluding the circumflex coronary artery for up to one minute. Values are meaned for 9 dogs and standard errors are shown.

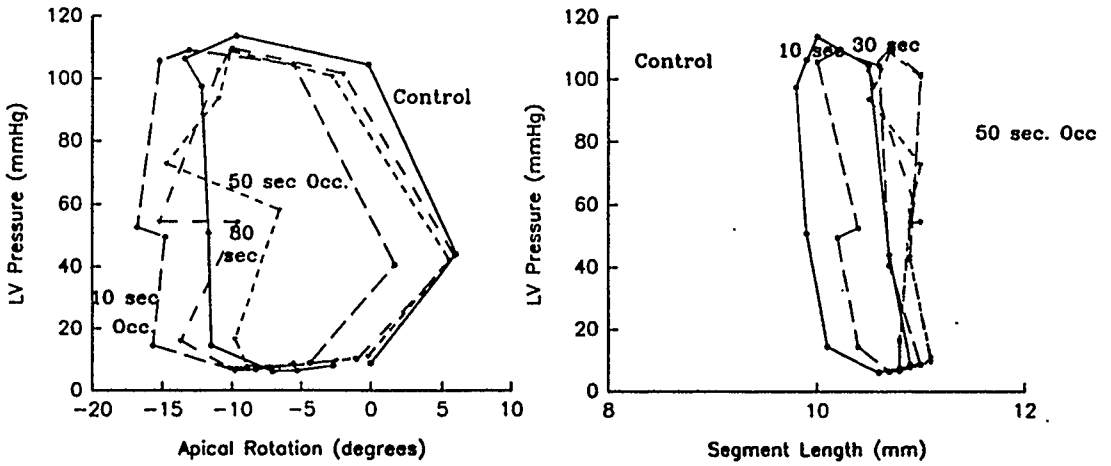


**Figure 5.7:** Mean plots of pressure--apex-rotation and pressure--segment-length loops under control conditions and after 10, 30, and 50 sec of circumflex ischemia.

delayed into the IVR period with a small twisting period occurring during the IVR untwisting phase. As seen with LAD ischemia at both 30 and 50 sec, the pressure-apex-rotation loops at 30 and 50 sec of LCX occlusion showed a pronounced sequence of untwisting/ twisting/ untwisting during the IVR period. Similarly, maximal apex-rotation was also delayed into the IVR period. Unlike the LAD ischemia at 50 sec, apex-rotation with LCX ischemia did not decrease significantly in amplitude. These results again indicate a probable change in the balance of fibre moments controlling twist. It is interesting to note the similarities and differences in LAD and LCX ischemia, considering the fact that the apex is mostly fed by the LAD and not the LCX artery.

### 5.4.3 The Effects of Ischemia on the Twist-Shortening Relationship and the Twist-Volume Relationship

Fractional shortening was calculated from both the ischemic and non-ischemic segment-lengths and plotted against apex-rotation. A typical example from one dog is shown in Fig. 5.8 of pressure--apex-rotation loops and apex-rotation--fractional shortening loops (for ischemic and non-ischemic segment-lengths) for control and during LAD ischemia. As shown previously by Beyar et al. (1989), the apex-rotation--fractional shortening loop under control conditions was linear during ejection, but becomes uncoupled during relaxation. With LAD ischemia, little change was seen in the shape of the non-ischemic apex-rotation--fractional

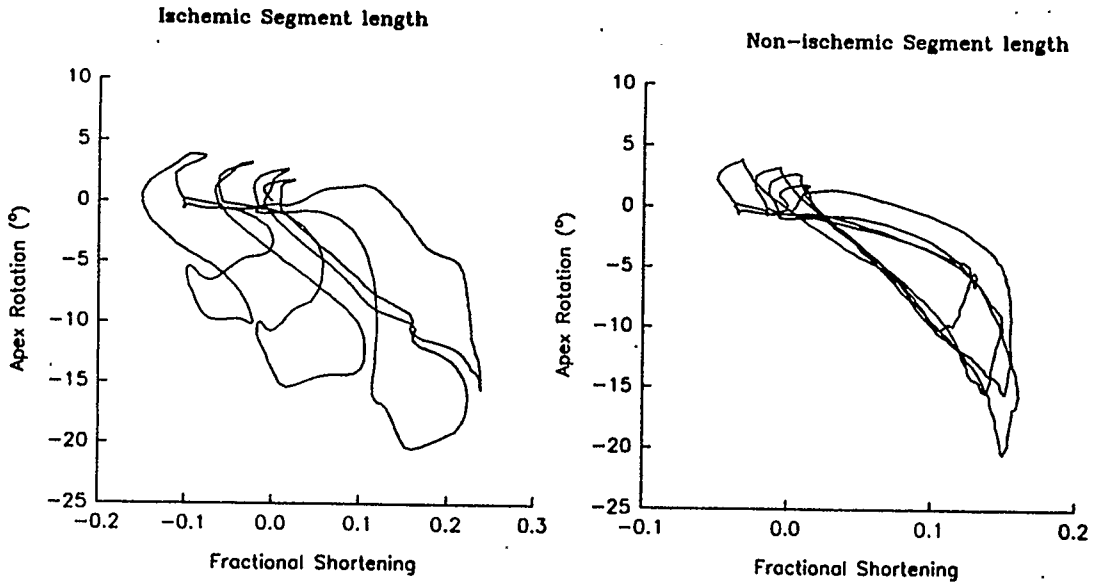


**Figure 5.8**: A typical example of apex-rotation--fractional shortening loops in the ischemic and non-ischemic zones under control conditions and after 10, 30, and 50 sec of LAD ischemia.

shortening loops. Although twist amplitude decreased, there was little left or right shift observed in the loops. When these apex-rotation--fractional shortening loops are plotted using the ischemic segment-length signal, however, there is a large change in both amplitude and shape of the loops. The linearity observed in the loop at control was reduced during ischemia, with a leftward shift in the loops seen. This may indicate that, with ischemia, apex-rotation and shortening become uncoupled throughout the cardiac cycle, rather than just during relaxation. Under control conditions, the apex-rotation--fractional shortening loop is also linear during the IVR period, although the slope of this portion is steeper than seen during ejection. When considering the ischemic segment-length signal, the apex-rotation--fractional shortening loops become non-linear during IVR under ischemic conditions. This is in contrast to the apex-rotation--segment-length loops from the non-ischemic area, which continue to show a linearity during IVR with ischemia (again, with a steeper slope than seen during ejection).

It was shown in Chapter 3 that there is a linear relationship between twist and volume at ED, which was significantly different than the linear relationship established at ES. In a similar fashion, ED and ES apex-rotation--area-index points have been plotted during an LAD occlusion for 9 dogs. Linear regressions at ED and ES were then plotted and compared to regressions obtained for VC occlusion and volume loading (Fig. 5.9). With ischemia, it can be seen that there is a large variance in slope and position of the regressions and there is no definite trend in

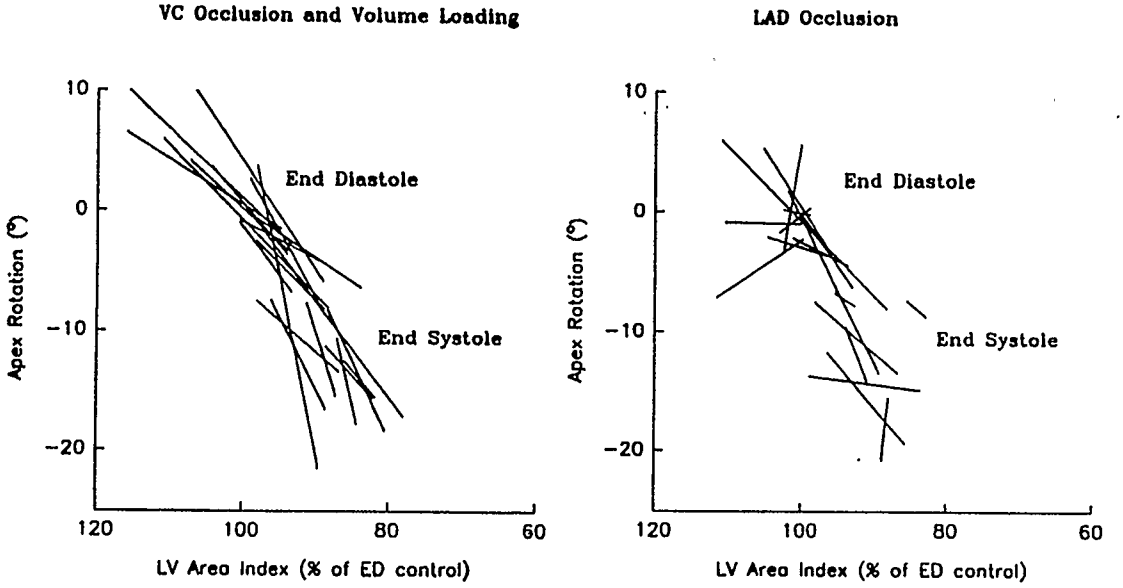


**Figure 5.9:** A plot showing regression lines from end-diastolic and end-systolic data during volume loading and VC occlusion (a). Regression lines from end-diastolic and end-systolic points were then plotted after 50 sec of LAD ischemia.

slopes at either ED or ES. This would indicate that LAD ischemia affects the twist-volume relationships at both ED and ES. This is particularly interesting since neither contractility, afterload, nor heart rate affect these relationships (Chapter 4).

## 5.5 Discussion

In this study, the effects of ischemia on apex-rotation were studied by using an optical method which allows for on-line recording of apex-rotation throughout the cardiac cycle. The method employed here allowed us to control the ischemic episodes. Indeed, other methods cannot be used to study many interventions such as ischemia because of their inability to record dynamic changes throughout the cardiac cycle continuously.

Pressure--segment-length loops can be used to quantitate segmental work and clearly demonstrate the temporal relation between ventricular pressure generation and segmental contraction. The effects of ischemia on these pressure--segment-length loops is well-known. The data is presented in the form of pressure--apex-rotation loops, as it is a simple way to correlate pressure and apex-rotation and allows for comparison between pressure--segment-length loops and pressure--apex-rotation loops. While previous studies have presented data in the form of twist-shortening loops (Beyar et al., 1989) or twist--ejection-fraction loops (Moon et al., 1994), such presentation is limited since it does not have the ability to show leftward or rightward shifts in twist and would mask valuable information about the

isovolumic periods. Pressure-apex-rotation loops allow for shifts in apex-rotation in subsequent beats to be observed.

### 5.5.1 The Effects of Ischemia on LV Twist Dynamics

Prinzen et al. (1986) found that, while endocardial and epicardial fibre shortening is the same under control conditions, endocardial fibre shortening decreased within 5 sec of the onset of ischemia, while epicardial fibre shortening was not affected until 30 sec of ischemia. (Endocardial shortening was not measured directly but estimated from epicardial deformation measurements.) In addition, their study found that the impairment of fibre shortening in the outer layers may be a direct result of the impairment of shortening of the inner fibres, rather than metabolic changes in the outer layers themselves. This is a result of tethering between the layers via the stiff collagen network. Gallagher et al. (1982) also found that endocardium segment-length shortening was reduced more than epicardial shortening during ischemia, as a result of decreased blood flow and altered metabolism in the endocardium (Bache et al., 1977). Thus, it appears that, in the first seconds of ischemia, outer layers remain unchanged while the endocardium becomes dysfunctional. Since the angle between epicardial and endocardial fibres is close to 90° (Streeter, 1979), the fibre moments produced in these layers would have opposite torques. Left ventricular twist is a result of a balance of moments between the endocardial fibres (untwist) and epicardial fibres (twist) (Ingels et al.,

1989). In the early stages of ischemia, the contribution of the endocardial "untwisting" moments would be reduced, and the epicardial moments would dominate even more, producing relatively more counter-clockwise apex-rotation during systole. An increase in apex-rotation amplitude seen after 10 sec of LAD ischemia would seem to support this view.

Also seen at 10 sec of ischemia was a delay in the maximal twist signal into the IVR period (rather than during ejection). This would also indicate a change in the balance of moments between the endocardium and epicardium (possibly delayed relaxation of the epicardium). Since rapid untwisting of the LV during the IVR period may play a role in restoring forces (Rademakers et al., 1992; Moon et al., 1994) and aid in early diastolic filling, this delay of maximal twist (into IVR) may affect the storage or release of potential energy and elastic recoil. This in turn may affect early diastolic filling.

At 30 and 50 sec of ischemia, maximal apex-rotation also occurred during the IVR period. In addition to this, there was a pattern during IVR of normal untwisting, followed by twisting, which was then followed by untwisting. With progressing ischemia, the shortening of the epicardial fibres decreases as discussed above (Prinzen et al., 1986). Normally, during IVR, untwisting occurs, in part, from the dominance of endocardial fibres (as the epicardial fibres are inactivated first). With the ischemic effects on both epicardial and endocardial fibre shortening at 30 and 50 sec of occlusion, the balance of moments during IVR may be markedly

altered, resulting in this ischemic untwisting / twisting / untwisting pattern. This may be a result of early endocardial relaxation. Without the contribution of endocardial "untwisting" moments during ischemia, twist relaxation may be slower, as was observed in this study. The decrease in total amplitude of apex-rotation observed at 50 sec may be a direct result of decreased epicardial fibre shortening with ischemia, resulting in less "twisting" torque. Just as Wiggers (1927) observed that increased temporal dispersion of "fractionate contractions" reduces the amplitude of peak negative and positive dP/dt, changing the time courses of endocardial and epicardial torques can affect the degree and timing of apex-rotation.

Hansen et al. (1987) and Yun et al. (1991) suggested that modification of the elastic properties of the left ventricle may affect relaxation. If fibre shortening is dysfunctional, as in ischemia, the elastic "spring" is not fully loaded during systole, which leads to reduced elastic recoil during relaxation. Similar to this study, Hansen et al. (1987) and Yun et al. (1991) found that untwisting during relaxation was reduced with cardiac allograft rejection.

The early untwisting observed during isovolumic contraction is a result of the endocardial fibres being activated before the epicardial fibres (Ingels et al., 1989). These "untwisting" moments may be reduced with ischemia but are not dominated by epicardial fibres until the outer fibres are activated. Thus, this IVC untwisting is seen throughout the ischemic episode.

It is interesting to note that the ischemic effects on apex-rotation of LAD and

LCX coronary occlusions are quite similar, since the apex is primarily fed by the LAD coronary artery. Buchalter et al. (1990) found that rotation of the apex with respect to the base increased from base to apex. Thus, at a given level of the heart, the muscle fibre shortening at that level translates its torque moment toward the apex, and contributes to the rotation of the heart more apical to that level. Therefore, it is suggested that although the LCX artery does not feed the apex directly, its occlusion affects large areas of muscle fibres that contribute to the balance of moments that produce apex-rotation. Supporting this, it was noted that with a smaller LAD ischemic zone, there was a reduced effect on apex-rotation, as a result of a smaller ischemic zone involving the apical portion of the LV.

### 5.5.2 The Effects of Ischemia on the Twist-Shortening and Twist-Volume Relationships

Beyar et al. (1989) showed a linear relationship between shortening and twist during the ejection period. Moon et al. (1994) also noted this linearity under control conditions. Beyar et al. (1989) noted an uncoupling of the twist-shortening relationship during relaxation. The experimental set-up of the present study allowed for the direct measurement of midwall segment-length in both ischemic and non-ischemic zones, so the effects of ischemia on the twist-shortening relationship could be well examined. As with the studies of Beyar et al. (1989) and Moon et al. (1994), a linear relationship between fractional shortening and apex-rotation was

noted through ejection under control conditions. With ischemia, a decrease in linearity of the apex-rotation--fractional shortening relationship was noted through ejection. This relationship was unaffected and remained linear in the non-ischemic zone. The loss of linearity of the apex-rotation--fractional shortening relationship in the ischemic zone may indicate that, with ischemia, apex-rotation and fractional shortening are not as tightly coupled as seen under control conditions. In this study, a linear relationship between apex-rotation and fractional shortening was noted during IVR, which had a steeper slope than during ejection. With LAD occlusion, this relationship was unaffected and remained linear in the non-ischemic zone. In the ischemic zone, however, this relationship became completely uncoupled. These results would indicate that ischemia has a notable effect on the twist-shortening relationship. The LV midwall fibres are oriented circumferentially and do not contribute significantly to apex-rotation, so it is interesting to note the linear relationship between midwall shortening and apex-rotation under control conditions. With ischemia, midwall shortening is affected by direct metabolic effects of ischemia, as well as tethering effects from the epicardial and endocardial layers via the collagen network. Apex-rotation also changes as a result of a changing balance of moments between epicardial and endocardial layers. These result in complex changes in the twist-shortening relationship, particularly during IVR.

Significantly different linear twist-volume relationships have previously been established for ED and ES (Chapter 3). These were found to be unaffected by

changes in contractility, afterload, and heart rate. When these points were compared during ischemia, the relationships were much more difficult to define. No trend in slopes or positions could be found between dogs when comparing regressions of the points at either ED or ES. This would seem to indicate that ischemia affects the twist-volume relationship. Ischemia changes the balance of moments between muscle fibres, and affects individual fibre shortening. This affects both apex-rotation and the ability of the heart to expel blood volume. Thus, it would seem reasonable that ischemia affects this twist-volume relationship.

### 5.5.3 Summary

By use of the optical device to measure apex-rotation, the effects of ischemia on LV twist have been studied. LAD ischemia resulted in delayed maximal apex-rotation into the IVR period at 10, 30, and 50 sec. An increase in apex-rotation amplitude at 10 sec of occlusion may be a direct result of less endocardial shortening and less endocardial "untwisting" contribution to the balance of moments. At 30 and 50 sec of occlusion, an ischemic pattern of untwisting/ twisting/ untwisting during IVR was noted. This ischemic pattern disappeared within one minute of reperfusion. Generally, similar results were achieved for both the LAD and LCX artery occlusions. Under control conditions, a linear relationship exists between apex-rotation and segment-length during ejection. With ischemia, this relationship may become uncoupled. These results show the effects of ischemia on the balance

of epicardial and endocardial moments which govern LV twist. This, in turn, may affect restoring forces and early diastolic filling.

# Chapter 6

# CONCLUSIONS

LV torsion is a result of a balance of moments between epicardial and endocardial fibres. As this balance of moments changes throughout the cardiac cycle and with interventions such as load or ischemia, different twisting and untwisting patterns occur. This study has shown that LV twist can be well-characterized by apex-rotation, since base-rotation is small. Apex-rotation was measured with an optical device, which had the advantage of being simple to use and providing a continuous recording which could be correlated to haemodynamic parameters such as LV pressure and shortening. The on-line data made analysis simpler than previous methods. The method was limited, however, by the invasive procedure (large thoracic opening) and because the measurements do not include base-rotation. When the optical device was used to measure base-rotation, it was found to be 1-2°. Although the apex-rotation values are an underestimation of LV twist, they remain a reliable index of torsion.

Because the optical device has the ability to measure rapid changes in apex-rotation (particularly during isovolumic periods), it was useful in the study of the effects of preload, afterload, contractility, heart rate, and ischemia.

The end-diastolic angular position is determined by the volume of the LV (a balance between fibre length and the load upon the collagen network). Previous methods (Hansen et al., 1991; Rademakers et al., 1992; Moon et. al, 1994) arbitrarily set the end-diastolic twist value at 0° each beat, and compare other points in the cycle to this value. Therefore, in the study of interventions, no shift in the end diastolic twist values could be seen as an effect of a particular intervention. Since each point in the cycle is compared to this end diastolic value, any shift in pressure-twist or twist-shortening loops would be lost. Valuable information about the effects of load and contractility could not be documented using these methods. The optical method allows for beat-to-beat shifts in apex-rotation to be observed and therefore, has a great advantage over previous methods in the study of intervention effects.

Chapter 3 showed the effects of changing preload on apex-rotation. By VC occlusion and volume loading, a direct, linear twist-volume relationship has been established at end diastole that is significantly different from the linear relationship established at end systole. In Chapter 4, it was shown that this twist-volume relationship was unaffected by changing contractility, afterload, or heart rate, as all the variance in apex-rotation with these interventions could be explained by changes in volume. The effects of ischemia on this relationship (Chapter 5) were harder to interpret, as ischemia seemed to reduce the strong linearity observed with load interventions.

The amplitude and dynamics of LV apex-rotation was also studied under these intervention conditions. In general, reduced preload increased apex-rotation amplitude (although not significantly) and caused maximal apex-rotation to occur earlier in the cycle. Increased preload, afterload, or heart rate, all decreased the amplitude of apex-rotation and caused maximal twist to be delayed into isovolumic relaxation. This may be a result of a change in the balance of endocardial and epicardial fibre moments with these interventions. Delayed untwisting during isovolumic relaxation may be associated with reduced restoring forces (due to reduced fibre shortening under these intervention conditions), less elastic recoil (less potential energy release), and less early diastolic filling..

The twist-shortening relationship, which was shown to be linear during the twisting phase, and linear (with a steeper slope) during isovolumic relaxation, was essentially unaffected by reduced preload. Those interventions which caused a delay of maximal apex-rotation (increased preload, afterload and heart rate) appeared to affect the isovolumic relaxation twist-shortening relationship, making the linearity less defined in this period.

Increased contractility increased both apex-rotation amplitude and the rate of twisting/untwisting in the isovolumic periods. An exception to this was that untwisting in the isovolumic relaxation period with paired-pacing was delayed, possibly because paired-pacing involves ventricular pacing which would affect activation pathways and the balance of fibre moments.

Ischemia affected both fibre shortening and LV apex-rotation. With LAD ischemia, there was an initial increase in apex-rotation, likely due to decreased endocardial shortening. With decreased endocardial torque, the balance of moments was more dominated by epicardial "twisting" fibres, and increased twist was observed. Late in the ischemic period, apex-rotation was decreased, as both endocardial and epicardial shortening is affected. During isovolumic relaxation, a paradoxical pattern of untwisting/ twisting/ untwisting was observed. These changes may be a direct result of changes in the balance of moments between epicardial and endocardial fibres, and may affect restoring forces and early diastolic filling.

The following conclusions can be made from these studies:

1) The measurement of apex-rotation by the optical device provides a direct, reliable index of LV twist, which has advantages over previous methods in its simplicity, analysis, ability to measure rapid changes with interventions, and its ability to measure shifts in apex-rotation at end diastole and throughout the cycle. Apex-rotation data obtained by this method are comparable to other methods and confirm that it can be used to characterize LV twist dynamics.

2) The angular position of the apex is determined by the volume of the LV at both end diastole and end systole (although these relationships are significantly different). This twist-volume relationship is not dependent on contractility, afterload, or heart rate. It may be affected by ischemia, which affects fibre shortening and LV volume. Changes in the dynamics and amplitude of apex-rotation may be mediated

by both end diastolic and end systolic volume effects.

3) Our observations are consistent with the conclusion that the pattern of torsion throughout the cardiac cycle is determined by the balance of epicardial and endocardial fibres. Untwisting observed during isovolumic contraction is likely due to the transient dominance of endocardial moments as they are activated first. Rapid untwisting during isovolumic relaxation is partially due to the dominance of still-activated endocardial fibres.

4) The exact timing of maximal twist in the cardiac cycle (before end systole at baseline) can be altered by different interventions. Increased load, heart rate, and afterload were shown to alter the onset of relaxation, by delaying maximal twist into the isovolumic relaxation period.

5) The rate of untwisting during isovolumic relaxation is a balance between restoring forces and torque moments at the time. In general, the lower the end-systolic volume (e.g. reduced preload), the higher the stored elastic energy (due to increased fibre shortening), the larger are the restoring forces, and the larger is the isovolumic relaxation untwist. This was confirmed with increased preload and afterload which increased end-systolic volume and decreased the rate of isovolumic relaxation untwist.

6) Contractility increased the amplitude of apex-rotation significantly and in general, increased the rate of twisting and untwisting during the isovolumic periods. This may increase restoring forces and early diastolic filling.

7) There is a twist-shortening relationship which is linear during the twisting phase and linear (with a steeper slope) during isovolumic relaxation. The relationship during the twisting phase appears unaffected by changes in load or contractility. Interventions which caused a delay in untwist appeared to affect the twist-shortening relationship during isovolumic relaxation.

8) Ischemia had a profound effect on fibre shortening, as well as apex-rotation. Both LAD and Circumflex ischemia affected torsion, although in general, the apex is fed by the LAD.

9) During early LAD ischemia, an increase in LV apex-rotation was observed. This may be a result of increased epicardial fibre dominance, as the endocardial fibres show reduced shortening first. Reduced opposition to twist by the endocardial fibres shifts the balance of moments to increase twist. A change in the balance of moments during isovolumic relaxation may also produce the paradoxical twisting observed during this period.

The optical device has been shown to be a simple and direct method to measure apex-rotation. It allowed for the study of dynamic changes in LV twist with changes to preload, afterload, contractility, heart rate, and ischemia to be documented. Because of the advantages to this method listed above, it has been possible to show effects of these interventions previously undocumented. LV twist provides a good index of LV contractile function, and the measurement of apex-

rotation by this method may be useful in many future studies. This device could be used to more fully describe the twist-volume relationship and the effects of contractility, afterload, and heart rate on this relation. A possible twist-shortening relationship may also be further established. The effects of activation patterns on twist dynamics could also be studied with this device.

It is hoped that these studies have expanded the knowledge of LV twist, its dynamics through the cardiac cycle, and how it relates to fibre shortening and LV volume. The effects of load, contractility, and ischemia help to more fully understand the balance of fibre moments that determine the dynamics of LV twist.

# References

1) Arts, T., R.S. Reneman, and P.C. Veenstra. A model of the mechanics of the left ventricle. Ann. Biomed. Eng. 7: 299-318, 1979.

2) Arts T, and Reneman RS. Measurement of deformation of canine epicardium in vivo during cardiac cycle. Am. J. Physiol. 1980; 239: H432-437.

3) Arts, T., P.C. Veentra, and R.S. Reneman. Epicardial deformation and left ventricular wall mechanics during ejection in the dog. Am. J. Physiol. 243:H379-H390, 1982.

4) Arts T, Meerbaum S, Reneman RS, and Corday E. Torsion of the left ventricle during the ejection phase in the intact dog. Cardiovasc. Res. 1984; 18:183-193.

5) Azhari, H., M. Buchalter, S. Sideman, E. Shapiro, and R. Beyar. A conical model to describe the nonuniformity of the left ventricular twisting motion. Ann. Biomed. Eng. 20: 149-165, 1992.

6) Bache, R.J., P.A. McHale, and J.C. Greenfield. Transmural myocardial perfusion during restricted coronary inflow in the awake dog. Am. J. Physiol. 232:H645-H651, 1977.

7) Beyar, R., and S. Sideman. A computer study of the left ventricular performance based on fibre structure, sarcomere dynamics, and transmural electrical propagation velocity. Circ. Res. 55:358-375, 1984.

8) Beyar, R., and S. Sideman. The dynamic twisting of the left ventricle: a computer study. Ann. Biomed. Eng. 14:547-562, 1986.

9) Beyar, R., F.C.P. Yin, M. Hausknecht, M.L. Wiesfeldt, and D.A. Kass. Dependence of left ventricular twist-radial shortening relations on cardiac cycle phase. Am. J. Physiol. 257:H1119-H1126, 1989.

10) Buchalter, M.B., J.L. Weiss, W.J. Rogers, E.A. Zerhouni, M.L. Wiesfeldt, R. Beyar, and E.P. Shapiro. Noninvasive quantification of left ventricular rotational deformation in normal humans using magnetic resonance imaging myocardial tagging. Circ. 81:1236-1244, 1990.

11) Caillet, D., and B. Crozatier. Role of myocardial restoring forces in the

determination of early diastolic peal velocity of fibre lengthening in the conscious dog. Cardiovasc. Res. 16:107-112, 1982.

12) Durrer, D., R.T. Van Dam, G.E. Freud, M.J. Janse, F.L. Meisler, R.C. Arzbaecher. Total excitation of the isolated human heart. Circ. 41:899-912, 1970.

13) Feigl, E.O., and D.L. Fry. Intramural myocardial shear during the cardiac cycle. Circ. Res. 14:536-540, 1964.

14) Feigl, E.O. Coronary physiology. Physiol. Rev., 63: 1-205, 1983.

15) Fenton, T.R., J.M. Cherry, and G.A. Klassen. Transmural myocardial deformation in the canine left ventricular wall. Am. J. Physiol. 235:H523-H530, 1978.

16) Gallagher, K.P., G. Osakada, O.H. Hess, J.A. Kozial, W.S. Kemper, and J. Ross. Subepicardial segmental function during coronary stenosis and the role of myocardial fibre orientation. Circ. Res. 50:352-359, 1982.

17) Greenbaum, R.A., S.Y. Ho, D.G. Gibson, A.E. Becker, and R.H. Anderson. Left ventricular fibre architecture in man. Br. Heart J., 45:248-263, 1981.

18) Hansen, D.E., G.T. Daughters, E.L. Alderman, E.B. Stinson, J.C. Baldwin, and D.C. Miller. Effect of acute human cardiac allograft rejection on left ventricular systolic torsion and diastolic recoil measured by intramyocardial markers. Circ. 76: 998-1008, 1987.

19) Hansen, D.E., G.T. Daughters, E.L. Alderman, N.B. Ingels, and D.C. Miller. Torsional deformation of the left ventricular midwall in human hearts with intramyocardial markers: Regional heterogeneity and sensitivity to the inotropic effects of abrupt rate changes. Circ. Res. 62: 941-952, 1988.

20) Hansen DE, Daughters GT, Alderman EL, Ingels NB, Stinson EB, and Miller DC. Effect of volume loading, pressure loading, and inotropic stimulation on left ventricular torsion in humans. Circ. 1991; 83:1315-1326.

21) Ingels NB, Daughters GT, Stinson EB, and Alderman EL. Measurements of midwall myocardial dynamics in intact man by radiography of surgically implanted markers. Circ. 1975; 52: 859-867.

22) Ingels, N.B., D.E. Hansen, G.T. Daughters, E.B. Stinson, E.L. Alderman, and D.C. Miller. Relation between longitudinal, circumferential, and oblique shortening and torsional deformation in the left ventricle of the transplanted human heart. Circ.

Res. 64:915-927, 1989.

23) Lower, R. Tractus de Corde, 1669. In: Early Science in Oxford, vol. 9, edited by R.T. Gunther. Oxford, UK: 1932. Reprint, London: Sawsons, Pall Mall, 1968.

24) MacGowan GA, Rogers WJ, Azhari H, Burkhoff D, Salvador D, Perry LV, Zweier JL, Shapiro EP, Weiss JL. The isovolumic left ventricle twists bi-directionally: a MRI tagging study. Circ. 1992; 86:I-82 (abstract).

25) McDonald, I.G. The shape and movements of the human left ventricle during systole: A study by cineangiography and by cineradiography of epicardial markers. Am. J. Cardiology, 26:221-230, 1970.

26) Moon MR, Ingels NB, Daughters GT, Stinson EB, Hansen DE, and Miller DC. Alterations in left ventricular twist mechanics with inotropic stimulation and volume loading in human subjects. Circ. 1994; 89:142-150.

27) Nevo, E., and Y. Lanir. Structural finite deformation model of the left ventricle during diastole and systole. Trans. ASME 111:342-349, 1989.

28) Nilolic, S., E.L. Yellin, K. Tamura, H. Vetter, T. Tamura, J.S. Meisner, and R.W.M. Frater. Passive properties of canine left ventricle: diastolic stiffness and restoring forces. Circ. Res. 62:1210-1222, 1988.

29) Ohayon, J., and R.S. Chadwick. Theoretical analysis of the effects of a radial activation wave and twisting motion on the mechanics of the left ventricle. Biorheology, 25:435-447, 1988.

30) Prinzen, F.W., T. Arts, G.J. Van der Vusse, and R.S. Reneman. Fibre shortening in the inner layers of the left ventricular wall as assessed from epicardial deformation during normoxia and ischemia. J. Biomech. 17:801-811, 1984.

31) Prinzen, F.W., T. Arts, T.T. Prinzen, and R.S. Reneman. Comments on "Relationship between myocardial fibre direction and segment shortening in the midwall of the canine left ventricle". Circ. Res. 57:909-910, 1985.

32) Prinzen, F.W., T. Arts, G.J. van der Vusse, W.A. Coumans, and R.S. Reneman. Gradients in fiber shortening and metabolism across ischemic left ventricular wall. Am. J. Physiol. 250:H255-H264, 1986.

33) Rademakers, F.E., M.B. Buchalter, W.J. Rogers, E.A. Zerhouni, M.L.

Weisfeldt, J.L. Weiss, and E.P. Shapiro. Dissociation between left ventricular untwisting and filling. Accentuation by catecholamines. Circ. 85:1572-1581, 1992.

34) Raff GL, and Glantz SA. Volume loading slows left ventricular isovolumic relaxation rate. Circ. Res. 1981; 48: 813-824.

35) Ross J, Sonnenblick EH, Kaiser GA, Frommer PL, and Braunwald E. Electroaugmentation of ventricular performance and oxygen consumption by repetitive application of paired electrical stimuli. Circ. Res. 1965; 16:332-342.

36) Rushmer, R.F., D.K. Crystal, C. Wagner. The functional anatomy of ventricular contraction. Circ. Res., 1:162-170, 1953.

37) Scher, A.M., and Spach, M.S. Cardiac depolarization and repolarization and the electrocardiogram, in Berne, R.M. (ed): Handbook of Physiology, Section 2: The Cardiovascular System, Vol. 1: The Heart. American Physiology Society, Washington, DC. p 357-395, 1979.

38) Streeter, D.D., H.M. Spotnitz, D.P. Patel, J. Ross, and E.H. Sonneblick. Fiber orientation in the canine left ventricle during diastole and systole. Circ. Res. 24: 339-347, 1969.

39) Streeter, D.D. Gross morphology and fiber geometry of the heart, in Berne, R.M. (ed): Handbook of Physiology, Section 2: The Cardiovascular System, Vol. 1: The Heart. American Physiological Society, Washington DC. p 61-112, 1979.

40) Tyberg, J.V., W.J. Keon, E.H. Sonnenblick, C.W. Urshel. Mechanics of ventricular diastole. Cardiovasc. Res. 4:423-428, 1970.

41) Tyberg, J.V., J.S. Forrester, H.L. Wyatt, S.J. Goldner, W.W. Parmley, and H.J.C. Swan. An analysis of segmental ischemic dysfunction utilizing the pressure-length loop. Circulation 49:748-754, 1974.

42) Waldman, L.K, Y.C. Fung, and J.W. Covell. Transmural myocardial deformation in the canine left ventricle. Normal in vivo three-dimensional finite strains. Circ. Res. 57: 152-163, 1985.

43) Waldman, L.K., and J.W. Covell. Effects of ventricular pacing on finite deformation in canine left ventricles. Am. J. Physiol. 252:H1023-H1030, 1987.

44) Waldman, L.K., D. Nosan, F. Villarreal, and J.W. Covell. Relation between transmural deformation and local myofiber direction in canine left ventricle. Circ. Res. 63:550-562, 1988.

45) Wiggers, C.J. The importance of dynamic factors in ventricular alternation. Am. J. Physiol. 81:516-517, 1927.

46) Yun, K.L., M.A. Niezyporak, G.T. Daughters, N.B. Ingels, E.B. Stinson, E.L. Alderman, D.E. Hansen, and D.C. Miller. Alterations in left ventricular diastolic twist mechanics during acute human cardiac allograft rejection. Circ. 83: 962-973, 1991.